2008

Experimental and simulation study of demand controlled ventilation

Li Zhang
Iowa State University

Experimental and simulation study of demand controlled ventilation

by

Li Zhang

A dissertation submitted to the graduate faculty

in partial fulfillment of the requirements for the degree of

DOCTOR OF PHILOSOPHY

Major: Mechanical Engineering

Program of Study Committee:
Gregory M. Maxwell, Major Professor
Ron M. Nelson
Kenneth Bryden
Steven J. Hoff
Michael Bence Pate

Iowa State University

Ames, Iowa

2008

UMI Number: 3307039

ProQuest Information and Learning Company
300 North Zeeb Road
P.O. Box 1346
Ann Arbor, MI 48106-1346

TABLE OF CONTENTS

LIST OF TABLES

LIST OF FIGURES

LIST OF SYMBOLS

Ci CO2 concentration in the space

Co CO2 concentration in outdoor air

G CO2 generation rate

Qo Outdoor air flow rate

m number of persons in the space

G1 CO2 generation rate per person

Q1 outdoor air flow rate per person

Qp Outdoor air flow rate decided by people

Qb Outdoor air flow rate decided by building

V_j Room Volume

C_j CO_2 concentration in the room

t Time

Q_{ij} Air flow rate into the room

C_{ij} CO_2 concentration of the air entering the room

Q_{ej} Air flow rate out of the room

C_{ej} CO_2 concentration of the air leaving the room

G_j CO_2 generation in the room

ν_{ej} the specific volume of air leaving the room

ν_{ij} the specific volume of air entering the room

T_{ei} the temperature of air leaving the room

T_{ij} the temperature of air entering the room

C_r CO_2 concentration of the return air

Q_{oa} Air flow rate of the outdoor air

C_{oa} CO_2 concentration of the outdoor air

Q_{ea} Air flow rate of the exit air

ν_{ea} the specific volume of air leaving the system

ν_{oa} the specific volume of the outdoor air entering the system

T_{ea} the temperature of air leaving the system

T_{oa} the temperature of outdoor air entering the system

Rp outdoor airflow rate required per person.

Pz the largest number of people expected to occupy the zone during typical usage.

Ra outdoor airflow rate required per unit area

Az zone flow area

Qot the design outdoor air intake flow

G_{qj}, the CO2 generation in the room

ρ density of CO2 gas

ABSTRACT

The purpose of this study is to compare energy use and CO_2 concentration for a multizone building utilizing three ventilation control strategies. The three strategies are occupancy-based demand controlled ventilation (DCV), carbon-dioxide based DCV and constant ventilation. The study compares the building's energy consumption using the three methods for summer, winter and transition seasons. To perform the study, an indoor air quality (IAQ) model was developed and used in conjunction with EnergyPlus to simulate the building. Experiments were conducted at the Iowa Energy Center's Energy Resource Station to validate the IAQ model. Results from the study show that occupancy based DCV requires the least amount of ventilation air which still meets the ASHRAE ventilation standard.

CHAPTER 1 INTRODUCTION

1.1 Motivation

The consumption of energy by HVAC systems in industrial and commercial buildings constitutes 14% of the United States primary energy consumption (DOE, 2003). About 32% of the electricity generated in the United States is consumed to heat, cool, ventilate, and light commercial buildings (ASHRAE, 2000). The loads due to ventilation typically account for about 20% to 40% of the annual heating and cooling loads (ASHRAE 1993). How to decrease the energy consumption of HVAC systems while maintaining the acceptable indoor air quality is the motivation of this study. Currently many HVAC systems operate at a fixed ventilation rate. This results in over ventilation and higher energy consumption. A method to solve the problem is demand controlled ventilation (DCV). In DCV, the outdoor airflow rate varies with the number of people and their location within the building.

1.2 Literature review

1.2.1 CO_2-based DCV

Conventional demand controlled ventilation (DCV) is usually CO_2-based. In CO_2-based DCV, the outdoor airflow rate is adjusted to maintain the indoor CO_2 concentration at a set point. The steady-state concentration for a single-zone model (as shown in Figure 1.1), is given by Equation 1.1.

$$C_i - C_o = G / Q_o \qquad (1.1)$$

Where

C_i = CO_2 concentration in the space

C_o = CO_2 concentration in outdoor air

G = CO_2 generation rate

Q_o = Outdoor airflow rate

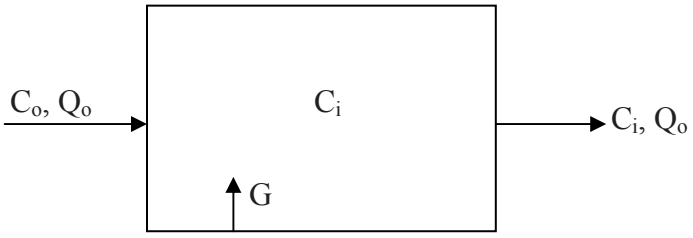

Figure 1.1 Single Zone Model

ASHRAE standard 62.1: Ventilation for acceptable indoor air quality is widely accepted as ventilation guideline. In ASHRAE standard 62.1-2001 (and previous versions), the outdoor airflow rate is proportional to occupancy (Stanke, 2005). As shown in Equation (1.2), assuming a fixed generation rate per person and constant outdoor air (OA) CO_2 concentration, the CO_2 concentration in the space is a constant.

$$C_i = C_o + G / Q_o = C_o + mG_1 / mQ_1 = C_o + G_1 / Q_1 \quad (1.2)$$

Where

m = number of persons in the space

G_1= CO_2 generation rate per person

Q_1 = outdoor airflow rate per person

The constant CO_2 concentration in the space can be used as the CO_2 concentration set point. For example, at an activity level of office work, corresponding to a person performing sedentary activity, the CO_2 generate rate per person is 0.31 L /min. The required outdoor airflow rate is 450 L/min (15 ft^3/min) per person. CO_2 concentrations in acceptable outdoor air typically range from 300 to 500 ppm. Assuming the outdoor air CO_2 concentration is 300 ppm, then

$$C_i - C_o = G_1 / Q_1$$

$$= (0.31 \text{ L/min}) / (450 \text{ L/ min})$$

$$= 0.0007 \text{ liters of } CO_2 \text{ per liter of air}$$

$$= 700 \text{ ppm}$$

C_i = 300 ppm + 700 ppm = 1000 ppm

Thus, maintaining the indoor CO_2 concentration no greater than 1000 ppm could meet the ventilation requirement.

Several researchers have shown that CO_2-based DCV saves energy and cost compared to constant outdoor air ventilation (Mercer and Braun, 2005; Krarti and Alalawi, 2004, Alalawi and Krarti, 2002; Emmerich and Persily, 1997).

However, the constant set point CO_2-based DCV is not valid for ASHRAE standard 62.1-2004. The new standard changes the method of determining the ventilation rate. The required outdoor airflow rate is no longer proportional to occupancy. It is related to both occupancy and building area.

$$Q_o = Q_b + Q_p \qquad (1.3)$$

Where

Q_p = Outdoor airflow rate required by the occupants

Q_b = Outdoor airflow rate based on building area

Thus,

$$C_i = C_o + G / Q_o = C_o + mG_1 / (mQ_1 + Q_b) \qquad (1.4)$$

The CO_2 concentration in the space is not a constant but varies with the number of people. The CO_2 set point should not be a constant since it may result in over-ventilation or under-ventilation. This change to the ventilation standard makes the CO_2-based demand controlled ventilation more difficult to implement. (Stanke, 2005).

1.2.2 Occupancy-based DCV

Another DCV strategy is occupancy-based (Yu-Pei Ke, 1997). In occupancy-based DCV, the outdoor airflow rate is calculated based on the method described in the ASHRAE Standard 62.1-2004. The actual occupancy and building information are used in the calculation. Occupancy-based DCV directly meets the ventilation requirement set forth by the Standard, and satisfies the dynamic ventilation. The simulation results (Lawrence and Braun, 2007) showed that in Occupancy-based DCV, no significant difference in energy cost were found when using overall average occupancy or a variable occupancy pattern. Therefore, using the simpler approach of using overall average occupancy for each hour of the day was recommended. A review of the literature shows that limited research on

occupancy-based DCV has been published. Furthermore, there is limited comparison of energy use between occupancy-based DCV and the other ventilation control strategies. More research is required in this area which is the focus of this research project.

1.3 Objectives

The objective of this study is to compare the energy use and CO_2 concentration for a multizone building utilizing three ventilation control strategies. The three strategies are occupancy-based demand controlled ventilation (DCV), carbon-dioxide based DCV and constant ventilation. To perform the study, an indoor air quality (IAQ) model must be developed and used in conjunction with EnergyPlus to simulate the building. Experiments were conducted at the Iowa Energy Center's Energy Resource Station to validate the ventilation model.

CHAPTER 2 EXPERIMENTAL SETUP

The experiments were performed in Energy Resource Center (ERS), which is located on the Des Moines Area Community College in Ankeny, Iowa.

.

2.1 Energy Resource Station

ERS is owned and operated by the Iowa Energy Center. It was established for the purpose of comparing different energy efficiency measures and record energy consumption. It combines laboratory testing capabilities with real building characteristics. Figure 2.1 shows a photograph of the building.

The building consists of 8 test rooms, a computer room, an office, a class room and other rooms necessary to support the operation of the building. Figure 2.2 shows the building floor plan. The ERS is equipped with three variable-air-volume air handling units (AHUs). AHU-1 serves the common areas of the building. AHU-A and AHU-B are identical and serve Test Rooms-A and Test Rooms-B, respectively. The Test Rooms-A and Test Rooms-B are mirror images. They allow simultaneous, side-by-side comparison testing of many types of HVAC systems and control schemes. Three pairs of the test rooms are located along the building perimeter, facing south, east, and west, respectively. The fourth pair is located in the interior of the building.

A more complete description about the ERS can be found in the report of Price and Smith (2000).

Figure 2.1 An Outlook of Energy Resource Station

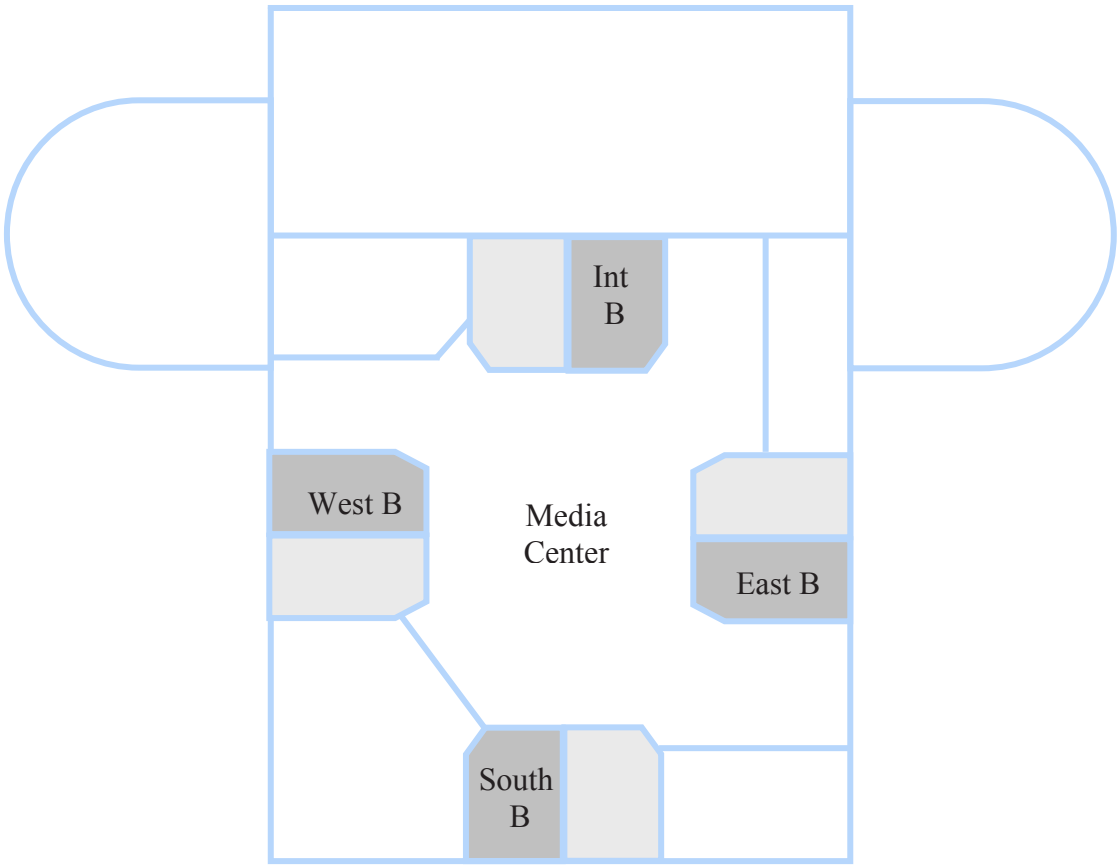

Figure 2.2 A Floor Plan of the Energy Resource Station

2.2 Test Rooms

A sheet metal cylinder, here after referred to as a tin man, was used to simulate a person who generates CO_2 gas and heat as a result of metabolism. Figure 2.3 shows four tin men in one of the test rooms. A flow meter with a needle valve was used to control a tin man's CO_2 generation rate, which is shown in Figure 2.4. The CO_2 gas was provided from a CO_2 gas cylinder. The light bulb simulated a person's heat generation. Figure 2.5 shows the inside of a tin man. The solenoid valve was connected with the flow meter. The solenoid valve and light bulb worked according to the same on-off control schedule. When the solenoid valve and light bulb were on, there were CO_2 and heat generation. It meant there was a person in the room. When the valve and light bulb were off, it meant the person left the room.

Only B Test rooms were used for the experiments. There were four tin men in west-B and east-B rooms, respectively. There was no tin man in south-B and interior-B rooms. In each B test room, two CO_2 sensors were used to measure the CO_2 concentration. One was Vaisala GMW 20 and placed on the wall. The other was the Vaisala GMD 20 and placed at the return duct of the room. Another three CO_2 sensors were also Vaisala GMD 20 and located at the AHU to measure the outdoor air, return air and supply air's CO_2 concentration. Figure 2.6 and 2.7 show photographs of the wall-mounted and duct-mounted CO_2 sensors, respectively. (In Figure 2.7, the duct sensor is shown removed from the duct.) Figure 2.8 shows the location of the CO_2 sensors. Appendix A provides the technical specifications of the CO_2 sensors. Based on ASHRAE standard 62.1-2004, CO_2 generation for a person doing office work was about 0.42L/min (0.015 ft^3/min), which was used as set point for each tin man's CO_2 generation rate during the experiments. Each CO_2 sensor and flow meter was calibrated before the experiment. For more information about the calibration work, please refer to Appendix B and C.

Figure 2.3 West B Room with Four Tin Men

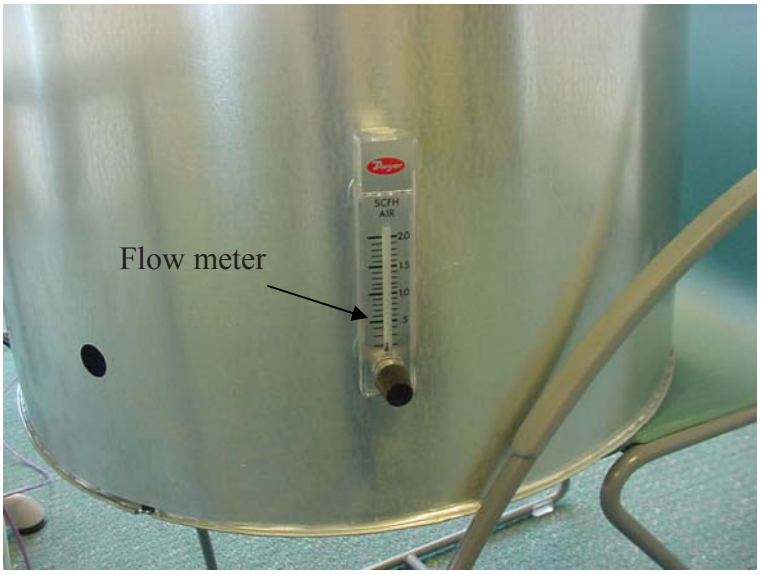

Figure 2.4 Flow Meter used to Control the CO2 Flow Rate

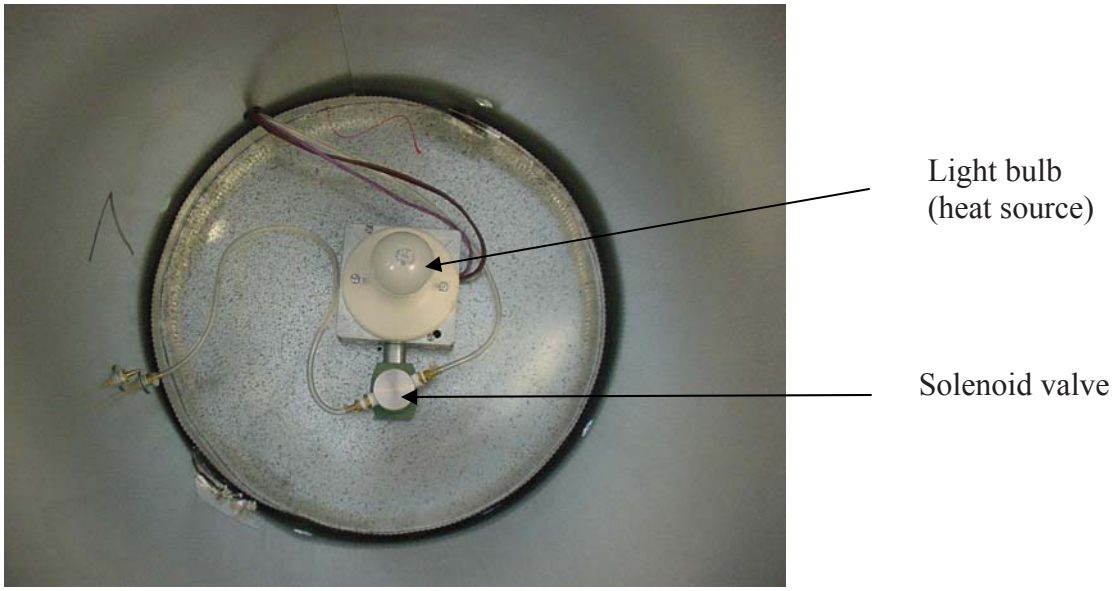

Figure 2.5 Inside of a Tin Man

Figure 2.6 Wall Mounted CO2 Sensor

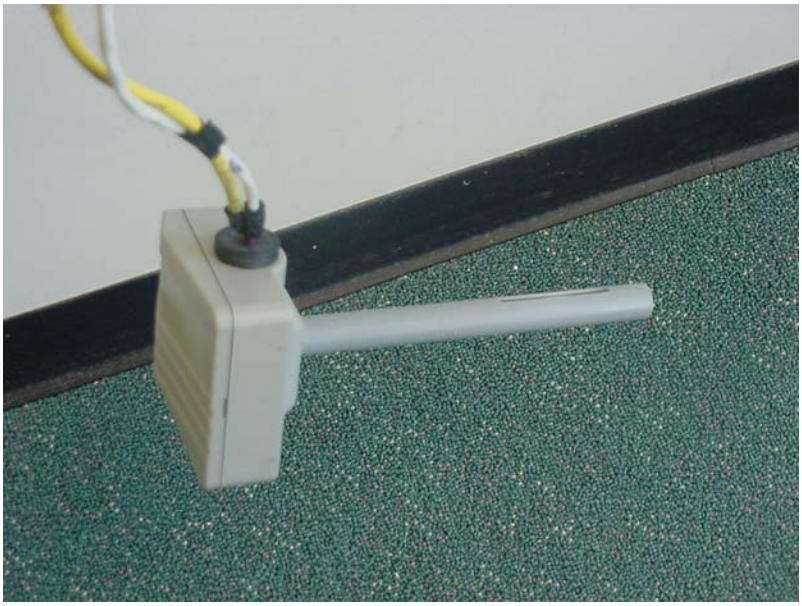

Figure 2.7 Duct Mounted CO2 Sensor

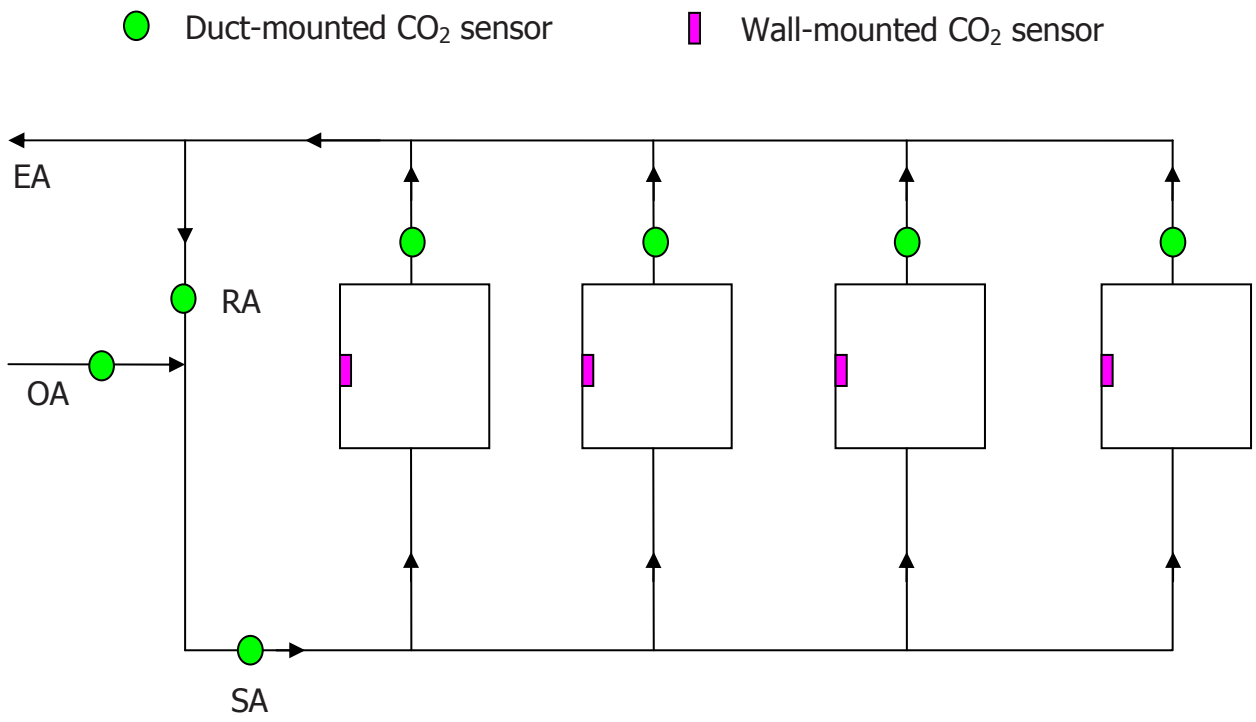

Figure 2.8 Location of CO_2 Sensors

CHAPTER 3 IAQ MODELS

3.1 General Models

The IAQ model was based on a CO_2 mass balance and assumed a uniform concentration throughout the room. Figure 3.1 illustrated the system. The equations for the CO_2 concentrations in the rooms, return air and supply air are derived below.

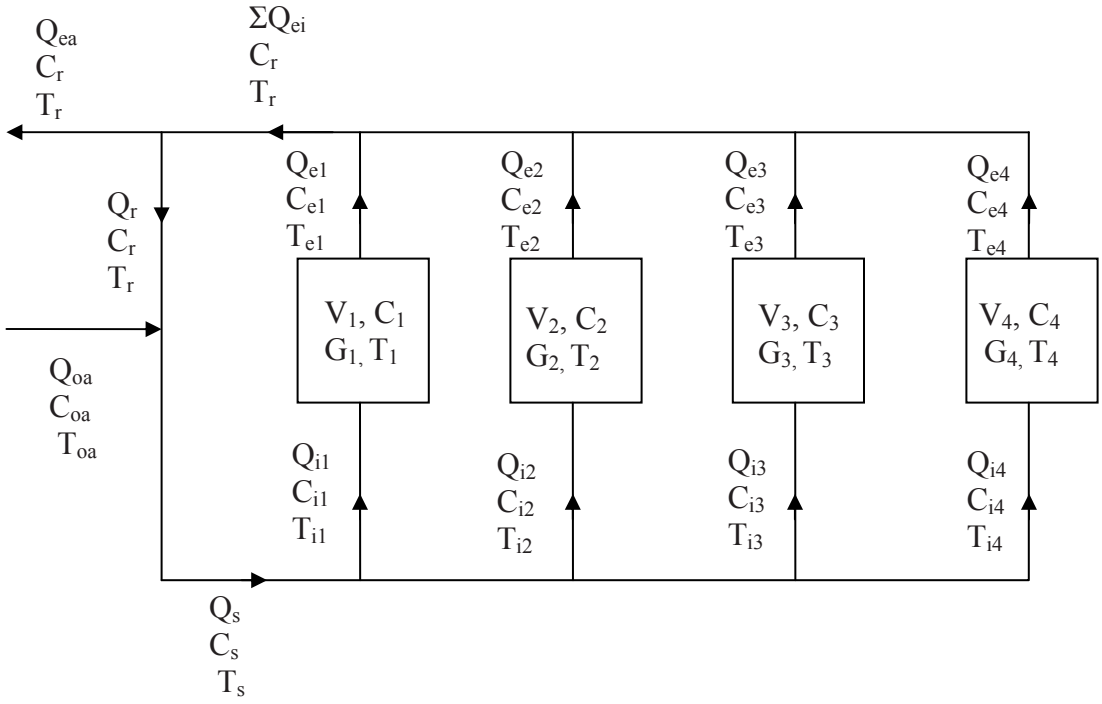

Figure 3.1 Schematic Diagram of the System

3.1.1 Room CO2 Concentration Model

Applying mass conservation of CO_2 to each room, the equation describes CO_2 balance is:

$$V_j \frac{dC_j}{dt} = Q_{ij} C_{ij} - Q_{ej} C_{ej} + G_j \quad (j = 1, 2, 3, 4) \tag{3.1}$$

where

j Room index. 1: East, 2: Interior, 3: West, 4: South

V_j Room Volume

C_j CO_2 concentration in the room

t Time

Q_{ij} Airflow rate into the room

C_{ij} CO_2 concentration of the air entering the room

Q_{ej} Airflow rate out of the room

C_{ej} CO_2 concentration of the air leaving the room

G_j CO_2 generation in the room

The left term in equation 3.1 is the rate of increase of CO_2 in the room. The first term on the right is the CO_2 that enters the room. The second term is the CO_2 that leaves the room. The last term is the CO_2 generation in the room, which is generated by occupancy in this study.

Since Q_{ij} was measured during the experiments, Q_{ei} was expressed by Q_{ij} as shown below. Assuming the mass of outdoor air entering the room is equal to the mass of air leaving the room, then

$$\frac{Q_{ej}}{\nu_{ej}} = \frac{Q_{ij}}{\nu_{ij}} \tag{3.2}$$

where

ν_{ej} the specific volume of air leaving the room

ν_{ij} the specific volume of air entering the room

Assuming the pressure of the outdoor air entering the system and the pressure of the air leaving the system are both equal to the atmosphere pressure P_{atm}, then based on the ideal gas law,

$$\frac{T_{ej}}{T_{ij}} = \frac{\nu_{ej}}{\nu_{ij}} \qquad (3.3)$$

where

T_{ei} the temperature of air leaving the room

T_{ij} the temperature of air entering the room

T_{ej} is equal to T_j which is the room air temperature. T_{ij} is equal to T_s which is the supply air temperature. Then

$$Q_{ej} = \frac{\nu_{ej}}{\nu_{ij}} Q_{ij} = \frac{T_j}{T_s} Q_{ij} \qquad (3.4)$$

C_{ij} is equal to C_s which is the CO_2 concentration of the supply air. C_{ej} is equal to C_j.

Applying these to equation 3.1, then

$$V_j \frac{dC_j}{dt} = Q_{ij} C_s - \frac{T_j}{T_s} Q_{ij} C_j + G_j \qquad (3.5)$$

3.1.2 Return Air CO2 Concentration Model

Applying mass conservation, as shown in Figure 3.1, the return air CO_2 concentration can be calculated by:

$$C_r = \frac{\sum_{j=1}^{4} Q_{ej} C_j}{\sum_{j=1}^{4} Q_{ej}} = \frac{\sum_{j=1}^{4} \frac{T_j}{T_s} Q_{ij} C_j}{\sum_{j=1}^{4} \frac{T_j}{T_s} Q_{ij}} \qquad (3.6)$$

Where

C_r CO_2 concentration of the return air

3.1.3 Supply Air CO_2 Concentration Model

Applying mass conservation, as shown in Figure 3.1, the supply air CO_2 concentration can be calculated by:

$$C_s = \frac{Q_{oa} C_{oa} + (\sum_{j=1}^{4} Q_{ej} - Q_{ea}) C_r}{\sum_{j=1}^{4} Q_{ij}} \qquad (3.7)$$

where

Q_{oa} Airflow rate of the outdoor air

C_{oa} CO_2 concentration of the outdoor air

Q_{ea} Airflow rate of the exit air

Since Q_{oa} was measured during the experiments, Q_{ea} was expressed by Q_{oa} as shown below. Assuming the mass of outdoor air entering the system is equal to the mass of air leaving the system, then

$$\frac{Q_{ea}}{\nu_{ea}} = \frac{Q_{oa}}{\nu_{oa}} \qquad (3.8)$$

where

ν_{ea} the specific volume of air leaving the system

ν_{oa} the specific volume of the outdoor air entering the system

Assuming the pressure of the outdoor air entering the system and the pressure of the air leaving the system are both equal to the atmosphere pressure P_{atm}, then based on the ideal gas law,

$$\frac{T_{ea}}{T_{oa}} = \frac{\nu_{ea}}{\nu_{oa}} \qquad (3.9)$$

where

T_{ea} the temperature of air leaving the system

T_{oa} the temperature of outdoor air entering the system

Then

$$Q_{ea} = \frac{\nu_{ea}}{\nu_{oa}} Q_{oa} = \frac{T_{ea}}{T_{oa}} Q_{oa} \qquad (3.10)$$

Applying this to Equation 3.7, and because T_{ea} is equal to T_r (return air temperature), Equation 3.7 is becomes

$$C_s = \frac{Q_{oa} C_{oa} + (\sum_{j=1}^{4} \frac{T_j}{T_s} Q_{ij} - \frac{T_r}{T_{oa}} Q_{oa}) C_r}{\sum_{j=1}^{4} Q_{ij}} \qquad (3.11)$$

The simulation model was implemented using the software Simulink (2002).

3.2 Leakage Model

Typically HVAC air-side systems are not completely sealed and when the air pressure inside the system differs from the surroundings, leakage occurs. The duct system at the ERS is well sealed, but access doors and duct connections at the air handling unit do allow for air leakage. Since the air handling unit is a "draw thru", the supply air fan pulls air through the unit thus creating a negative pressure (relative to the surroundings) inside the unit. Thus a small amount of air from the mechanical room (with ambient levels of CO_2) was assumed to

be drawn into the unit where it would mix with the CO_2 levels in the system. The test rooms used for the research were pressure neutral with respect to the rest of the building. This was accomplished using a commercial pressure control system which adjusted the return air damper for each room to maintain neutral pressure. Each test room door was equipped with door seals to insure minimal air transfer between the test rooms and the rest of the building. Figure 3.2 provides an indication of relative air pressure between the system and the surroundings.

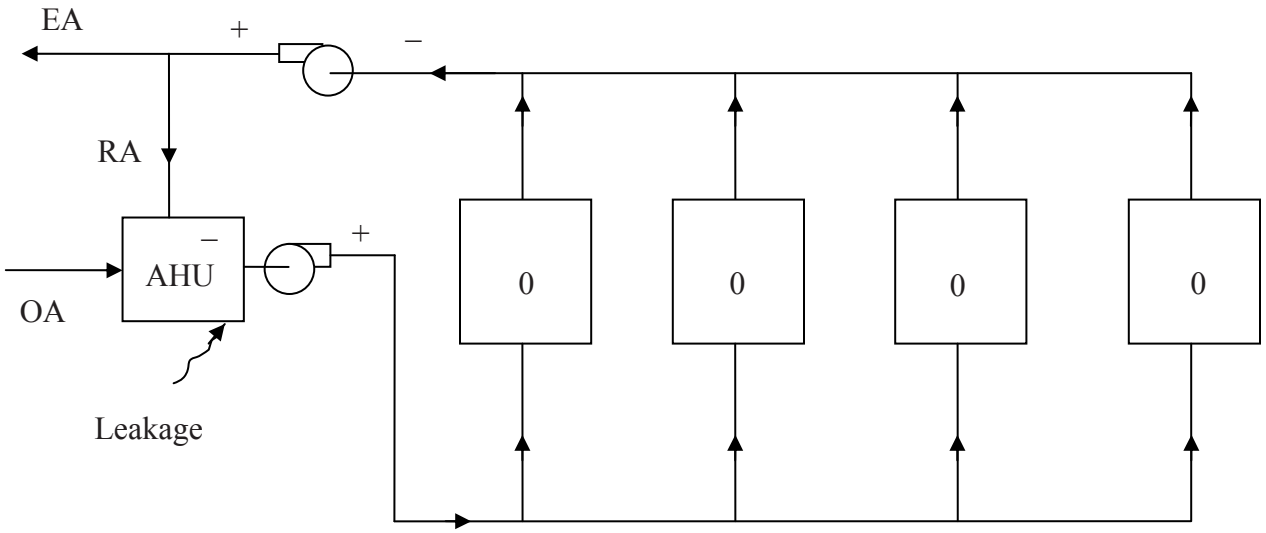

Figure 3.2 Relative Air System Pressures

The air leakage into the system was modeled as shown in Figure 3.3. Since the CO2 concentration for the air in the mechanical room (source of leakage air) was essentially the same as the outdoor air, the total outdoor airflow rate, Q_{oa} , is given by Equation (3.12).

$$Q_{oa} = Q_{DCV} + Q_{leakage} \qquad (3.12)$$

Where

Q_{DCV} Outdoor airflow rate required for ventilation

$Q_{leakage}$ Airflow rate caused by leakage into the AHU

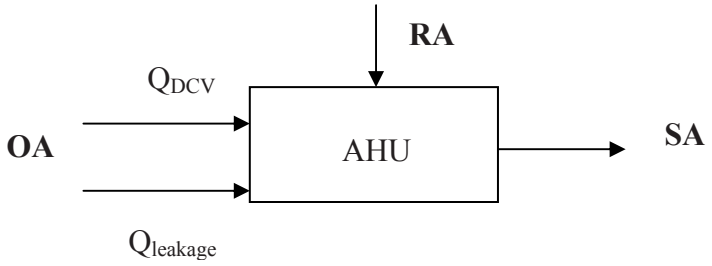

Figure 3.3 Air Leakage Model

CHAPTER 4 IAQ MODEL VALIDATION

4.1 Introduction

Experiments were performed at ERS in order to validate the IAQ model. The results of IAQ model and experiment were compared and are presented in this chapter. The experiments were performed from March 23 to March 25, 2005. During the tests, the air temperature in each test room was maintained at 72 ^{o}F. On March 23rd, the weather was mostly sunny with outdoor air temperature ranging from about 32 ^{o}F to 52 ^{o}F. The following two days were mostly cloudy with the outdoor air temperature varying from 33 ^{o}F to 38 ^{o}F. Figure 4.1 shows the air temperature in the test rooms as well as the outdoor air temperature during the tests. Figure 4.2 shows the solar irradiation (direct normal and total horizontal) during the tests. As seen in the figure, March 23rd was a mostly sunny day with intermittent cloud cover. March 24th and 25th were overcast with little direct solar irradiation.

The supply airflow rate to each test room is shown in Figure 4.3. The system type used during this test was variable air volume with terminal reheat. For this system type, the supply airflow increases as the cooling load on the room increases. In the heating mode, the supply airflow rate is set to a minimum and the supply air is heated using electric heating coils in the variable air volume terminal units. The effects of solar irradiation on March 23rd can be seen on the test room airflow rate by examining the room airflow plots in Figure 4.3.

The concentration of CO_2 in the outdoor air is not constant, but varies based on atmospheric conditions and local production and consumption of CO_2. Figure 4.4 shows the concentration of CO_2 in the outdoor air during the three days of testing.

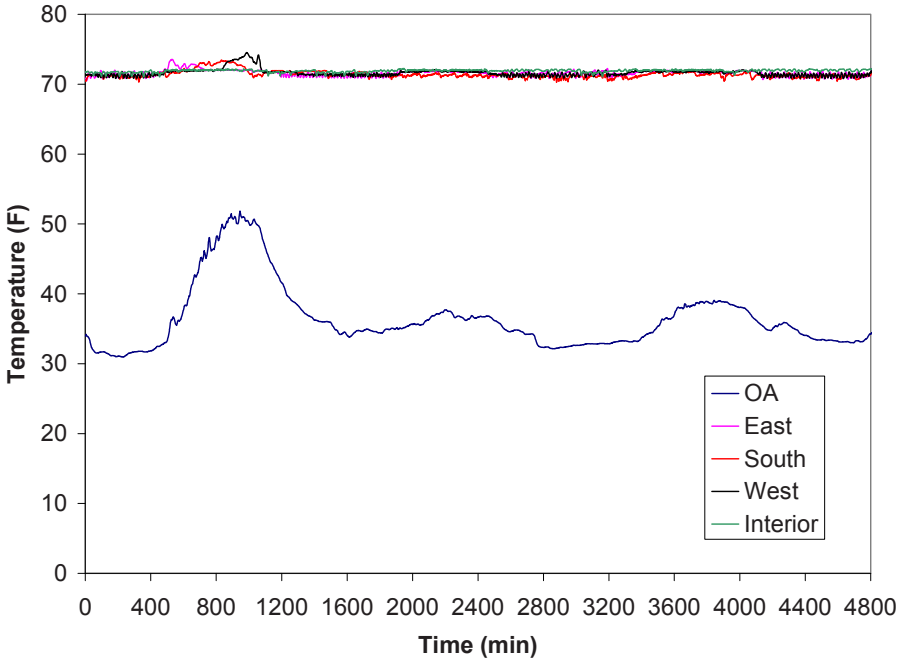

Figure 4.1 Test Room and Outdoor Air Temperatures

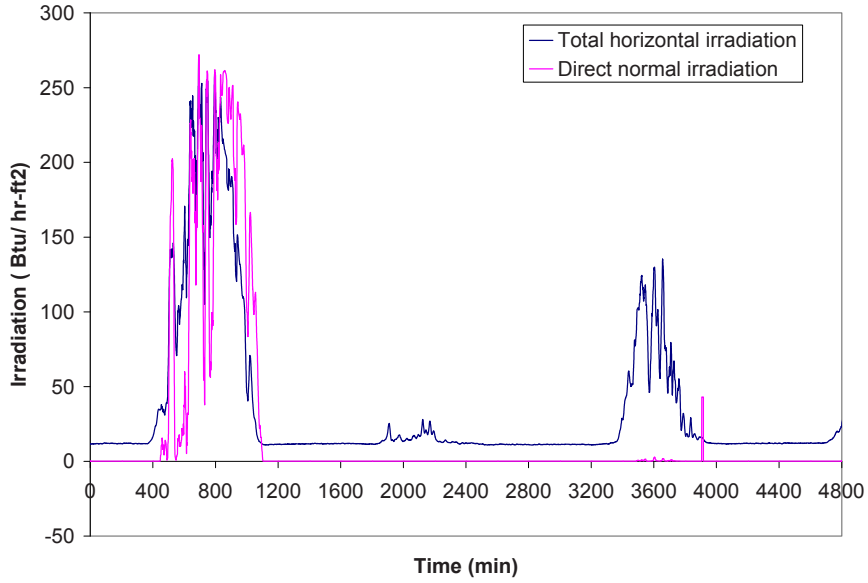

Figure 4.2 Solar Irradiation

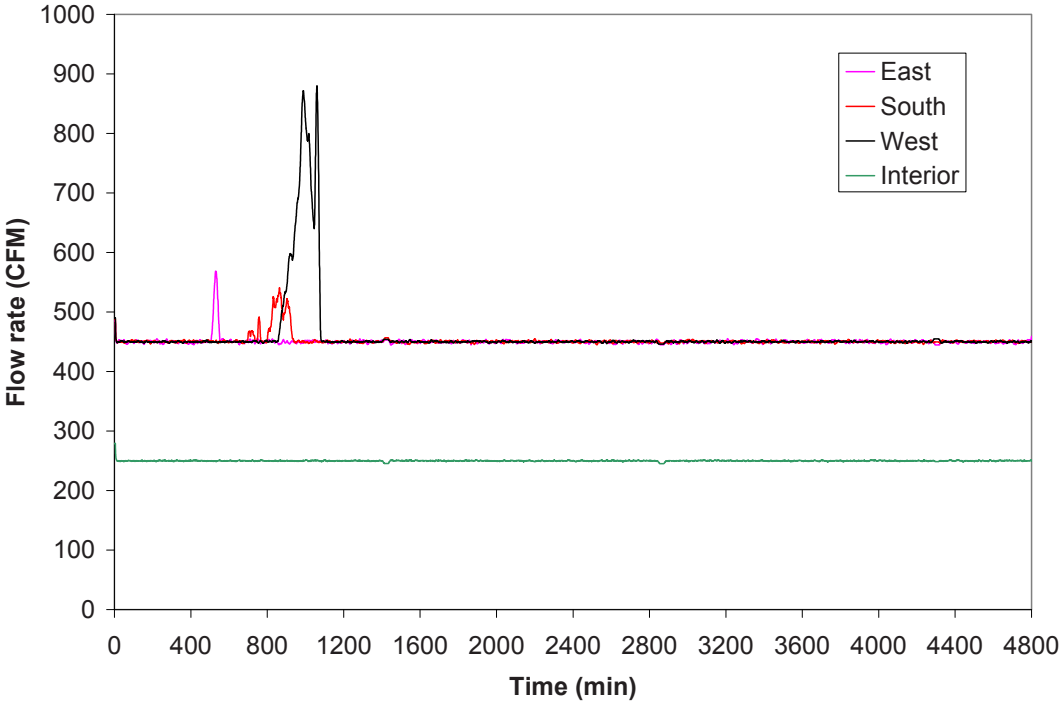

Figure 4.3 Supply Airflow Rate to Each Room

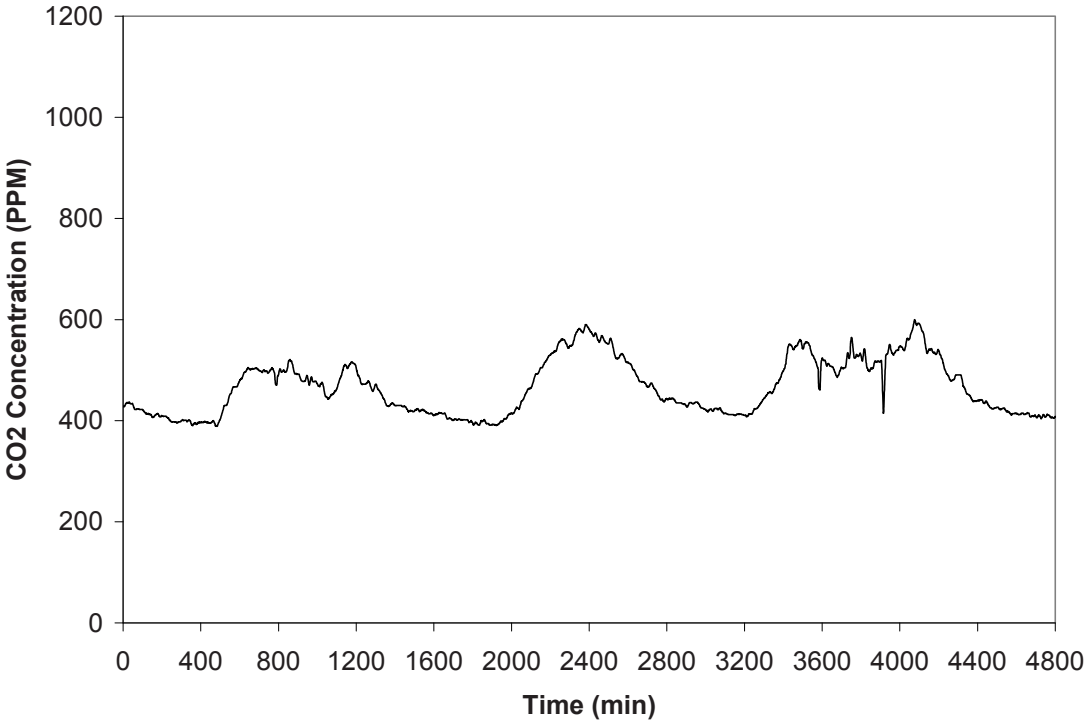

Figure 4.4 Outdoor Air CO_2 Concentration

Three different occupancy schedules were used for the ventilation model verification tests. Occupants were simulated for the East and West test rooms while the Interior and South test room were unoccupied. Figure 4.5 illustrates the occupancy schedule for the East and West rooms. For the first day, four occupants in each room were present for a full eight hours. For the second day, the number of occupants increased by one each hour during the morning then decreased by one each hour during the afternoon. On the third day, a stepped increase of occupants occurred during the morning with all occupants leaving the space at one time. This was repeated during the afternoon.

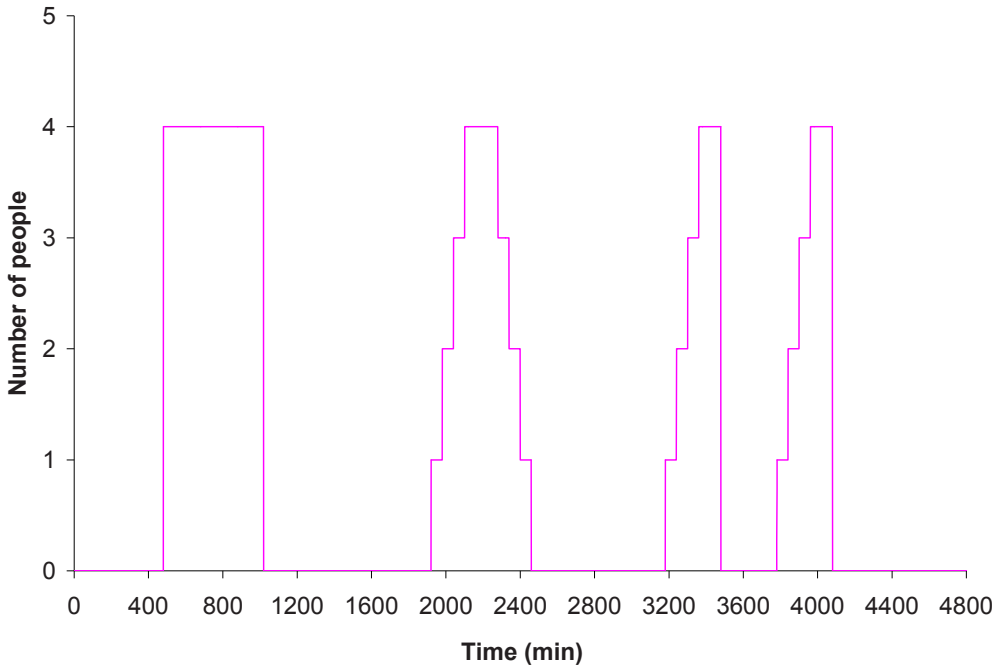

Figure 4.5 Occupancy Schedule

For each level of occupancy, the ventilation airflow rate was calculated based on ASHRAE Standard 62.1 (2004). Table 4.1 summarizes the parameters used to calculate the outdoor air ventilation airflow rate required for different levels of occupancy within the building.

Table 4.1 Outdoor airflow rate under different occupancy conditions.

Case	Room	Rp	Pz	Ra	Az	V_{ot}
1	I	5	0	0.06	267	65
	E	5	0	0.06	267	
	S	5	0	0.06	267	
	W	5	0	0.06	267	
2	I	5	0	0.06	267	75
	E	5	1	0.06	267	
	S	5	0	0.06	267	
	W	5	1	0.06	267	
3	I	5	0	0.06	267	85
	E	5	2	0.06	267	
	S	5	0	0.06	267	
	W	5	2	0.06	267	
4	I	5	0	0.06	267	95
	E	5	3	0.06	267	
	S	5	0	0.06	267	
	W	5	3	0.06	267	
5	I	5	0	0.06	267	105
	E	5	4	0.06	267	
	S	5	0	0.06	267	
	W	5	4	0.06	267	

where:

Rp: outdoor airflow rate required per person, ft^3/min.

Pz: the largest number of people expected to occupy the zone during typical usage.

Ra: outdoor airflow rate required per unit area, ft^3/min per ft^2

Az: zone flow area, ft^2

V_{ot}: design outdoor airflow rate, ft^3/min.

The control system on the air handling unit provided the capability of holding the outdoor airflow rate to a desired set point value. The set point values were varied based on the ventilation demand as calculated using the ASHRAE standard. Figure 4.6 shows the outdoor airflow set point and corresponding outdoor airflow rate (Q_{DCV}) measured during the tests. The leakage was assumed to be 150 ft^3/min based on tuning the ventilation model.

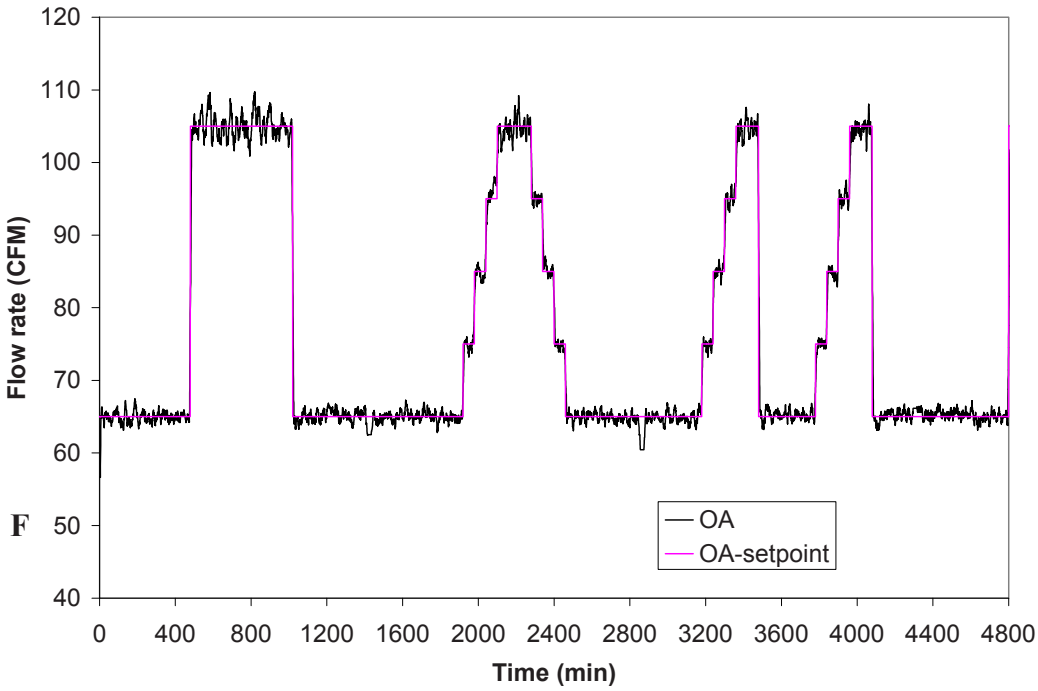

F

i

Figure 4.6 Outside Airflow Rate

4.2 Experimental and Simulation Results

Figures 4.7-4.12 show the measured CO_2 concentrations along with the CO_2 concentrations computed for each test room as well as the return-air and supply-air duct systems. For each test room, the CO_2 concentration is measured by a wall mounted sensor and a duct mounted sensor located in the return air duct.

Figure 4.7 and 4.8 show the CO_2 concentrations in the West and East rooms, respectively. The influence of the occupants is readily seen in the concentration levels. In most cases the simulation results compare more favorably with the CO_2 concentrations measured by the return duct sensors rather then the wall mounted sensors.

Figures 4.9 and 4.10 show the CO_2 concentrations in the South and Interior rooms, respectively. Even though there are no occupants in these rooms, the CO_2 concentrations are seen to follow the concentration pattern of the occupied rooms; although, with lower levels of concentration. This is a result of the re-circulation of air from all rooms back into the supply air system.

Figures 4.11 and 4.12 show the CO_2 concentrations in the return-air duct and supply-air duct (after the supply air fan), respectively. While the results for the return-air duct compare favorably, the peak concentrations in the supply air duct show some differences of approximately 100 ppm.

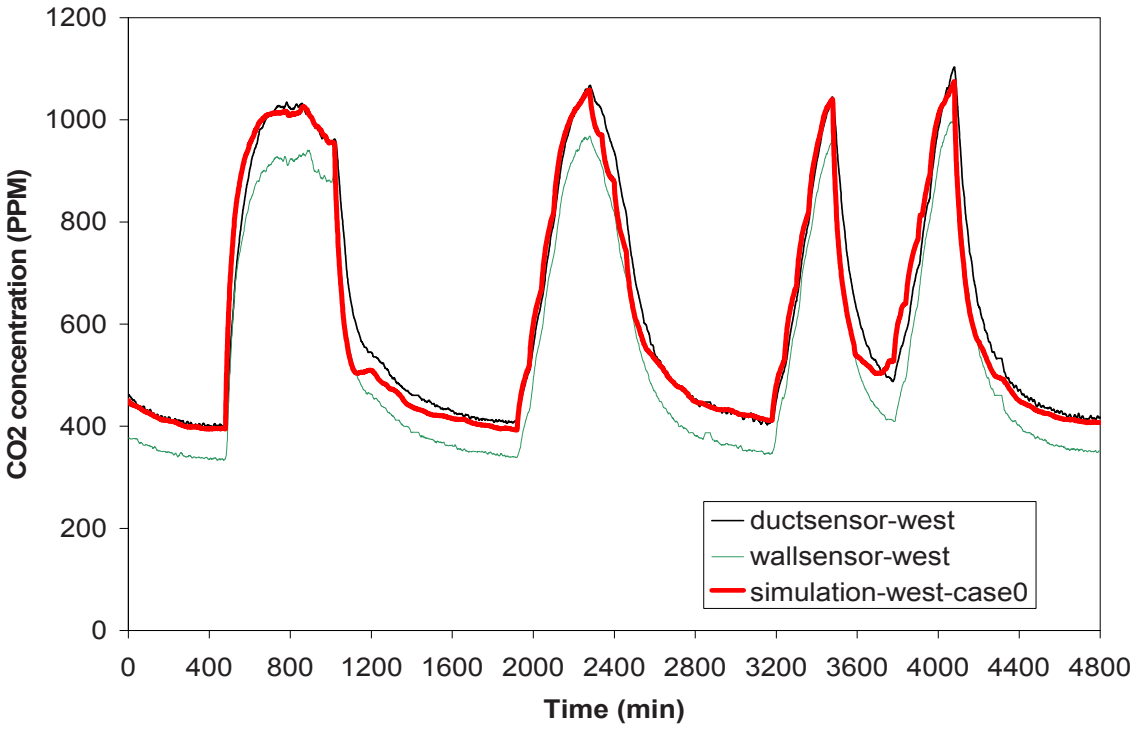

Figure 4.7 CO_2 Concentration in West Room

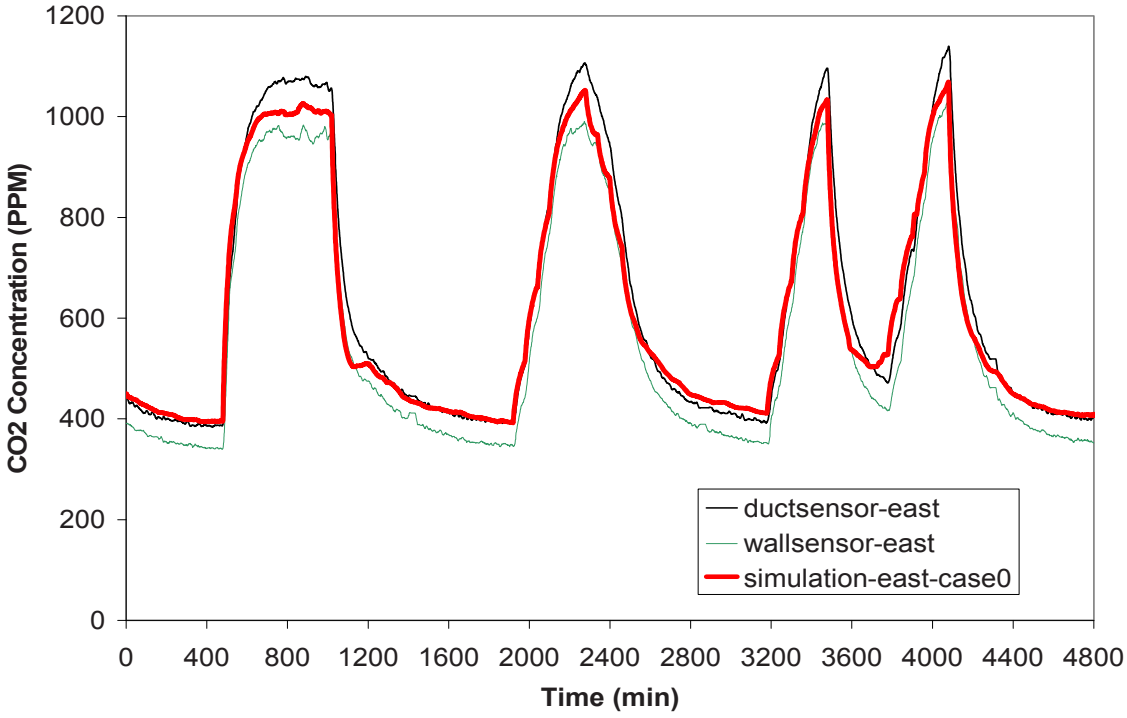

Figure 4.8 CO_2 Concentration in East Room

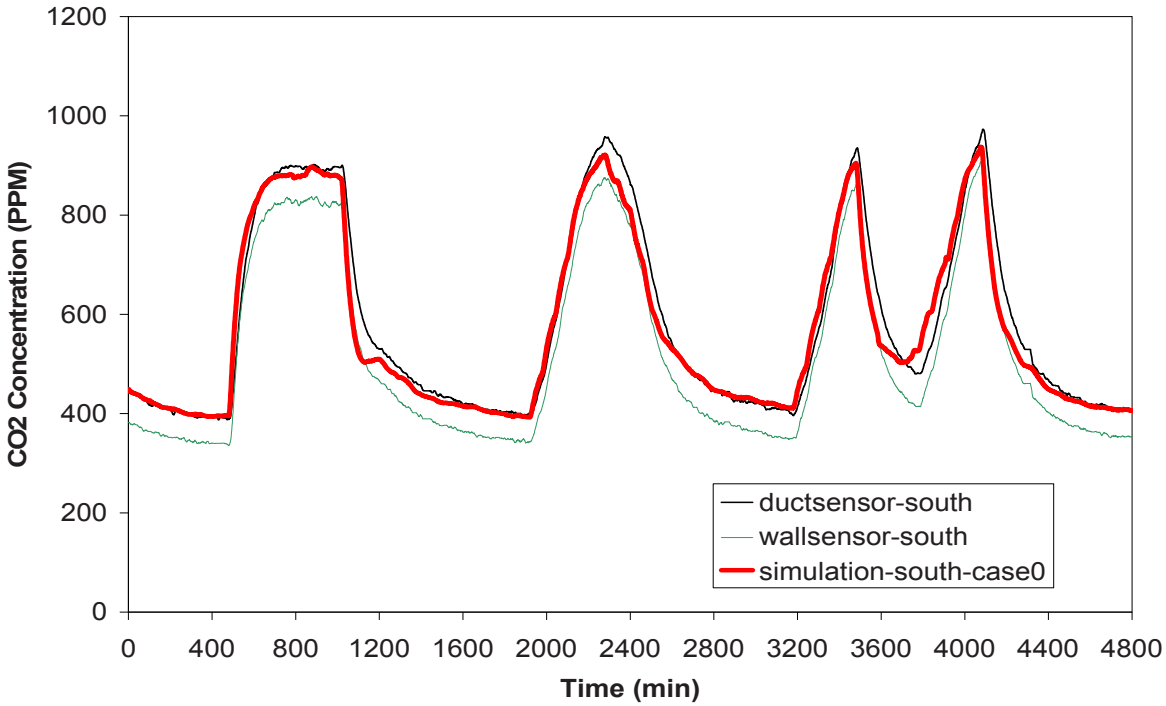

Figure 4.9 CO_2 Concentration in South Room

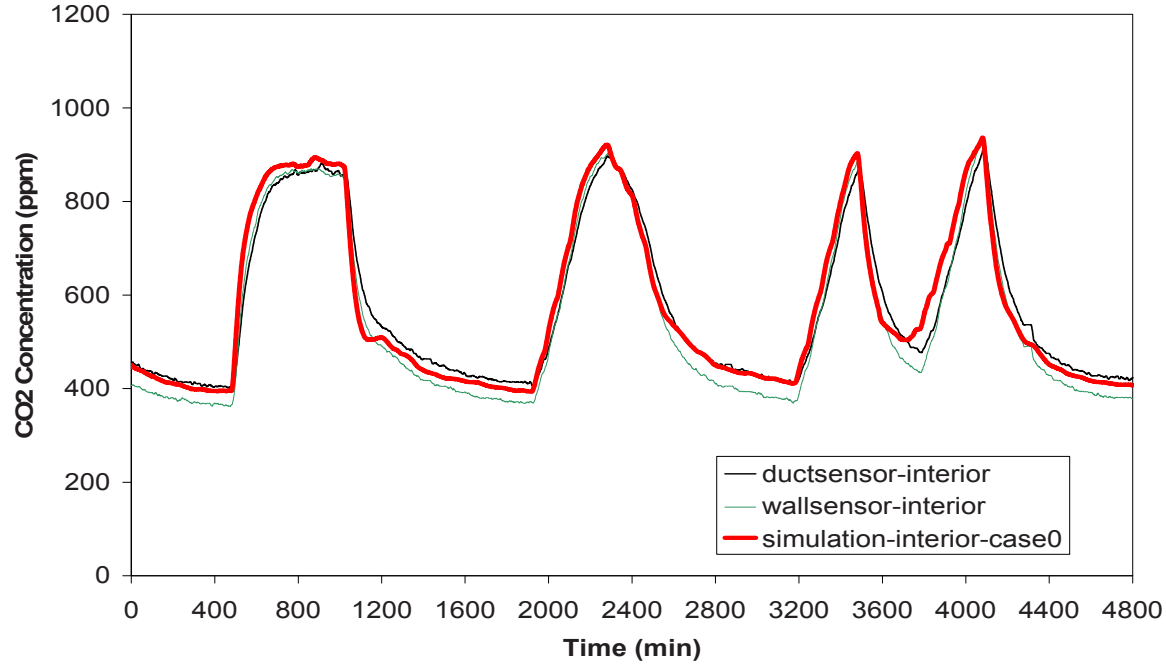

Figure 4.10 CO_2 Concentration in Interior Room

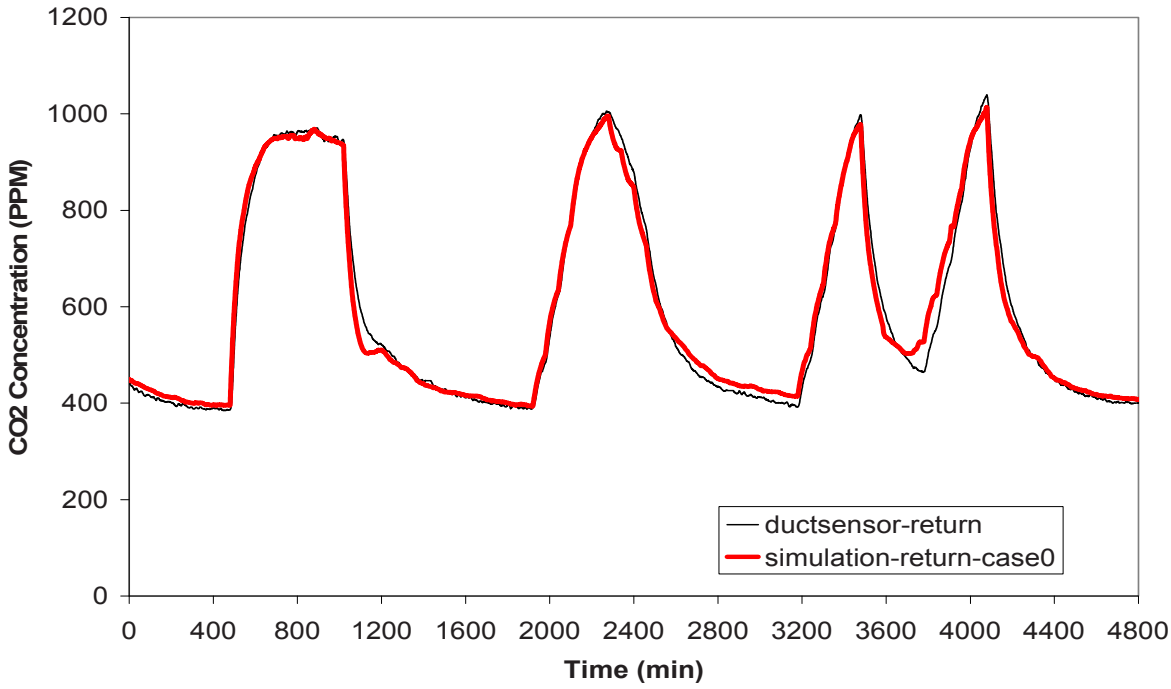

Figure 4.11 CO_2 Concentration in Return Air

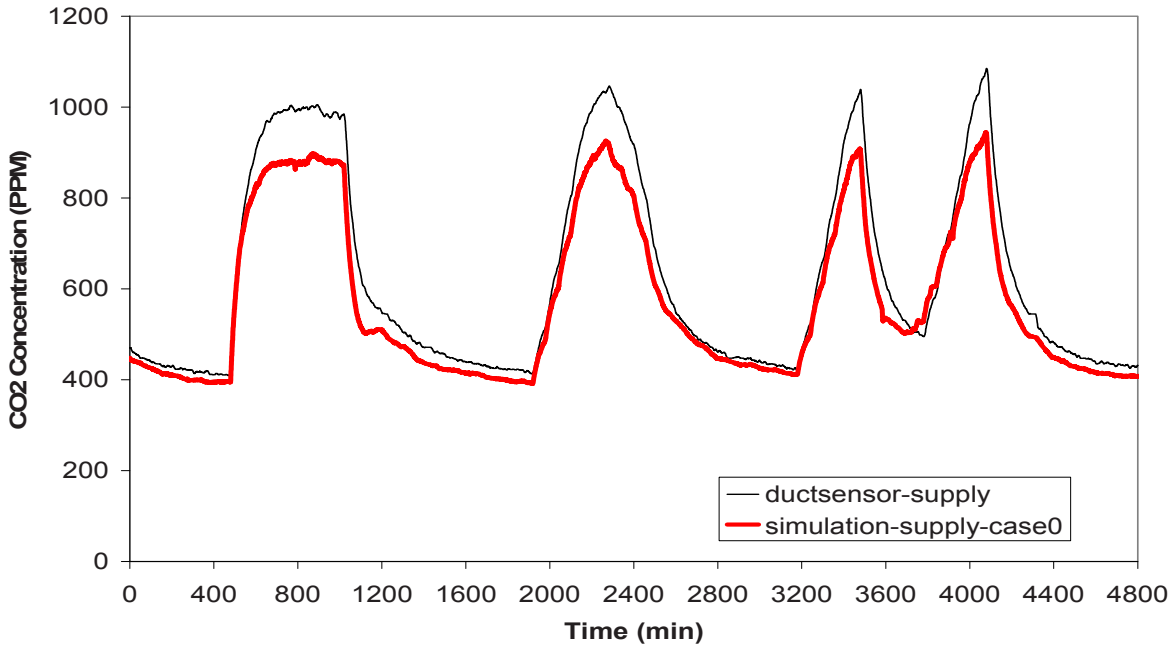

Figure 4.12 CO_2 Concentration in Supply Air

4.3 Error analysis

Since the input file to the simulation model included the outdoor air CO_2 concentration, CO_2 generation rate in the room, outdoor airflow rate and supply airflow rate to each room, their effects on the simulation results were studied one by one. Table 4.2 lists the different cases and the parameter value used. The symbol "-" means that the parameter value was the same as that in Case 0. Case 0 represents the base case for which the results have already been shown in Figures 4.7 through 4.12.

In Cases 1 and 2, the effect of outdoor air CO_2 concentration was studied. In Case 1, the outdoor air CO_2 concentration was the value used in Case 0 plus the uncertainty of outdoor air CO_2 sensor, which was 50 ppm. In Case 2, the outdoor air concentration was the value used in Case 0 minus the uncertainty of outdoor air CO_2 sensor. When the outdoor air CO_2 concentration increased or decreased, the CO_2 concentration in each room increased or decreased accordingly. The maximum difference of Case 1 and Case 2 compared with Case 0 was about +50 ppm and -50 ppm, respectively. As an example, Figure 4.13 shows the results of Case 1 and 2 compared with Case 0 for the West room. Table 4.3 lists the maximum variation of CO_2 concentrations in each case.

In Cases 3 and 4, the effect of CO_2 generation rate was studied. In Case 3, the CO_2 generation rate was the value used in Case 0 which was 0.014 CFM per flow meter plus the uncertainty which was 0.00115 CFM per flow meter. In Case 4, the CO_2 generation rate was the value used in Case 0 minus the error bar of the flow meters. When the CO_2 generation rate increased or decreased, the CO_2 concentration in each room increased or decreased accordingly. The maximum difference of Case 3 and Case 4 compared with Case 0 was about 50 ppm and -50 ppm, respectively. Figure 4.14 shows the results of Case 3 and 4 compared with Case 0 in the West room.

In Cases 5 and 6, the effect of outdoor airflow rate was studied. Based on the information from ERS, the uncertainty of the flow rate was within 5%. In Case 5, the

outdoor airflow rate was 1.05 the value used in Case 0. In Case 6, the outdoor airflow rate was 0.95 the value used in Case 0. When the outdoor airflow rate increased or decreased, the CO_2 concentration in each room decreased or increased accordingly. The maximum difference of Case 5 and Case 6 compared with Case 0 was about -10 ppm and 10 ppm, respectively. Figure 4.15 shows the results of Case 5 and 6 compared with Case 0 in the West room.

In Cases 7 and 8, the effect of west room flow rate was studied. In Case 7, the flow rate entering the west room was 1.05 the value used in Case 0. In Case 8, the flow rate was 0.95 the value used in Case 0. The maximum difference of Case 7 and Case 8 compared with Case 0 in the West room was about -6 ppm and 6 ppm, respectively. There were nearly no change of CO_2 concentration in other places. Figure 4.16 shows the results of Case 7 and 8 compared with Case 0 in the West room.

In Cases 9 and 10, the effect of the East room flow rate was studied. In Case 9, the flow rate entering the East room was 1.05 the value used in Case 0. In Case 10, the flow rate was 0.95 the value used in Case 0. The maximum difference of Case 9 and Case 10 compared with Case 0 in the East room was about -6 ppm and 6 ppm, respectively. There were nearly no change of CO_2 concentration in other places. Figures 4.17 shows the results of Case 9 and 10 compared with Case 0 in the East room.

In Cases 11 and 12, the effect of the South room flow rate was studied. In Case 11, the flow rate entering the south room was 1.05 the value used in Case 0. In Case 12, the flow rate was 0.95 the value used in Case 0. The maximum difference of Case 11 and Case 12 compared with Case 0 in the South room was about 2 ppm and -2 ppm, respectively. The maximum difference of Case 11 and Case 12 compared with Case 0 in other places was about 1 ppm and -1 ppm, respectively. Figure 4.18 shows the results of Case 11 and 12 compared with Case 0 in the South room.

In Cases 13 and 14, the effect of the Interior room flow rate was studied. In Case 13, the flow rate entering the Interior room was 1.05 the value used in Case 0. In Case 14, the flow rate was 0.95 the value used in Case 0. The maximum difference of Case 13 and Case 14 compared with Case 0 in the Interior room was about 3 ppm and -3 ppm, respectively. The maximum difference of Case 13 and Case 14 compared with Case 0 in other places was about 1 ppm and -1 ppm, respectively. Figure 4.19 shows the results of Case 13 and 14 compared with Case 0 in the Interior room.

In Case 15 and 16, the combination effect of factors considered above was studied. Since the uncertainty of flow rate to each room affected the simulation results very little, their effect was ignored. In Case 15, the outdoor air CO_2 concentration was the value used in Case 0 plus the uncertainty of outdoor air CO_2 sensor. The CO_2 generation rate was the value used in Case 0 plus the uncertainty of the flow meters. The outdoor airflow rate was 0.95 the value used in Case 0. In Case 16, the outdoor air CO_2 concentration was the value used in Case 0 minus the uncertainty of outdoor air CO_2 sensor. The CO_2 generation rate was the value used in Case 0 minus the uncertainty of the flow meters. The outdoor airflow rate was 1.05 the value used in Case 0. In Case 15, the CO_2 concentration in each room increased compared with Case 0. In Case 16, the CO_2 concentration in each room decreased compared with Case 0. The maximum difference of Case 15 and Case 16 compared with Case 0 was about 110 ppm and -110 ppm, respectively. Figure 4.20 shows the results of Case 15 and 16 compared with Case 0 in the West room.

Now, re-examine Figures 4.7 – 4.12. Considering the error band of the sensor, it is seen that the simulation results agree with experimental results. As an example, Figure 4.21 shows the results of CO2 concentration in supply air. The wide black line shows the readings of sensor. The two thin black lines above and below it shows its error band. The wide red line shows the simulation. The two thin red lines above and below it shows its error band.

Table 4.2 Simulation cases

Case	OA CO_2 Concentration (PPM)	CO_2 gas generation/ flow meter (CFM)	OA flow rate (CFM)	West room flow rate (CFM)	East room flow rate (CFM)	South room flow rate (CFM)	Interior room flow rate (CFM)
0	$(OACO2)_0$	$(CO2gen)_0$	$(OACFM)_0$	$(WCFM)_0$	$(ECFM)_0$	$(SCFM)_0$	$ICFM)_0$
1	$(OACO2)_0$ + 50	-	-	-	-	-	-
2	$(OACO2)_0$ - 50	-	-	-	-	-	-
3	-	$(CO2gen)_0$ + 0.00116	-	-	-	-	-
4	-	$(CO2gen)_0$ - 0.00116	-	-	-	-	-
5	-	-	$(OACFM)_0$ X 1.05	-	-	-	-
6	-	-	$(OACFM)_0$ X 0.95	-	-	-	-
7	-	-	-	$(WCFM)_0$ X 1.05	-	-	-
8	-	-	-	$(WCFM)_0$ X 0.95	-	-	-
9	-	-	-	-	$(ECFM)_0$ X 1.05	-	-
10	-	-	-	-	$(ECFM)_0$ X 0.95	-	-
11	-	-	-	-	-	$(SCFM)_0$ X 1.05	-
12	-	-	-	-	-	$(SCFM)_0$ X 0.95	-
13	-	-	-	-	-	-	$(ICFM)_0$ X 1.05
14	-	-	-	-	-	-	$(ICFM)_0$ X 0.95
15	$(OACO_2)_0$ + 50	$(CO_2gen)_0$ + 0.00116	$(OACFM)_0$ X 0.95	-	-	-	-
16	$(OACO_2)_0$ - 50	$(CO_2gen)_0$ - 0.00116	$(OACFM)_0$ X 1.05	-	-	-	-

Table 4.3 Maximum variation of CO_2 concentrations (ppm)

Case	West room	South room	East room	Interior room	Supply air	Return air
1&2	50/-50	50/-50	50/-50	50/-50	50/-50	50/-50
3&4	55/-55	41/-41	53/-53	41/-41	41/-41	47/-47
5&6	-9.5/9.9	-9.5/9.8	-9.4/9.8	-9.4/9.8	-9.5/9.9	-9.5/9.9
7&8	-5.6/6.3	-0.07/0.08	-0.07/0.08	-0.06/0.08	-0.10/0.12	-0.60/0.65
9&10	-0.07/0.13	-0.07/0.12	-5.5/6.1	-0.06/0.11	-0.11/0.15	-0.63/0.70
11&12	1.2/-1.2	1.7/-1.8	1.2/-1.2	1.1/-1.2	1.3/-1.3	0.68/-0.72
13&14	0.88/-0.92	0.88/-0.92	0.88/-0.92	2.5/-2.7	0.92/-0.96	0.70/-0.74
15&16	115/-113	102/-99	113/-111	102/-99	102/-99	108/-105

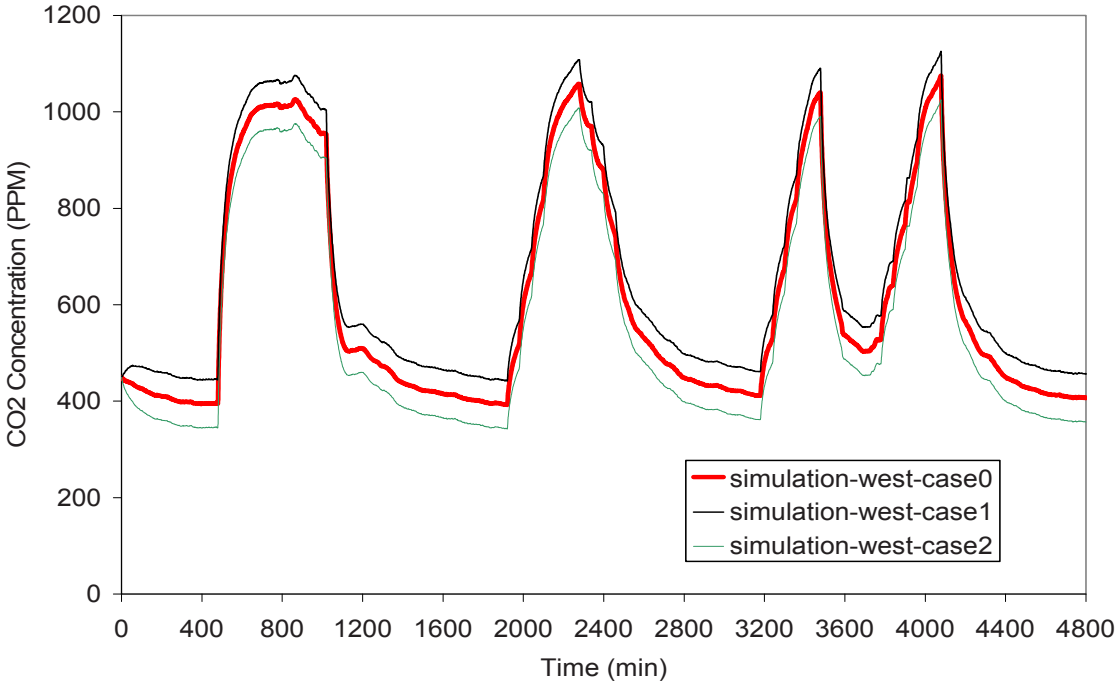

Figure 4.13 Simulation Results of Case 0, 1, and 2 in West Room

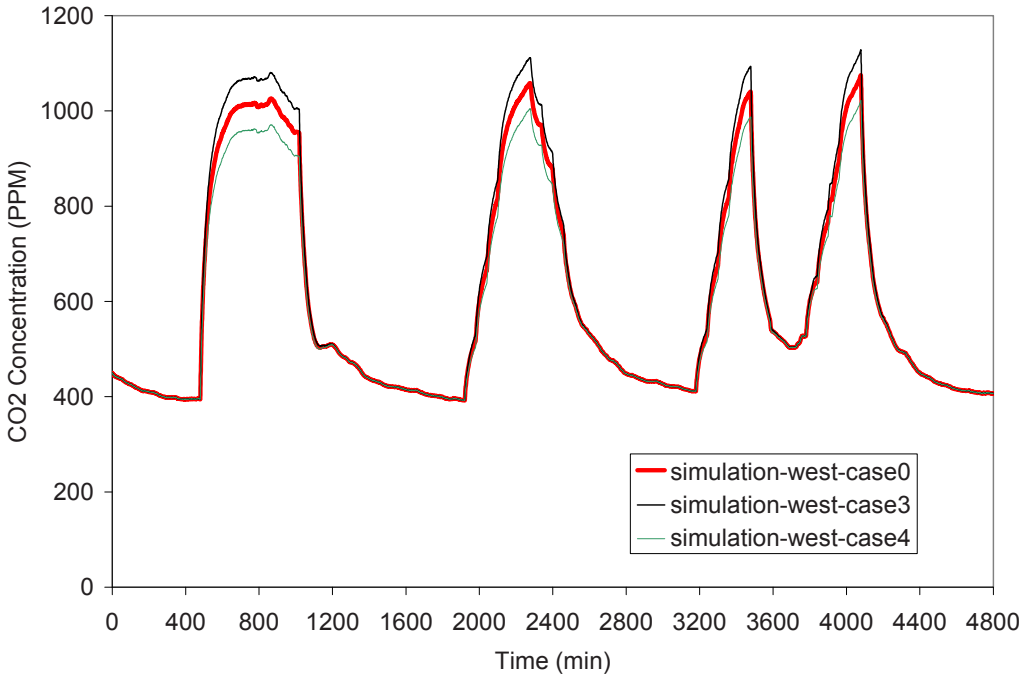

Figure 4.14 Simulation Results of Case 0, 3, and 4 in West Room

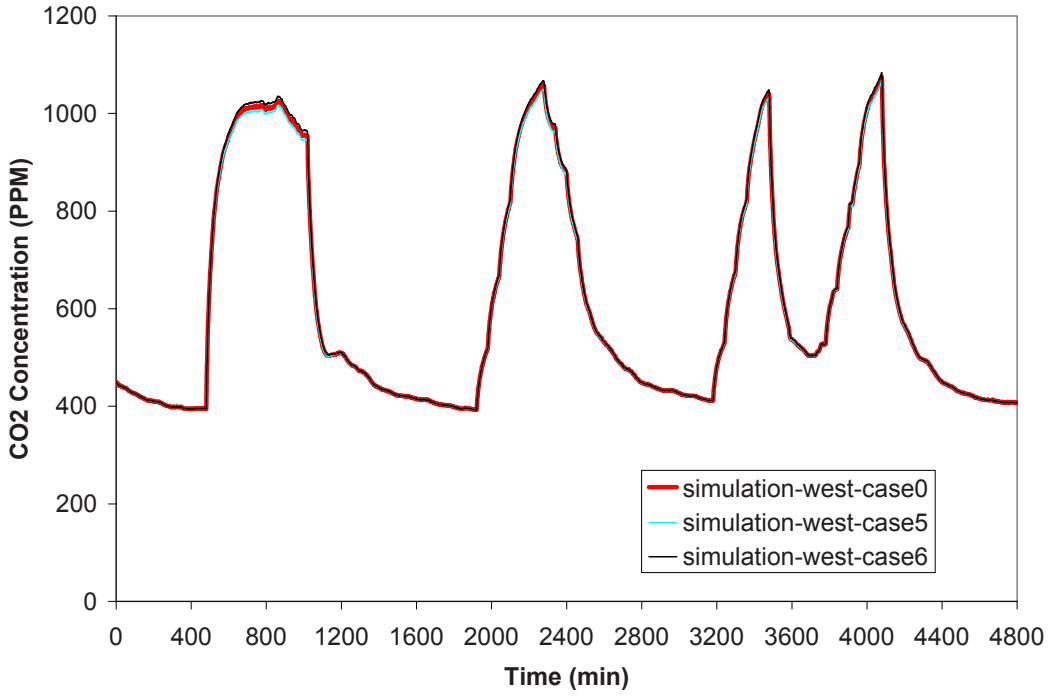

Figure 4.15 Simulation Results of Case 0, 5, and 6 in West Room

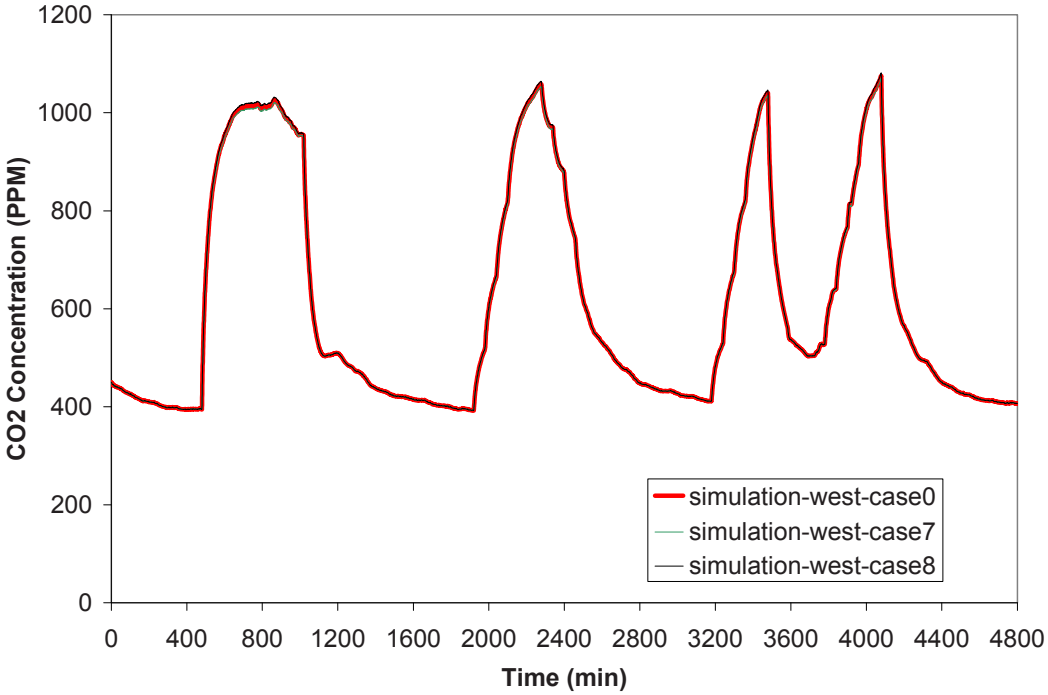

Figure 4.16 Simulation Results of Case 0, 7, and 8 in West Room

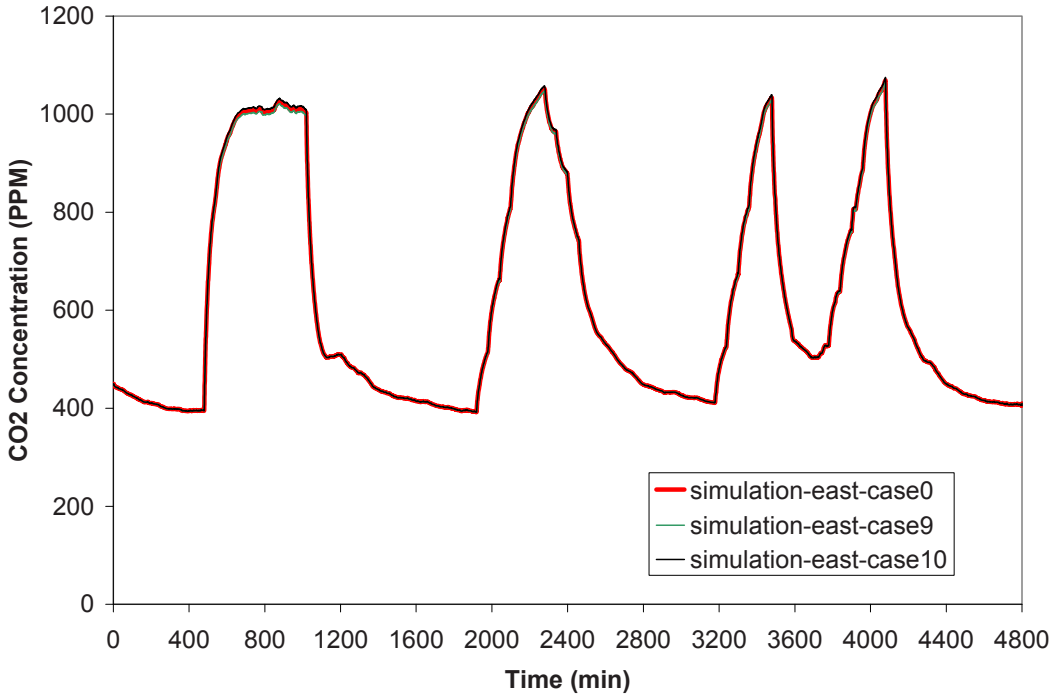

Figure 4.17 Simulation Results of Case 0, 9, and 10 in East Room

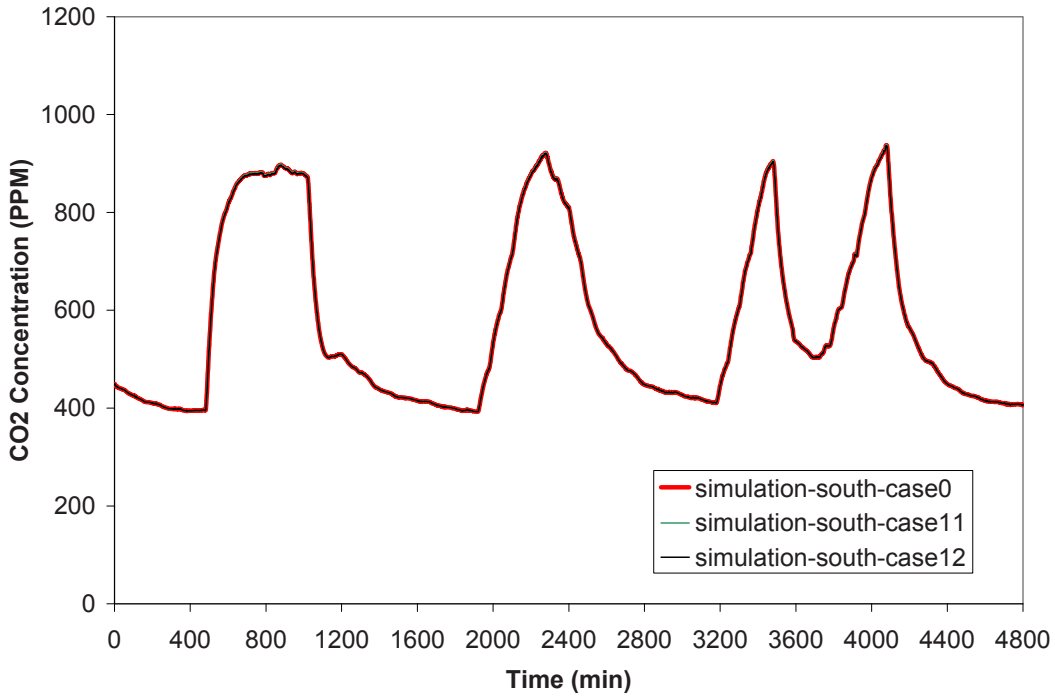

Figure 4.18 Simulation Results of Case 0, 11, and 12 in South Room

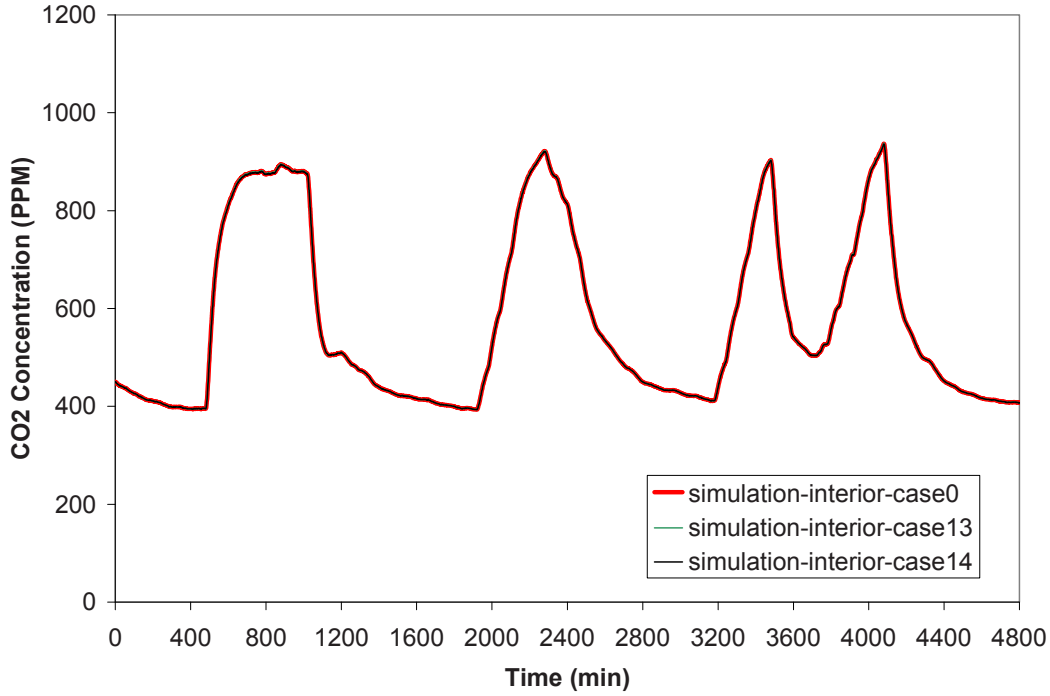

Figure 4.19 Simulation Results of Case 0, 13, and 14 in Interior Room

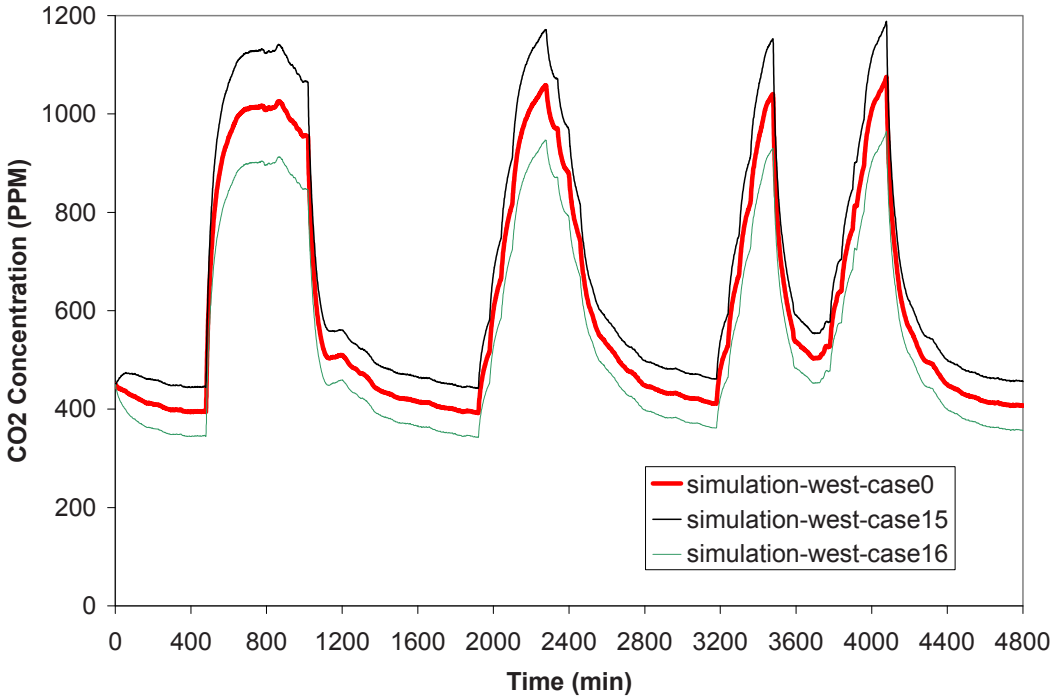

Figure 4.20 Simulation Results of Case 0, 15, and 16 in West Room

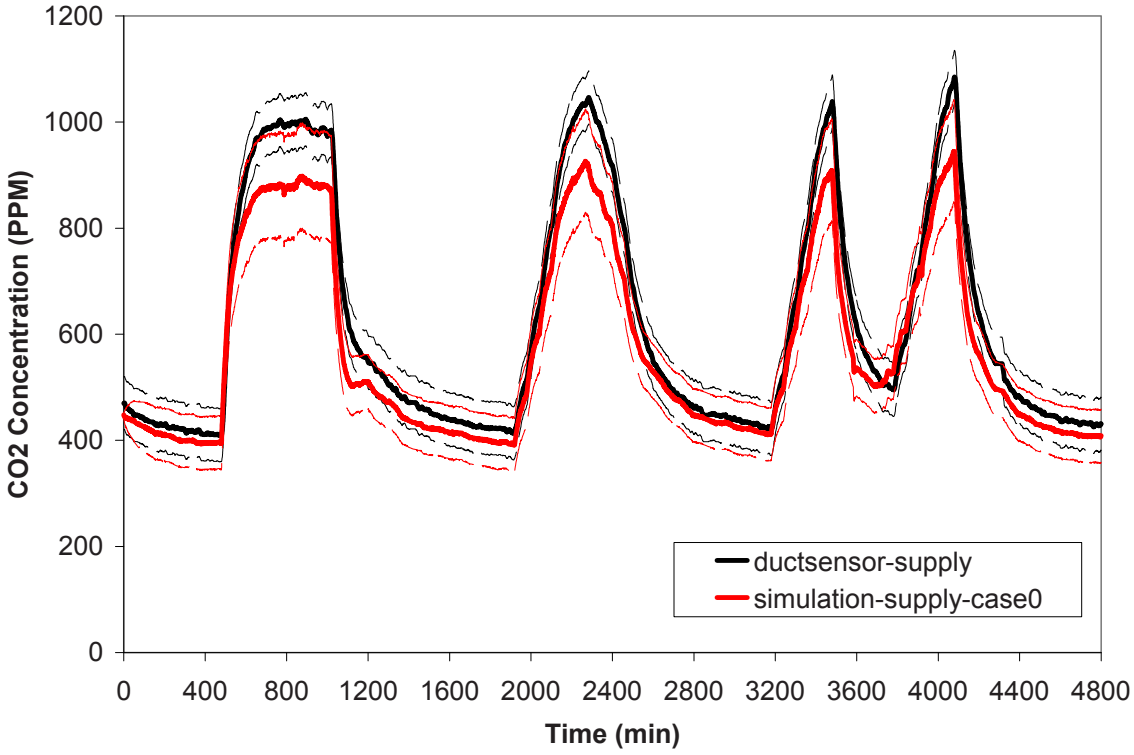

Figure 4.21 Results of CO_2 Concentration in Supply Air Considering Error Band

CHAPTER 5 INTEGRATED IAQ AND ENERGYPLUS MODELS

5.1 Introduction

This Chapter describes how to use IAQ and EnergyPlus models together to compare energy use and indoor CO_2 concentrations when using three different outdoor aid control strategies.

The B Test Rooms in ERS and related HVAC system were modeled using EnergyPlus. This program calculates cooling and heating loads necessary to maintain thermal control set points as well as providing many other simulation details. The important information about the models is introduced in this chapter.

The energy use of an HVAC system includes the energy used by fans, reheat coils, and the chilled water coil in the air handling unit. Since the supply air temperature was set to 60°F, and the room temperatures were set to 72-73°F no matter what outdoor air control strategy was used, with the same weather conditions and indoor loads, three different outdoor air control strategies resulted in the same airflow rate to each room, the same indoor temperatures, and thus the same power consumed by fan and reheat coils. The only energy use difference caused by different outdoor air control strategies was from the energy used to provide cooling water in AHU, which could be represented by cooling load in AHU. So cooling load differences in AHU when using different outdoor air control strategies represented the energy use differences and were compared here.

5.2 EnergyPlus

Figure 5.1 shows the schematic of the system simulated using EnergyPlus. To simplify the model, the fan group just included the supply fan. In a VAV reheat system, the air is cooled by the chilled water coil to the supply air set-point temperature. This air is

supplied to all rooms with a flow rate proportional to the cooling load. When a room has a call for heat, the supply airflow rate is reduced to the minimum setting and an electric heat coil in the terminal unit is energized in response to the heating load.

The main input parameters for the EnergyPlus model are outlined as follows:

Building location and characteristics

The location information of the building is: latitude 41.71 degrees North, longitude 93.61 degrees West, elevation 938 feet, and time-zone 6 which is central time zone in USA. For the details of the geometry and constructions of wall, door, window etc., please see the documents of Lee (1999), Price and Smith (1999).

Weather

EnergyPlus weather file for Des Moines, Iowa was used.

Zone controls

The temperature set points were made for supply air temperature after cooling coil and room temperatures. Based on the regular operations in ERS, their values are:

Supply air temperature: 60F

Heating thermostat set point: 72F

Cooling thermostat set point: 73F

Equipments of HVAC system

The HVAC equipment includes the cooling coil, supply fan, and VAV reheat system.

Internal loads

The internal loads included lights, baseboard heat, and occupancy.

Schedules

The schedules for the HVAC equipment and internal loads are listed in Chapter 6.

The main output parameters of the EnergyPlus model included cooling and heating loads, power of the equipment, weather parameters (including solar irradiation and outdoor temperature), indoor temperatures, and airflow rates.

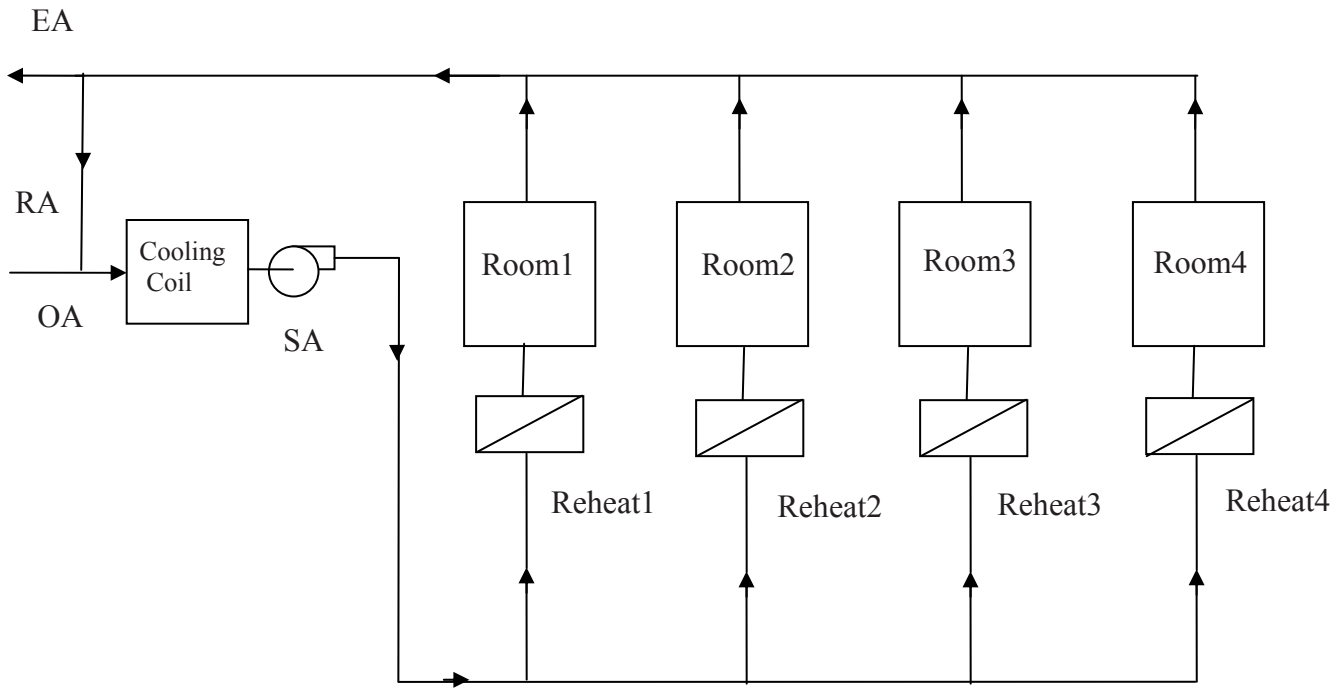

Figure 5.1 Schematic Diagram of EnergyPlus model

5.3 Integrated IAQ and EnergyPlus Models

The way to use IAQ and EnergyPlus models for Occupancy-based DCV and constant outdoor air strategy is a little different from that for CO_2-based DCV. The outdoor airflow rate required by the former two strategies can be calculated by using the Standard 62-2004; however, the IAQ model must be used to determine the outdoor airflow rate needed under CO_2 control.

5.3.1 Simulation Steps for Occupancy-based DCV and constant outdoor air strategy

As illustrated in Figure 5.2 A and Figure 5.2 B, the following steps were used to simulate Occupancy-based DCV or constant control strategy:

1. The outdoor airflow rate required by strategy was calculated based on Standard 62 and used as input to the EnergyPlus model. More details about the calculation are introduced in Chapter 6.
2. Run the EnergyPlus model and get the actual outdoor airflow rate based on both the strategy and economizer operation. The output data also include the airflow rate to each room, the outdoor and indoor temperatures, and the cooling load.
3. Use the actual outdoor airflow rate, the airflow rate to each room, and the outdoor and indoor temperatures as input to the IAQ model. Run the IAQ model and get the indoor CO_2 concentrations.

5.3.2 Simulation Steps for CO_2-based DCV

As illustrated in Figure 5.2 C, the following steps were used to perform simulations when the outdoor air control strategy was CO_2-based DCV:

1. Because three different outdoor air control strategies have the same airflow rate to each room, and the same indoor temperatures, use those values obtained in section 5.3.1 as input to the IAQ mode. Run IAQ model and get the outdoor airflow rate required by CO_2-based DCV. Use this outdoor airflow rate as input to EnergyPlus model.
2. Run the EnergyPlus model and get the actual outdoor airflow rate based on both the strategy and economizer operation, and the cooling load.
3. Use the actual outdoor airflow rate, the airflow rate to each room, and the outdoor and indoor temperatures as input to the IAQ model. Run the IAQ model and get the indoor CO_2 concentrations.

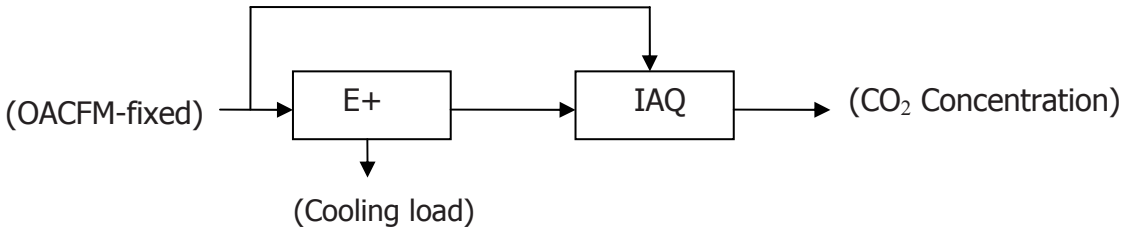

A. Constant OA Flow Rate Strategy

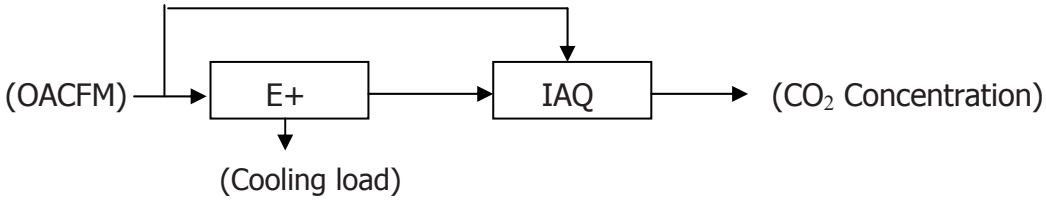

B. Occupancy-based DCV

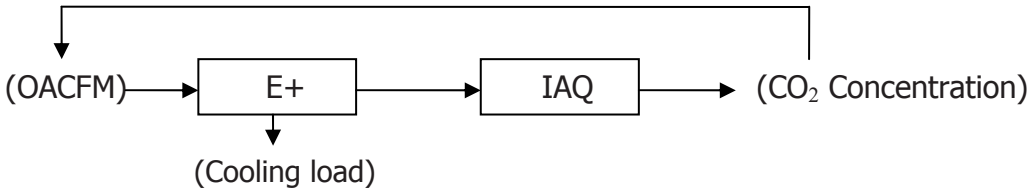

C. CO_2-based DCV

Figure 5.2 EnergyPlus model integrated with IAQ model

CHAPTER 6 RESULTS AND DISCUSSION

6.1 Introduction

In this chapter the results of EnergyPlus and IAQ models are examined. The models simulate the building and HVAC system as shown in Figure 5.1. The summer, winter and transition season cases are studied. In each season case, the models investigate the performance of three ventilation control strategies: (1) constant outdoor airflow rate control, (2) Occupancy-based DCV and (3) CO_2-based DCV.

Each case uses the same people, HVAC equipment, lighting and internal heat generation schedules. Figure 6.1 shows the people schedule. The exterior rooms, namely, the East, West and South rooms are treated as office space, and have the same people schedule. Two people are assumed to occupy each office. The interior room is treated as a meeting room with a maximum occupancy of eight people. The maximum number of people is based on the requirements of office and meeting room in ASHRAE 62.1-2004. Figure 6.1 also shows the outdoor airflow rate required by two ventilation control strategies: Occupancy-based DCV and constant outdoor airflow rate control. In Occupancy-based DCV, the outdoor airflow rate is determined from ASHRAE 62.1-2004. In the plot, it is named as “OA flow rate in Standard”. The maximum occupancy for the building exists when there are two people in each office space and eight people in the conference room. This situation establishes the maximum outdoor airflow rate as determined using ASHRAE 62.1-2004. This value is used in the constant outdoor airflow rate control strategy. This flow rate is referred to as “OA flow rate in Standard Max” in the plot. For clarity, the people schedule and outdoor airflow rate schedule are also listed in Table 6.1. The period between 6am-8am is pre-occupancy ventilation time. That ventilation is mainly to purge the building

before people enter it. The 350 CFM OA flow rate is used here, so after 2 hour purging, the indoor CO_2 concentration is nearly the same as that in the outdoor air.

The HVAC system is turned on from 6am to 7pm. The economizer works when the outdoor air temperature is lower than that of the return air. The lights and baseboard heaters are turned on from 8am to 5pm. The room temperature set point is 72°F-73°F. The supply air temperature after AHU is set to 60°F. The energy of the HVAC system is used in three parts: providing cooling water in AHU, fans, and reheat coils. With the same weather conditions, when using three different OA control strategies, the energy use of fans and reheat coils in each case are the same, because the air temperature before and after the fans and reheat coils, and the flow rate through fans and reheat coils in each case are the same. The only energy use difference in each case is the energy used to provide cooling water, which is reflected by the cooling load of the system. So only cooling load is studied and compared here.

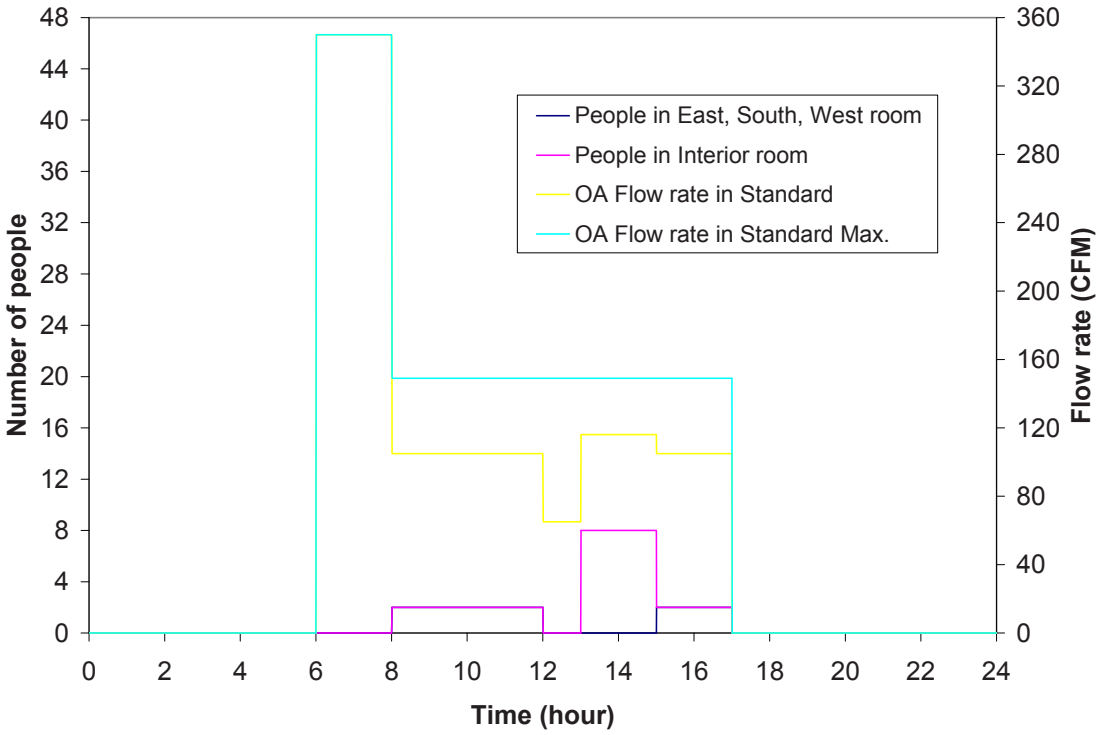

Figure 6.1 People and OA Flow Rate Schedules

Table 6.1 People schedule and OA flow rate schedule.

Time (hr)	People # in Interior room	People # in East, South, and West rooms	OA flow rate in Standard (CFM)	OA flow rate in Standard Max. (CFM)
0:00	0	0	0	0
1:00	0	0	0	0
2:00	0	0	0	0
3:00	0	0	0	0
4:00	0	0	0	0
5:00	0	0	0	0
6:00	0	0	350	350
7:00	0	0	350	350
8:00	2	2	105	149
9:00	2	2	105	149
10:00	2	2	105	149
11:00	2	2	105	149
12:00	0	0	65	149
13:00	8	0	116	149
14:00	8	0	116	149
15:00	2	2	105	149
16:00	2	2	105	149
17:00	0	0	0	0
18:00	0	0	0	0
19:00	0	0	0	0
20:00	0	0	0	0
21:00	0	0	0	0
22:00	0	0	0	0
23:00	0	0	0	0

6.2 Summer Cases (July 1-2)

The summer cases were run from July 1st to 2nd. The purpose of running these cases was to show how different OA control strategies would affect energy use and indoor CO_2 concentration in cooling season.

Figure 6.2 shows the solar irradiation during the two days. Figure 6.3 shows the outdoor air temperature and room temperatures. The HVAC system works from 6am to 7pm. During that period, the room temperatures were controlled between 72°F and 73°F. As shown in Figure 6.2, the sun rose at 5am, accordingly the temperature in the East room increases at that time. Unlike the exterior rooms, the interior room temperature didn't change much when HVAC system was off, because of less heat gain through walls. Figure 6.4 shows the airflow rate to each room. When HVAC system is turned on at 6 am, the temperatures in each exterior room were much higher than the temperature setpoint; therefore, the cooling airflow rate is a maximum for each room. During the day, the sun moved from the east to the west, and the airflow rate to the East, South, and West rooms reached its peak value accordingly. The airflow rate to the Interior room is only affected by the internal loads.

Figures 6.5 to 6.7 show the results when using Occupancy-based DCV. As shown in Figure 6.5, the OA temperature was higher than the return air temperature, so the economizer was off, and the OA flow rate was totally decided by Occupancy-based DCV. The plot also shows the supply air temperature was controlled at 60°F. Figure 6.6 shows the results of cooling load. Figure 6.7 shows the results of CO_2 concentration. The highest CO_2 concentration was over 1600 ppm, which happened in the Interior room when the room is fully occupied. During night time, the indoor CO_2 concentrations were kept about 1600 ppm. The purging time began at 6 am and ended at 8 am the next day. During this time, sufficient amounts of OA air was introduced in to the building and to decrease the indoor CO_2

concentrations. After the purging time, the indoor CO_2 concentrations were nearly the same as that of the outdoor air.

Figures 6.8 to 6.10 show the results when using constant OA flow rate control strategy. Similar to the former case, the OA temperature was higher than the return air temperature, so the economizer was off, and the OA flow rate was completely decided by constant control strategy as shown in Figure 6.8. Figure 6.9 shows the results of cooling load. Figure 6.10 shows the results of CO_2 concentration. The highest CO_2 concentration was about 1400 ppm, which was lower than that in Occupancy-based control case. That was because in constant control strategy, more OA flow rate was required compared to the Occupancy-based control strategy.

Figures 6.11 to 6.14 show the results when using CO_2-based DCV. The indoor CO_2 concentration was kept about 700 ppm above the outdoor air CO_2 concentration. Here, the OA CO_2 was 400 ppm, so the setpoint was 1100 ppm. The OA flow rate was adjusted to keep the indoor CO_2 concentration under the setpoint. The required OA flow rate was obtained by using the IAQ model and shown in Figure 6.11. The plot also shows the indoor CO_2 concentrations were kept near or below 1100 ppm. The OA flow rate was used as input to the EnergyPlus model. Since EnergyPlus only uses hourly-based schedules, the original OA flow rate obtain from IAQ model was hourly averaged. The results are shown in Figure 6.12. Similar to the cases before, the OA temperature was higher than the return air temperature, so the economizer was off, and the OA flow rate was totally decided by CO_2-based DCV. These results are shown in Figure 6.13. Figure 6.14 shows the cooling load of this case.

The OA flow rate and cooling load under three different control strategies were compared and shown in Figure 6.15 and 6.16, respectively. As shown in Figure 6.15, CO_2-based DCV requires the most OA flow rate, and the Occupancy-based DCV requires the least OA flow rate. Because in summer season, the OA temperature is much higher than the

required supply air temperature (60 °F), more OA flow rate resulted in more cooling load or energy use. So the cooling load in CO_2-based DCV was the highest, and the cooling load in Occupancy-based DCV was the lowest as shown in Figure 6.16.

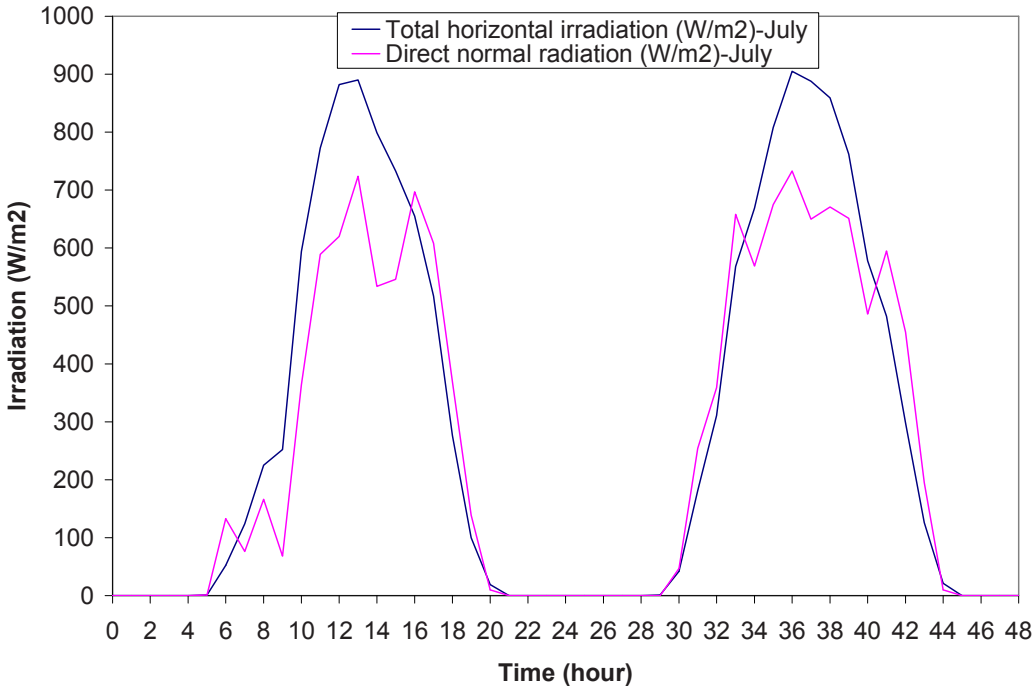

Figure 6.2 Solar Irradiation in July Cases

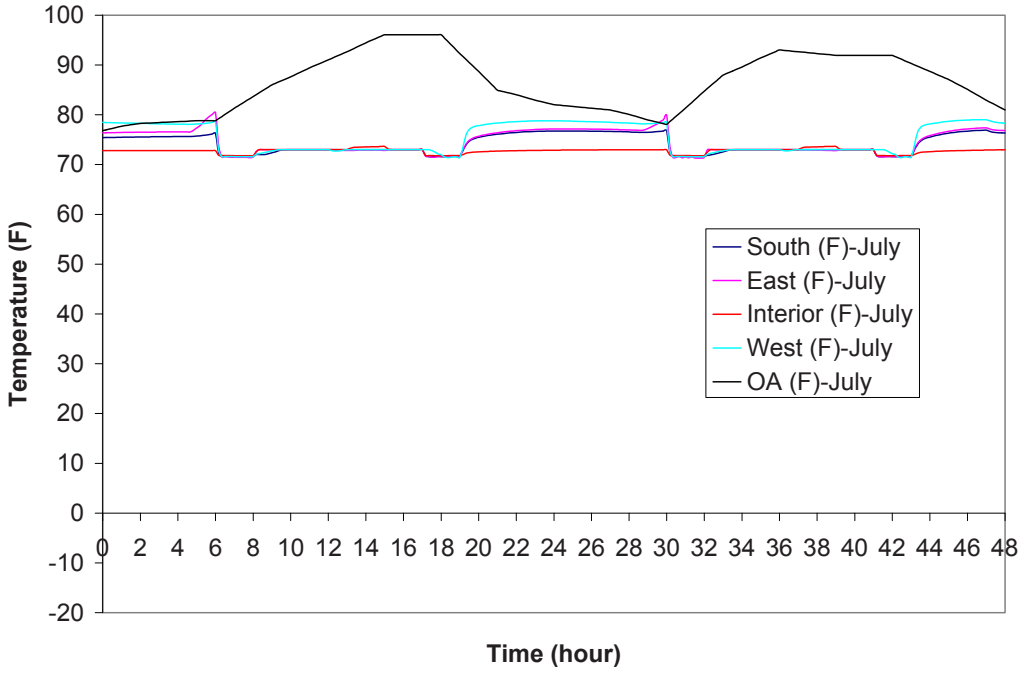

Figure 6.3 Temperature in July Cases

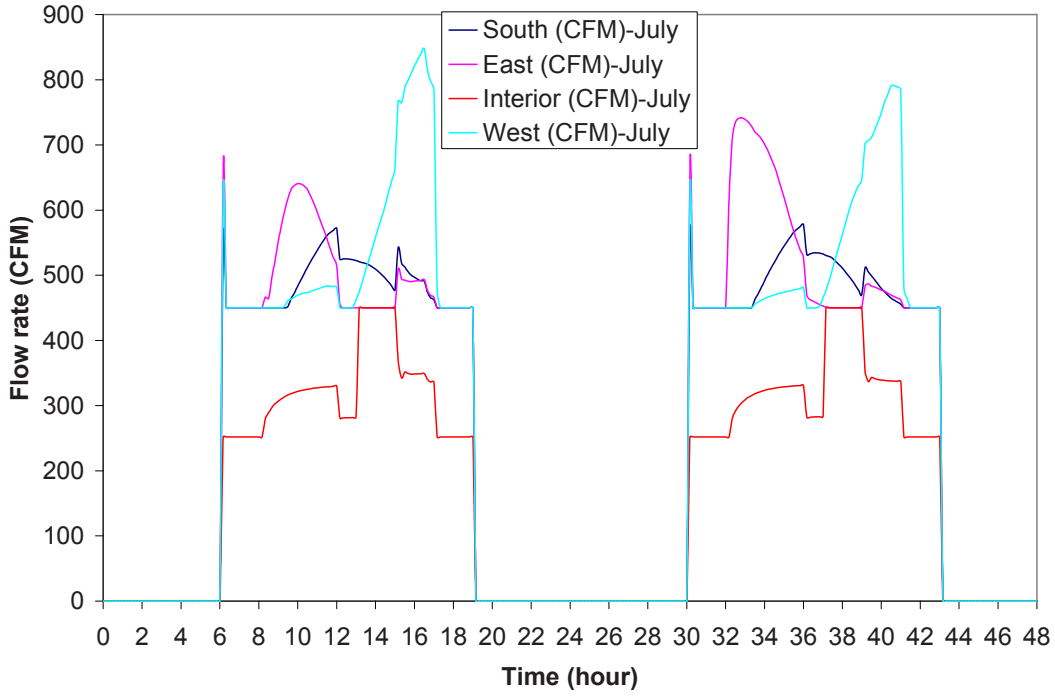

Figure 6.4 Air Flow Rate to Each Room in July Cases

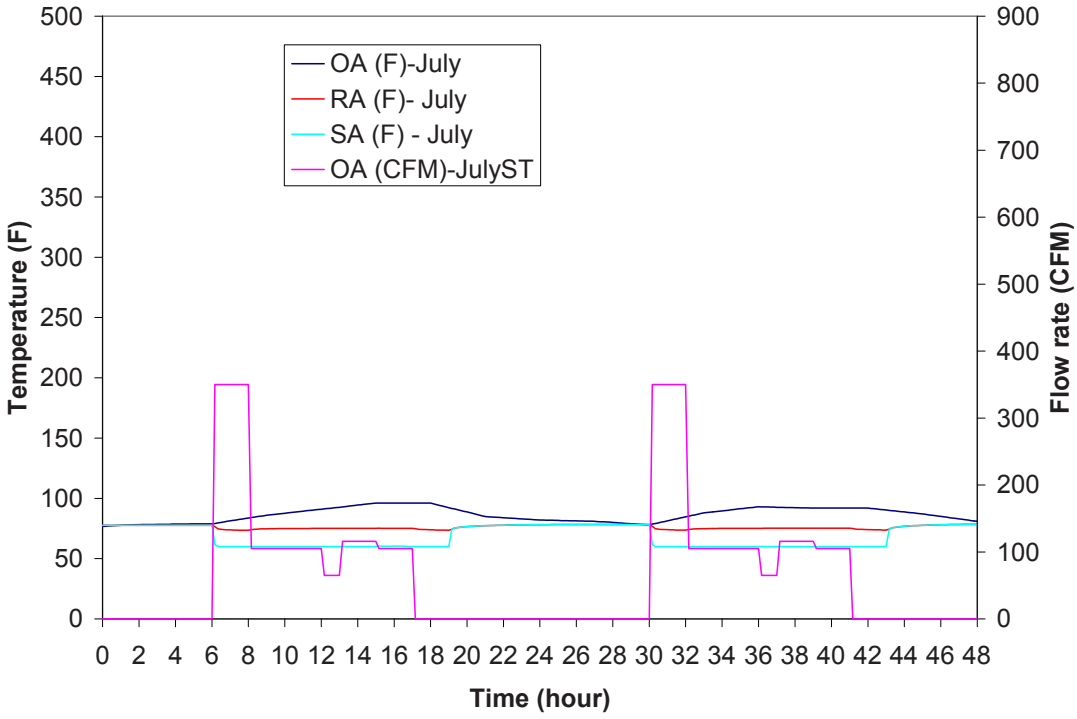

Figure 6.5 OA Flow Rate in July Standard Case

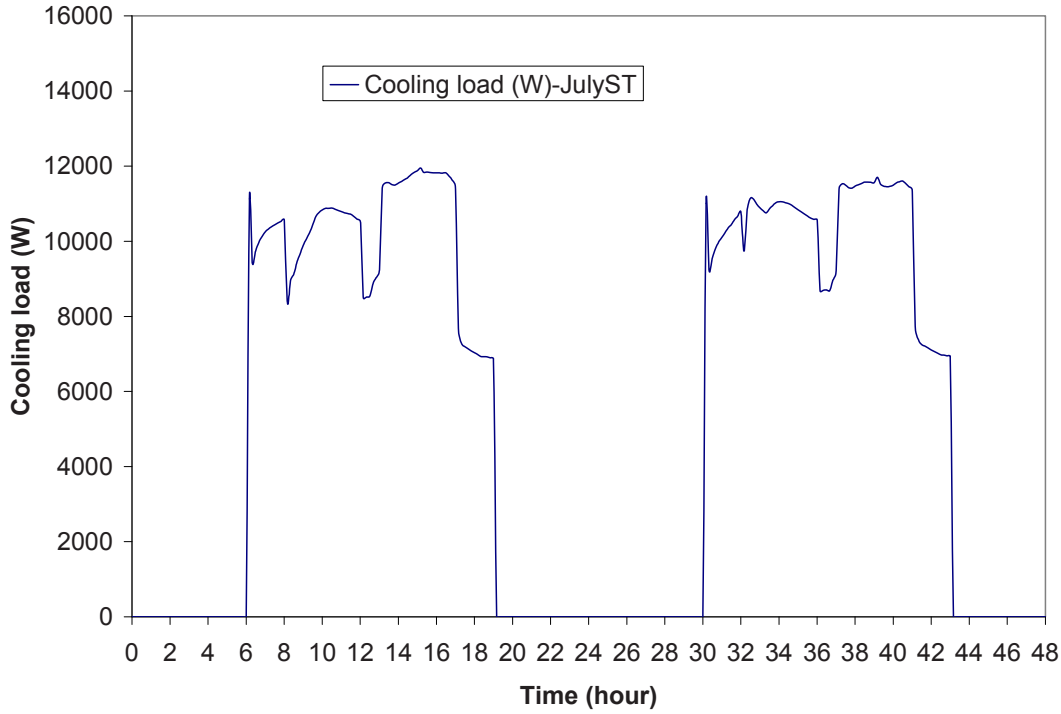

Figure 6.6 Cooling Load in July Standard Case

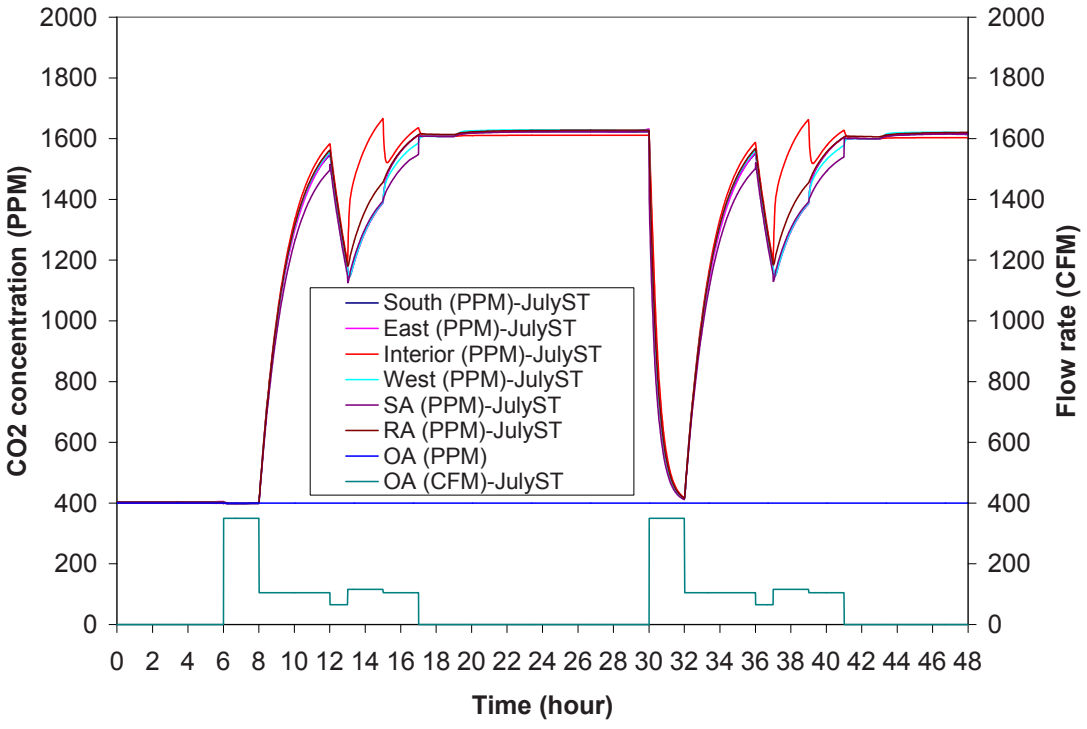

Figure 6.7 CO_2 Concentration in July Standard Case

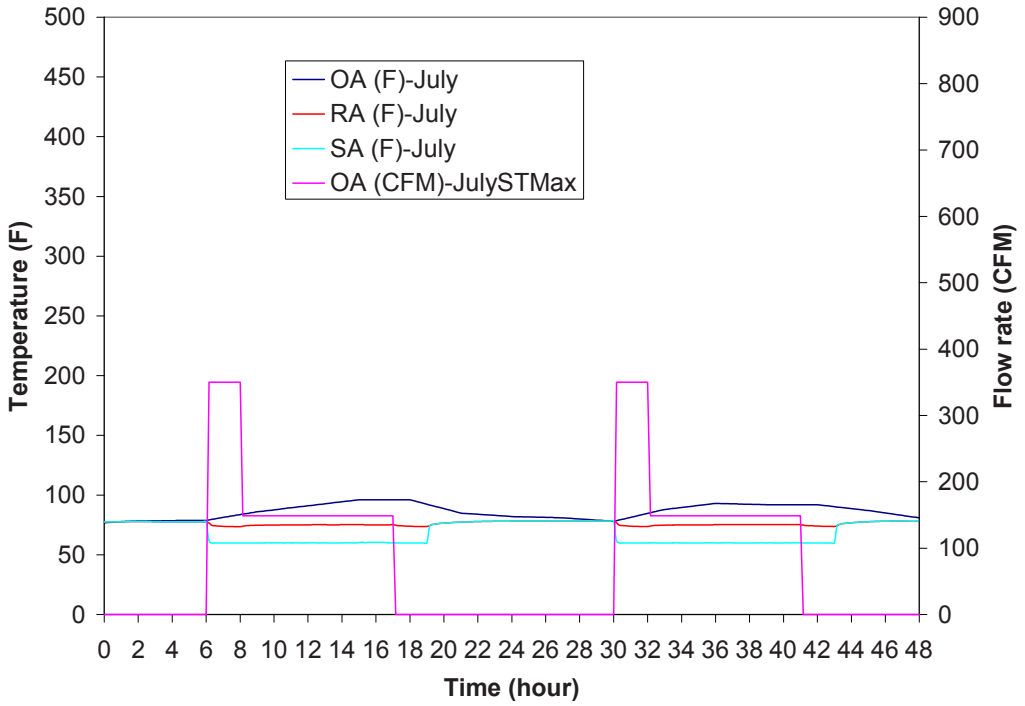

Figure 6.8 OA Flow Rate in July Standard Maximum Case

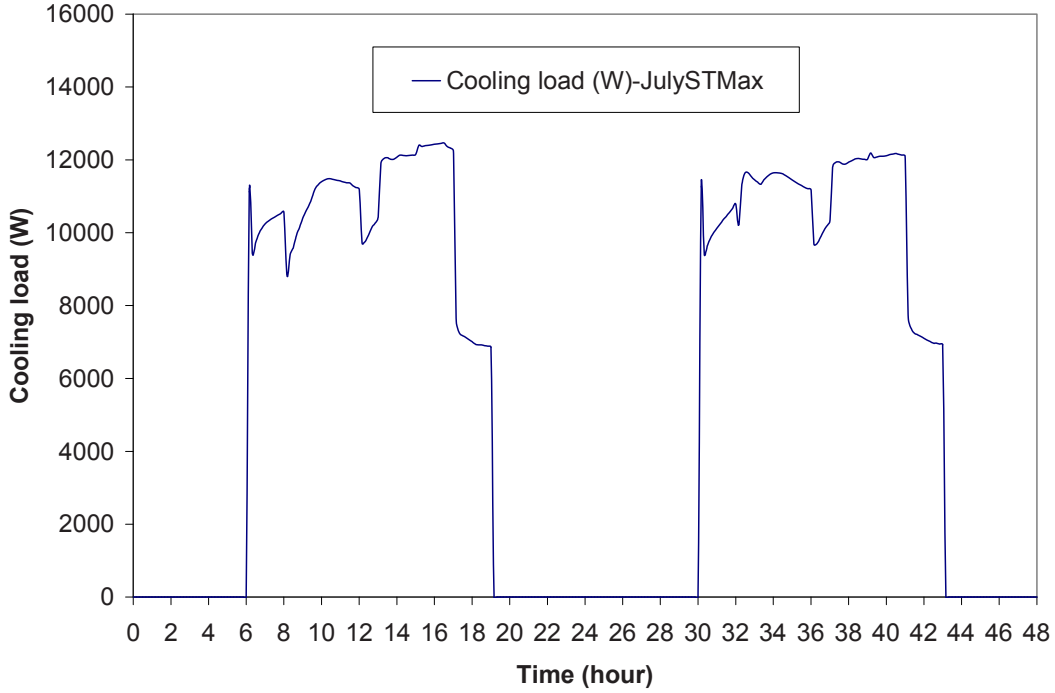

Figure 6.9 Cooling Load in July Standard Maximum Case

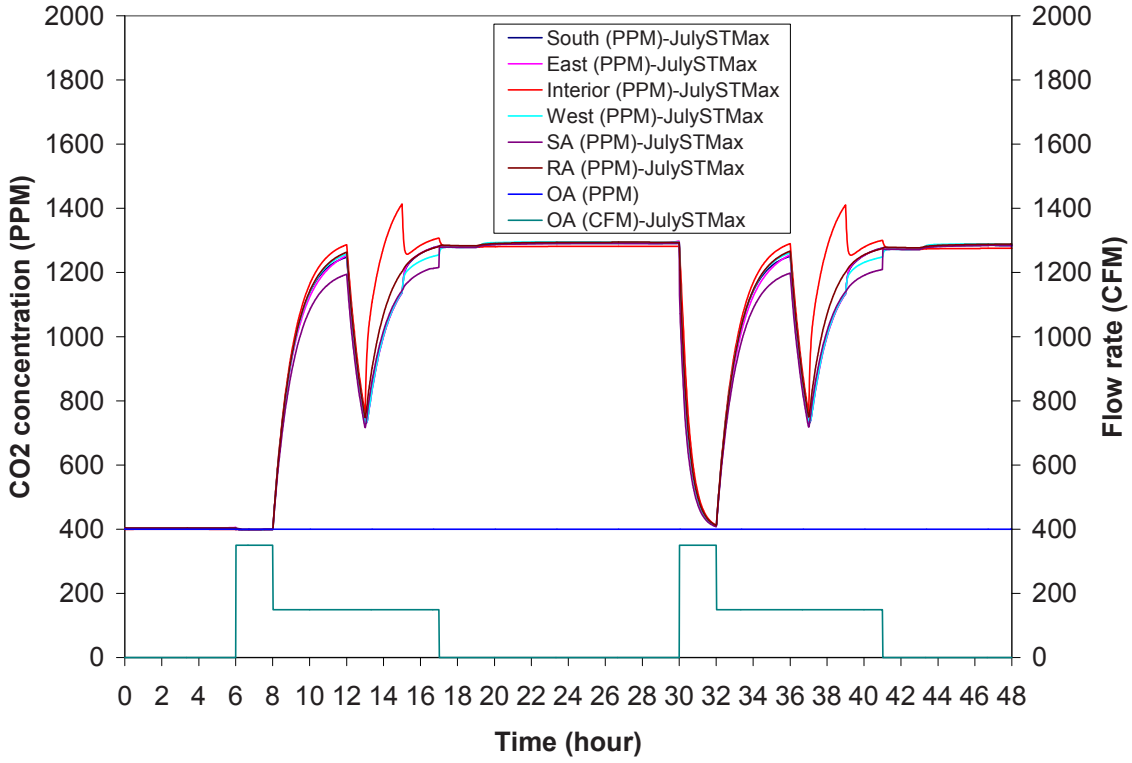

Figure 6.10 CO_2 Concentration in July Standard Maximum Case

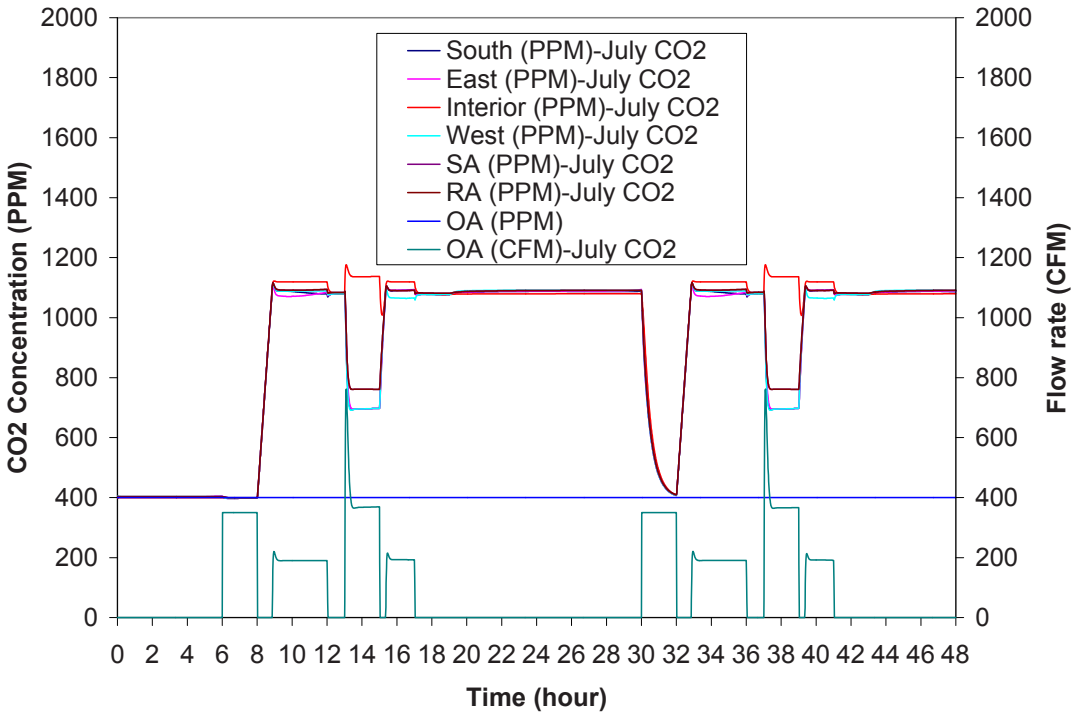

Figure 6.11 CO_2 Concentration in July CO2 Control Case

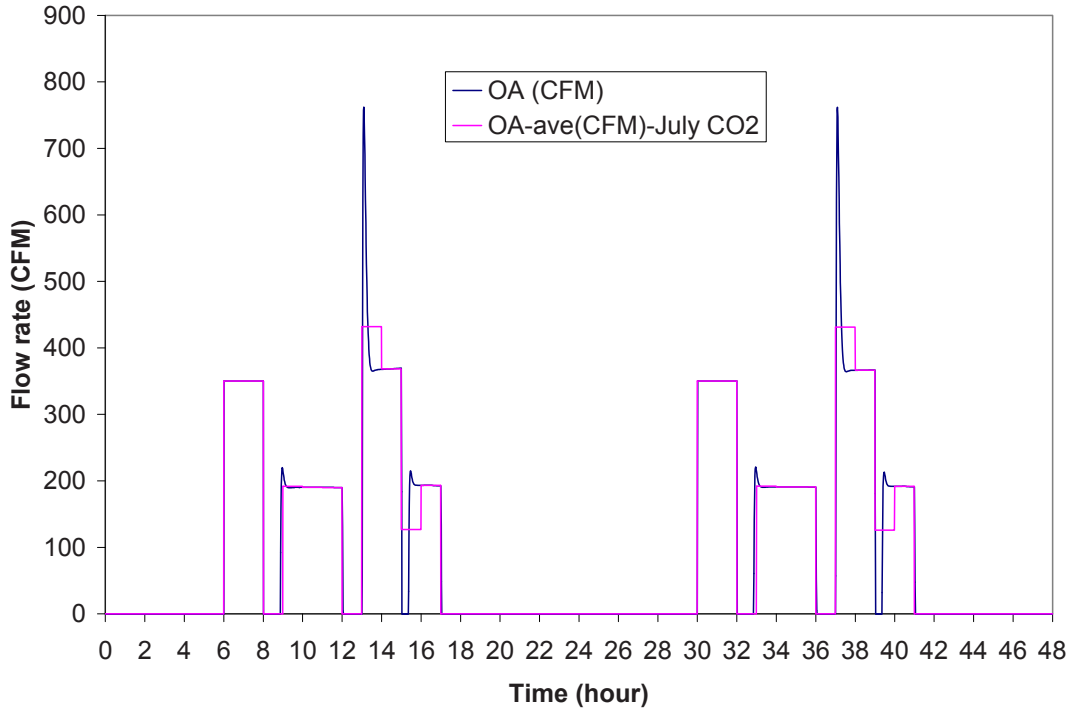

Figure 6.12 Hourly-Average OA Flow Rate in July CO_2 Control Case

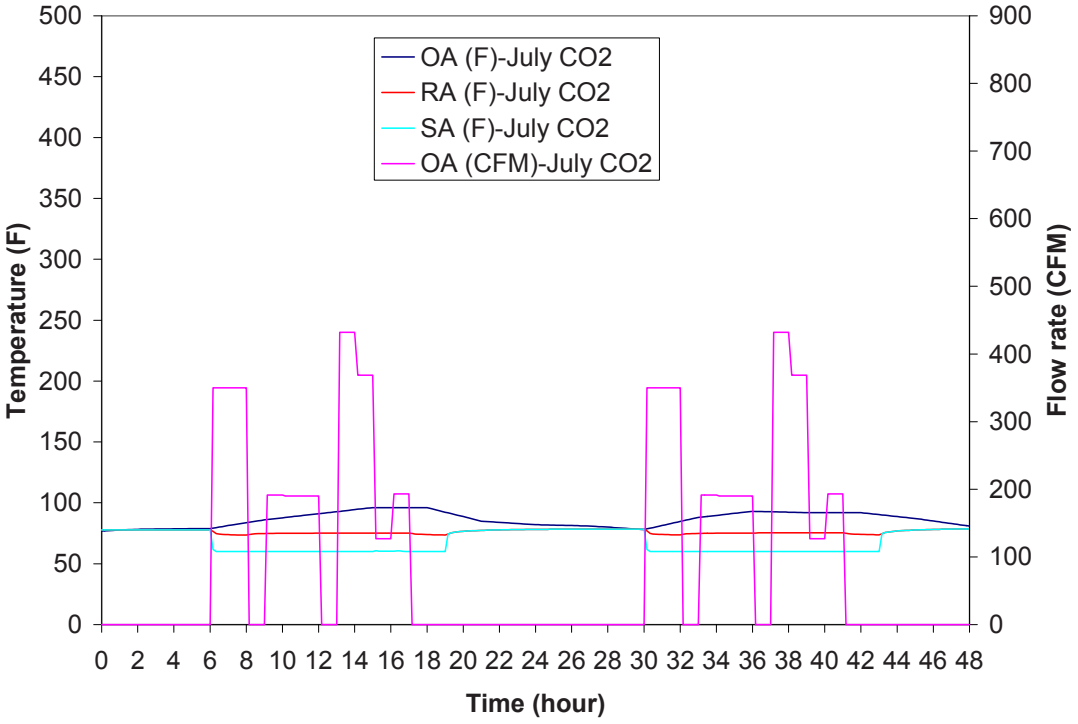

Figure 6.13 OA Flow Rate in July CO_2 Control Case

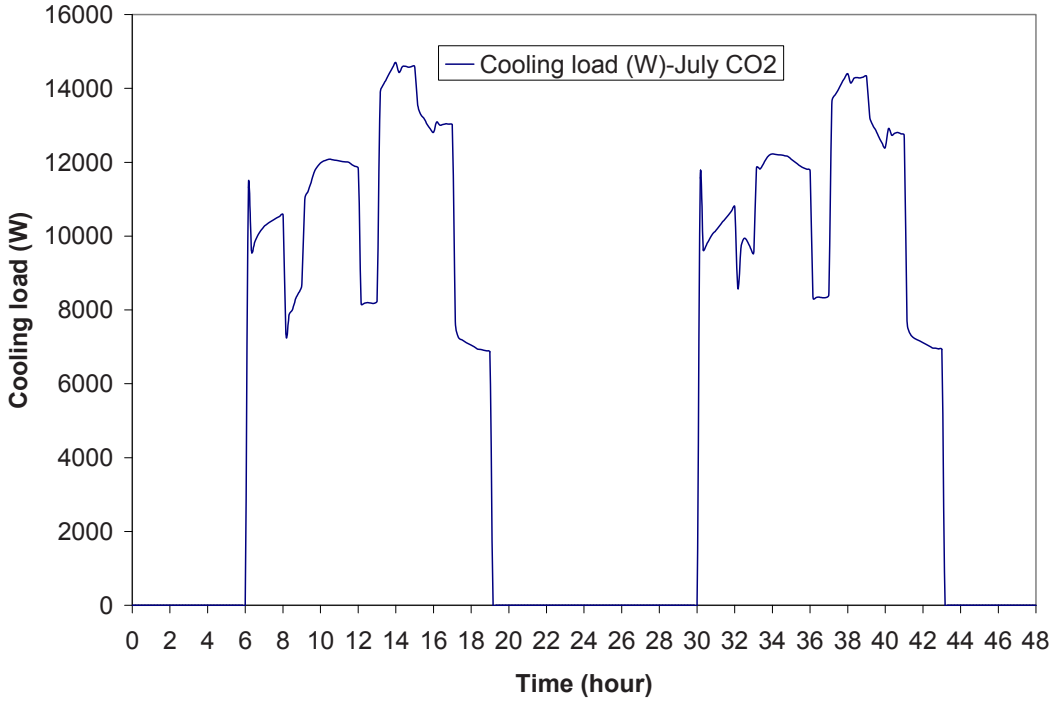

Figure 6.14 Cooling Load in July CO_2 Control Case

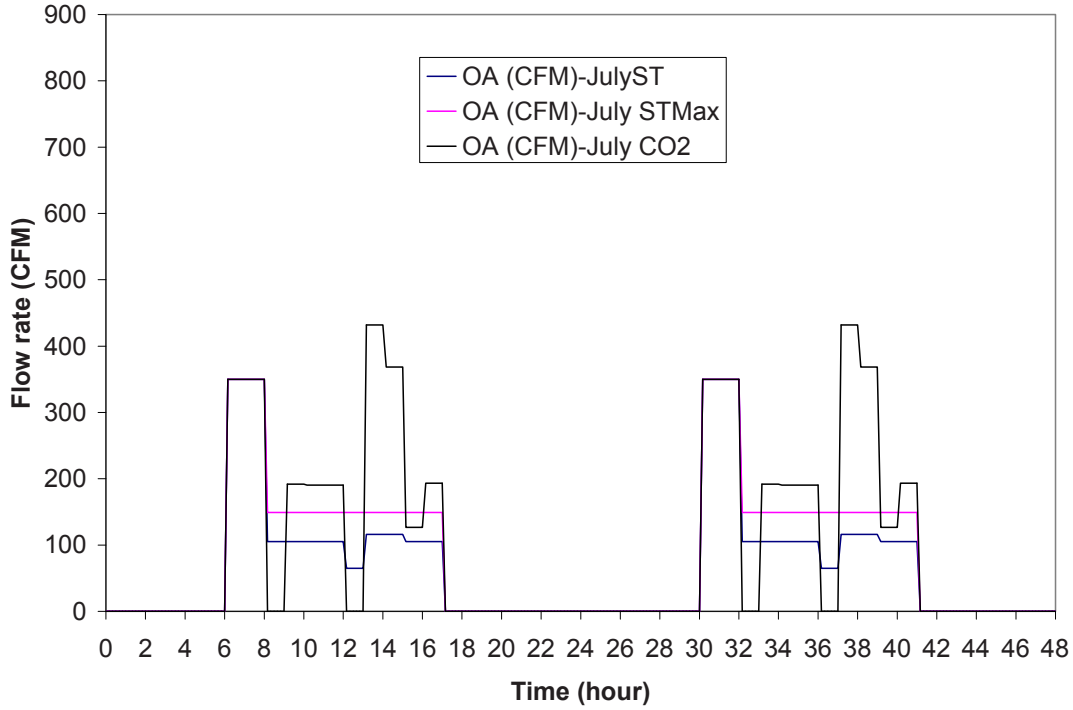

Figure 6.15 OA Flow Rate Comparison in July Cases

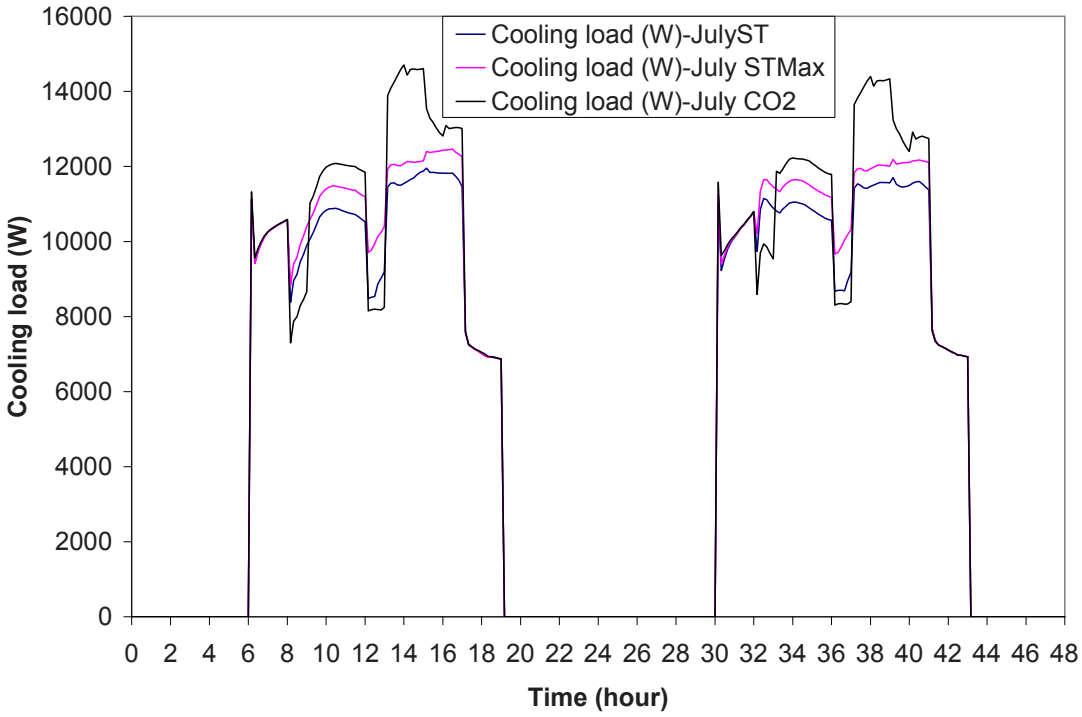

Figure 6.16 Cooling Load Comparison in July Cases

6.3 Winter Cases (January 13-14)

The winter cases were run from January 13 to 14. Figure 6.17 shows the solar irradiation during the two days. Figure 6.18 shows the outdoor air temperature and room temperatures. Similar to summer cases, the HVAC system works from 6 am to 7 pm. During that period, the room temperatures were controlled between 72°F and 73°F. As shown in Figure 6.17, the sun rose at 5 am, accordingly the temperature in east room increases at that time. Different from that of the exterior rooms, the interior room temperature didn't change much when HVAC system was off, because of less heat gain through walls. Figure 6.19 shows the flow rate to each room. When the HVAC system turns on at 6am, the temperature in each room was below the temperature setpoint, so each room was in heating mode, and the flow rate was at the minimum value. As time went on, the South room gained more heat than the other exterior rooms causing the South room to go into cooling mode. During that cooling period, the flow rate to south room increased and was above the minimum airflow rate value. The airflow rate to the Interior room was mainly affected by the internal heat loads.

Figures 6.20 to 6.22 show the results when using Occupancy-based DCV. The OA temperature was lower than the return air temperature, so the economizer was on. As shown in Figure 6.20, except the purging time, the OA flow rate decided by Occupancy-based DCV was lower than that decided by economizer, the latter was the actual OA flow rate. Figure 6.21 shows the OA temperature and the return air temperature. It also shows the supply air temperature was controlled at 60°F except during the purge time. During purge, a lot of low temperature OA was introduced to the system, so the supply air temperature was below 60°F. Since only using OA could make the supply air reach the setpoint, no extra cooling was required and the cooling load was 0. Figure 6.22 shows the results of CO_2 concentration. The highest CO_2 concentration was about 900 ppm. It was much lower than that in summer cases because of much larger OA flow rate.

Figure 6.23 shows the results when using constant OA flow rate control strategy. Same as the Occupancy-based DCV case, the OA temperature was lower than the return air temperature and the economizer was on. As shown in Figure 6.23, except during purge, the OA flow rate determined by Occupancy-based DCV was lower than that required by the economizer, the latter was the actual OA flow rate. After purge, the OA flow rate was determined by the economizer, which was the same as that in Occupancy-based DCV case. Again, since only using OA could make the supply air reach the setpoint, no extra cooling was required and the cooling-coil load was 0. Because the OA flow rate was the same as that in Occupancy-based DCV case, the results of CO_2 concentrations were the same as those in Occupancy-based DCV case.

Figure 6.24 to 6.26 show the results when using CO_2-based DCV. The OA flow rate required by CO_2-based DCV was obtained by using the IAQ model and shown in Figure 6.24. The plot also shows the indoor CO_2 concentrations were kept near or below 1100 ppm. The hourly-averaged OA flow rate is shown in Figure 6.25, which was used as input to the EnergyPlus model. Same as the former winter cases, the OA temperature was lower than the return air temperature and the economizer was on. As shown in Figure 6.26, except during purge, the OA flow rate determined by Occupancy-based DCV was lower than that determined by the economizer, the latter was the actual OA flow rate. After purge, the OA flow rate was determined by the economizer, and the cooling-coil load was 0, which were the same as those in former winter cases.

In conclusion, three different control strategies resulted in the same OA flow rate, cooling load and CO_2 concentrations in the winter cases. The OA flow rate was determined by the use of the economizer, and the cooling-coil load was 0.

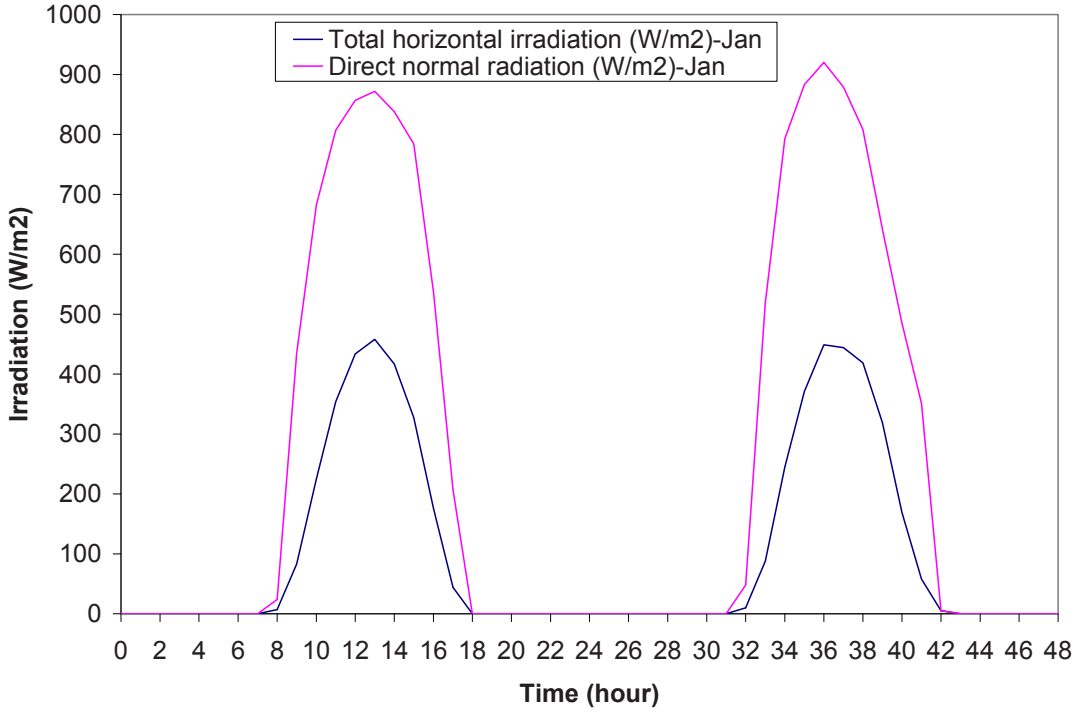

Figure 6.17 Solar Irradiation in January Cases

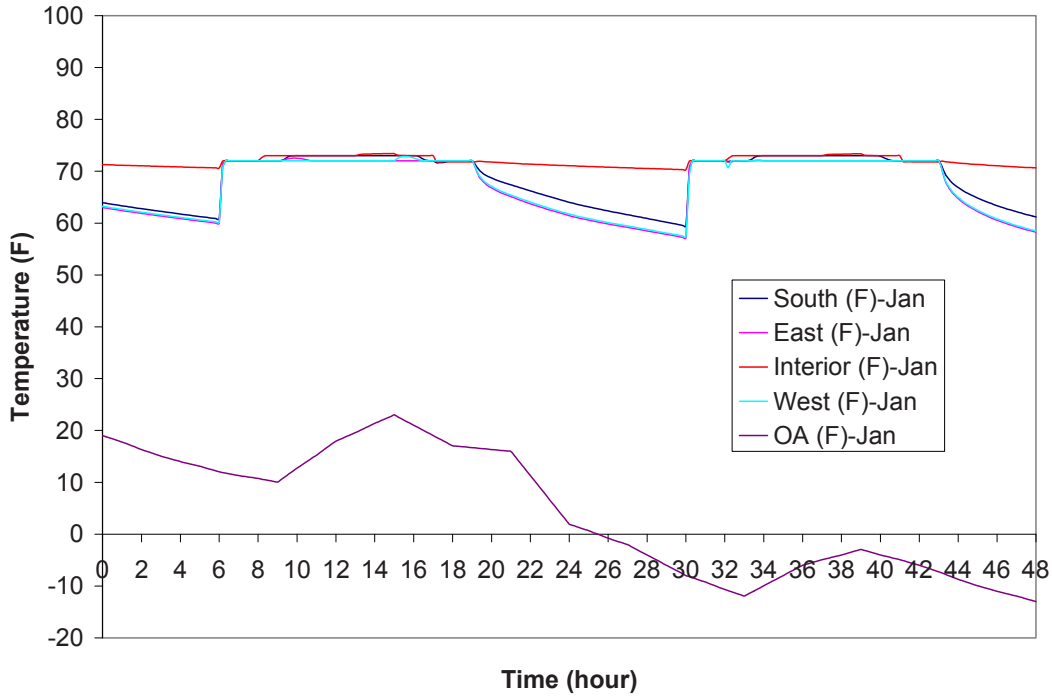

Figure 6.18 Temperature in January Cases

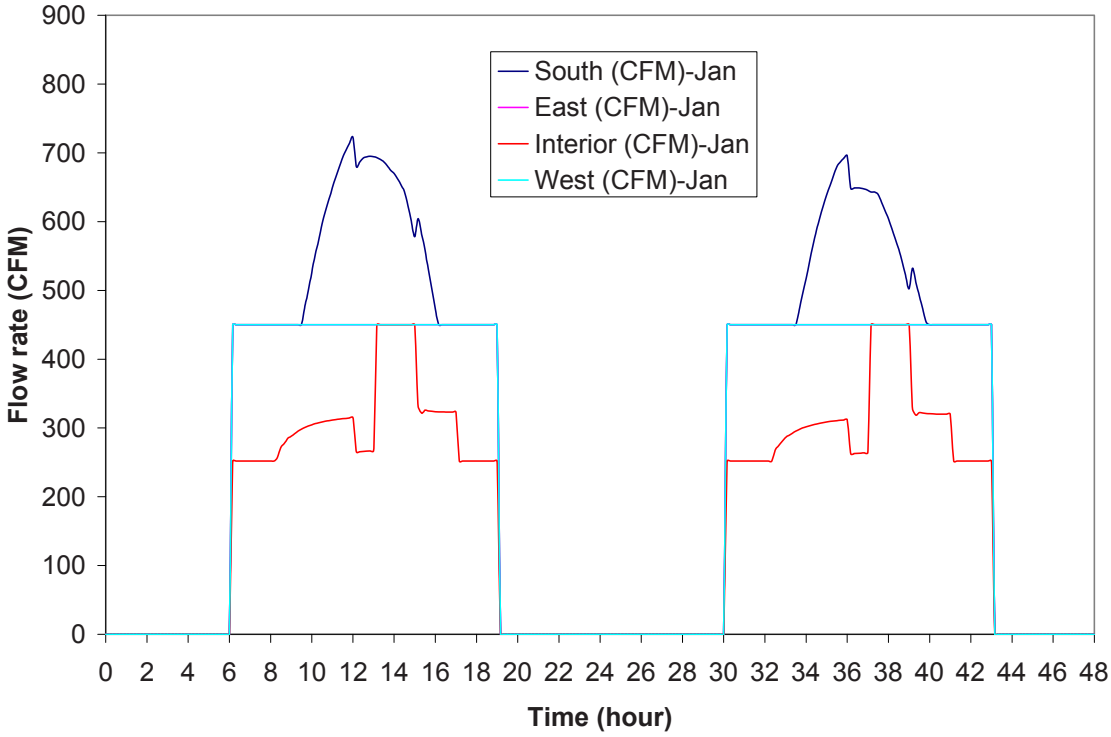

Figure 6.19 Airflow Rate to Each Room in January Cases

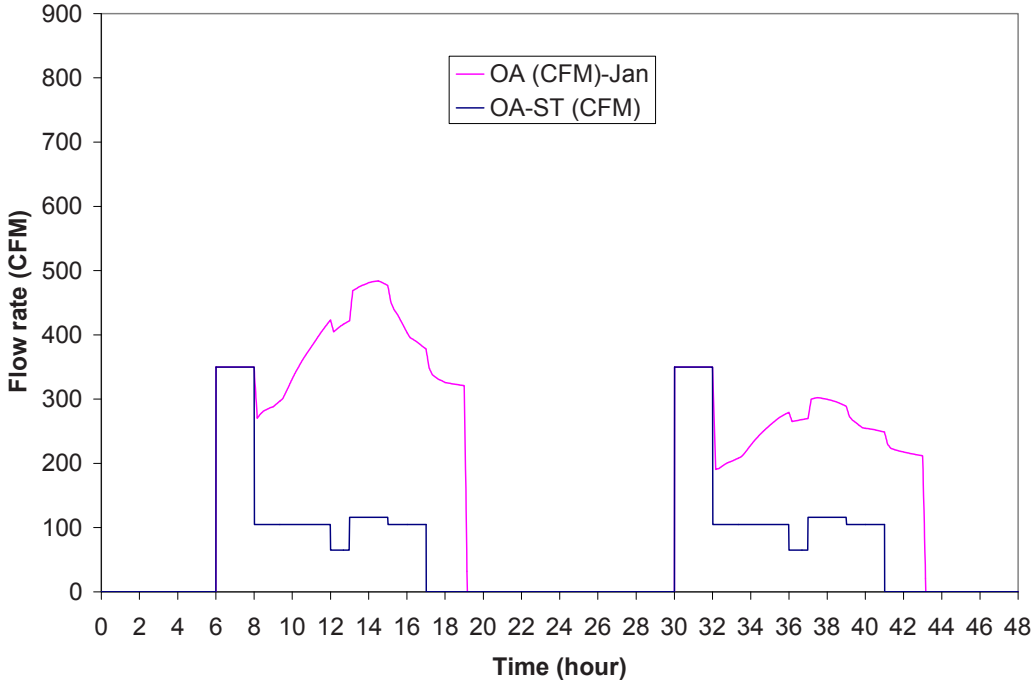

Figure 6.20 OA Flow rate comparison in January Standard Case

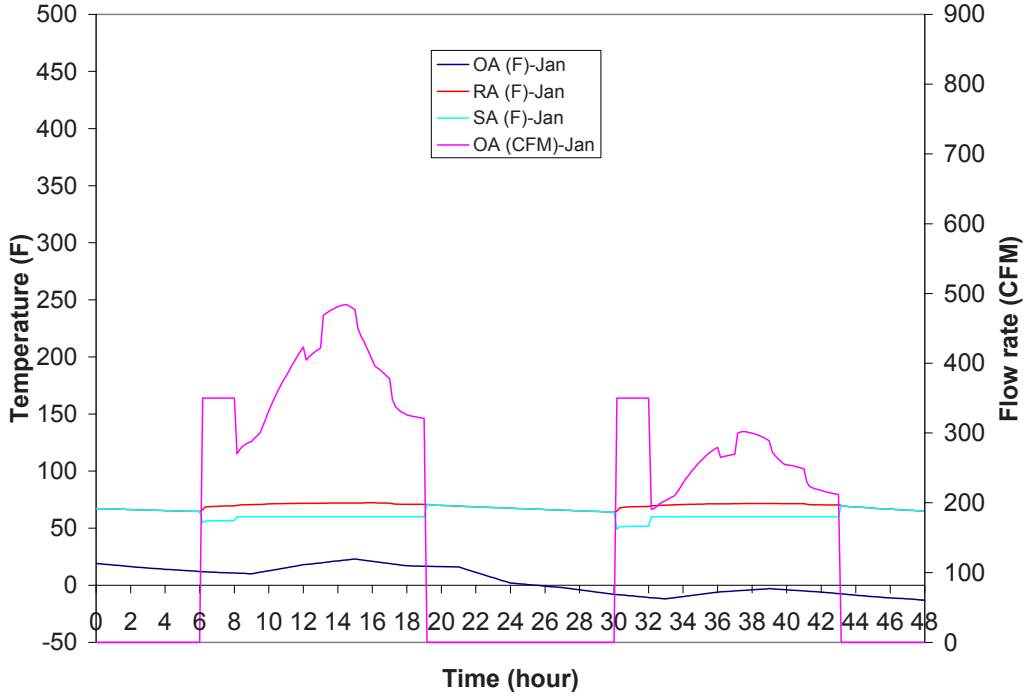

Figure 6.21 OA Flow Rate in January Cases

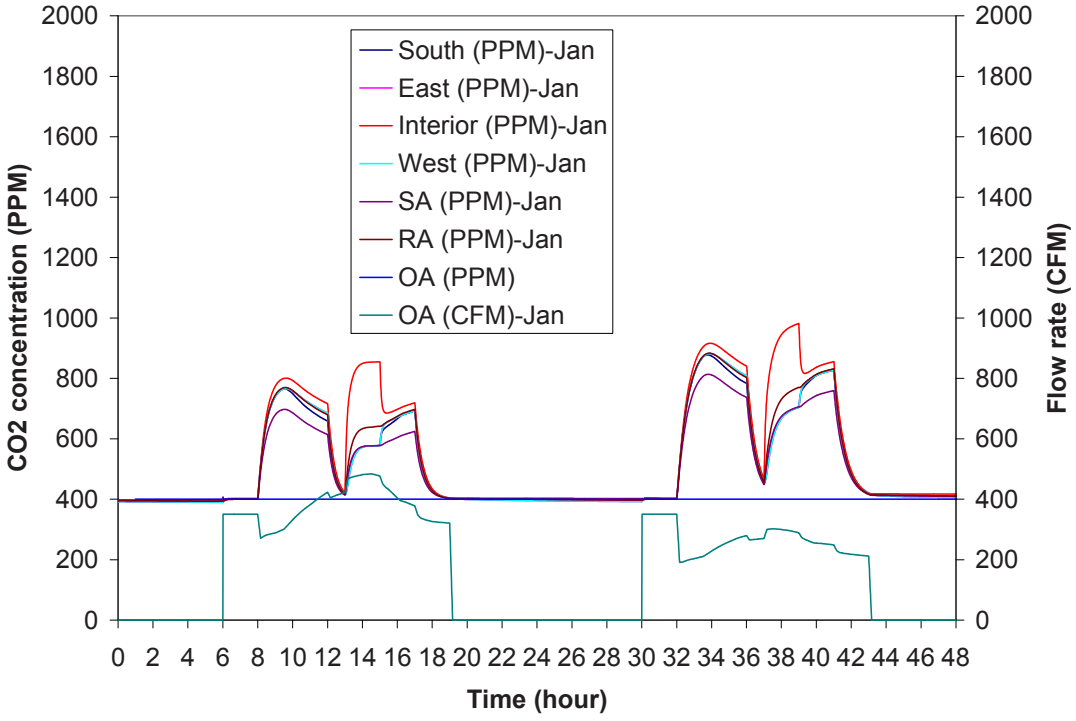

Figure 6.22 CO_2 Concentration in January Cases

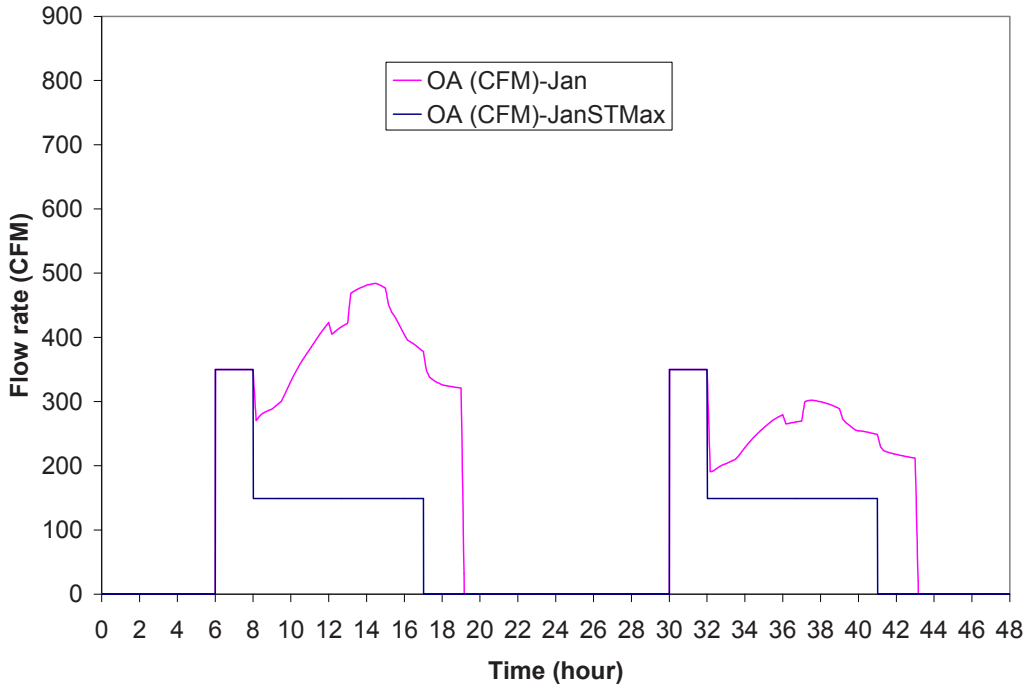

Figure 6.23 OA Flow rate comparison in January Standard Maximum Case

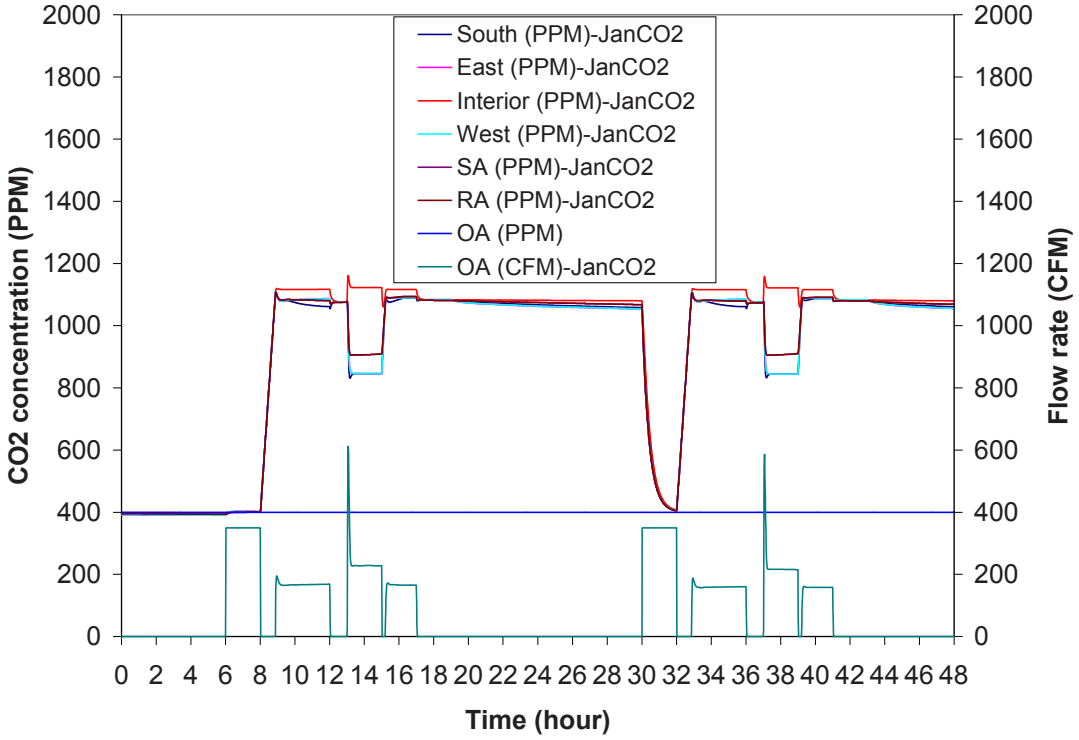

Figure 6.24 OA Flow rate in January based on CO_2 Control

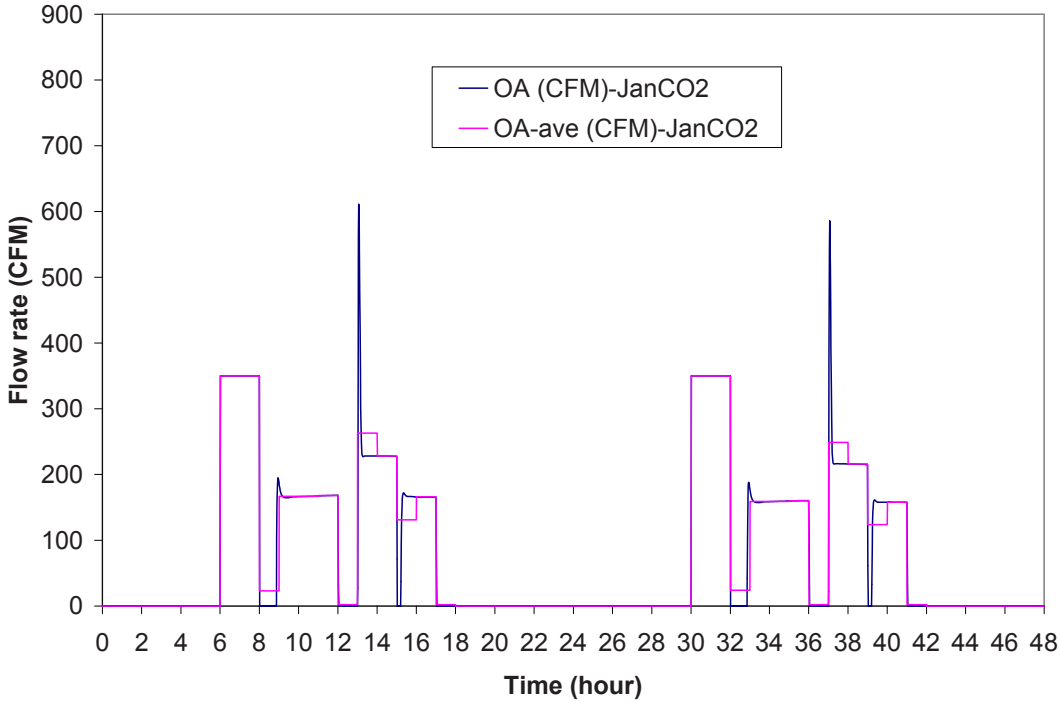

Figure 6.25 Hourly-Average OA Flow Rate in January Based on CO_2 Control

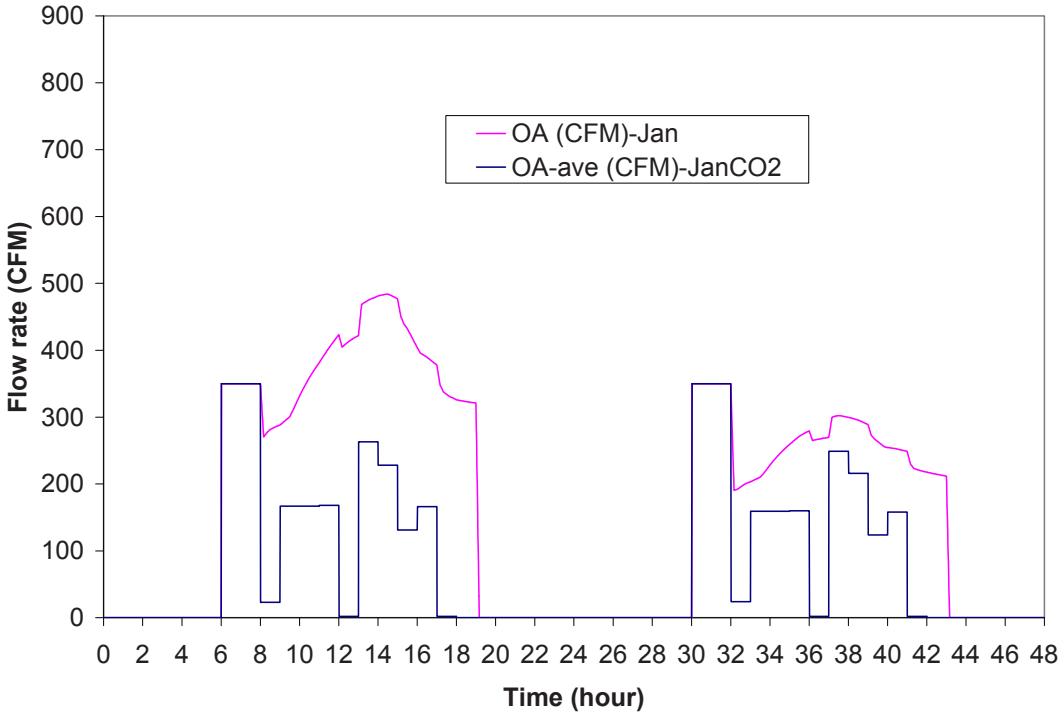

Figure 6.26 OA Flow rate comparison in January CO_2 Control Case

6.4 Transition season Cases (October 1-2)

The transition season cases were run from October 1st to 2nd. Figure 6.27 shows the solar irradiation during the two days. Figure 6.28 shows the outdoor air temperature and room temperatures. Same as that in summer and winter cases, the HVAC system works from 6am to 7pm, and the room temperatures were controlled between 72°F and 73°F. Figure 6.29 shows the flow rate to each room. As time went on, the sun moved from the east to the west, and the flow rate to the east, south, and west rooms reached its peak value accordingly. The flow rate to the interior room was mainly affected by the people number in it.

Figure 6.30 to 6.34 show the results when using Occupancy-based DCV. In Figure 6.30, the blue line was the OA flow rate required by Occupancy-based DCV. The pink line was the actual OA flow rate meeting the requirement of Occupancy-based DCV and economizer. For most of the time, the pink line was above the blue line, that was because during that time, the OA temperature was lower than the return air temperature as shown in Figure 6.31, so the economizer was on. When the OA temperature was higher than the return air temperature from 11 am to 5 pm in the first day, the economizer was off, and the OA flow rate was determined by the Occupancy-based DCV. Figure 6.31 also shows the supply air temperature was controlled at 60°F. Figure 6.32 shows the results of cooling load. After about 3 pm the second day, the cooling load was 0, although the HVAC system still worked until 7 pm. That was because during that time, using OA alone could make the supply air reach the setpoint as shown in Figure 6.31, no extra cooling was required and the cooling load was 0. Figure 6.33 shows the OA flow rate and the totally supply airflow rate.

Figure 6.34 shows the results of CO_2 concentration. When the economizer was active, the OA flow rate was high, accordingly, the indoor CO_2 concentrations were low. When economizer was off, the OA flow rate was low, and the indoor CO_2 concentrations were high. The highest CO_2 concentration was about 1600 ppm.

Figure 6.35 to 6.39 show the results when using constant OA flow rate control strategy. Figure 6.35 shows the OA flow rate required only by ventilation control strategy and the actual OA flow rate meeting the requirements of both ventilation and economizer. Same to the Occupancy-based DCV case, for most of the time, the OA temperature was lower than the return air temperature, so the economizer was on. When economizer was on, the OA flow rate was the same as that in Occupancy-based DCV case. When the OA temperature was higher than the return air temperature from 11 am to 5 pm in the first day, the economizer was off, and the OA flow rate was determined by the Occupancy-based DCV as shown in Figure 6.36. Figure 6.37 shows the results of cooling-coil load. After about 3 pm the second day, only using OA could make the supply air reach the setpoint as shown in Figure 6.36, no extra cooling was required and the cooling load was 0. Figure 6.38 shows the OA flow rate and the totally supply airflow rate.

Figure 6.39 shows the results of CO_2 concentration. When the economizer is active, the OA flow rate was high, accordingly, the indoor CO_2 concentrations were low. When economizer was off, the OA flow rate was low, and the indoor CO_2 concentrations were high. The highest CO_2 concentration was about 1400 ppm, which was lower than that in the Occupancy-based DCV case because of higher OA flow rate.

Figure 6.40 to 6.47 show the results when using CO_2-based DCV. The OA flow rate required by CO_2-based DCV was obtained by using the IAQ model and shown in Figure 6.40. The plot also shows the indoor CO_2 concentrations were kept near or below 1100 ppm. The hourly-averaged OA flow rate is shown in Figure 6.41, which was used as input to the EnergyPlus model. Figure 6.42 shows the OA flow rate required only by ventilation control strategy and the actual OA flow rate meeting the requirements of both ventilation and economizer. Same as the former transition season cases, for most of the time, the OA temperature was lower than the return air temperature, so the economizer was on. When economizer was on, the OA flow rate was the same as that in Occupancy-based DCV case

and constant OA flow rate control strategy case. When the OA temperature was higher than the return air temperature from 11am to 5 pm in the first day, the economizer was off, and the OA flow rate was decided by the CO_2-based DCV as shown in Figure 6.43. Figure 6.44 shows the results of cooling-coil load. After about 3 pm the second day, only using OA could make the supply air reach the setpoint as shown in Figure 6.43, no extra cooling was required and the cooling load was 0. Figure 6.45 shows the OA flow rate and the totally supply airflow rate.

Figure 6.46 shows the results of CO_2 concentration. When the economizer is active, the OA flow rate was high, accordingly, the indoor CO_2 concentrations were low. When economizer was off, the OA flow rate was low, and the indoor CO_2 concentrations were high. The highest CO_2 concentration was about 1300 ppm instead of 1100 ppm, that was because the OA flow rate required by CO_2-based control strategy was hourly averaged. If the actual OA flow rate required by CO_2-based control strategy was applied, the highest CO_2 concentration was about 1100 ppm as shown in Figure 6.47.

The OA flow rate and cooling load under three different control strategies were compared and shown in Figure 6.48 and 6.49, respectively. The only difference happened during the time when the OA temperature was higher than the return air temperature and the OA flow rate was only decided by the ventilation strategies. As shown in the plots, CO_2-based DCV requires the most OA flow rate, and the Occupancy-based DCV requires the least. Accordingly, the cooling load in CO_2-based DCV was the highest, and the cooling load in Occupancy-based DCV was the lowest.

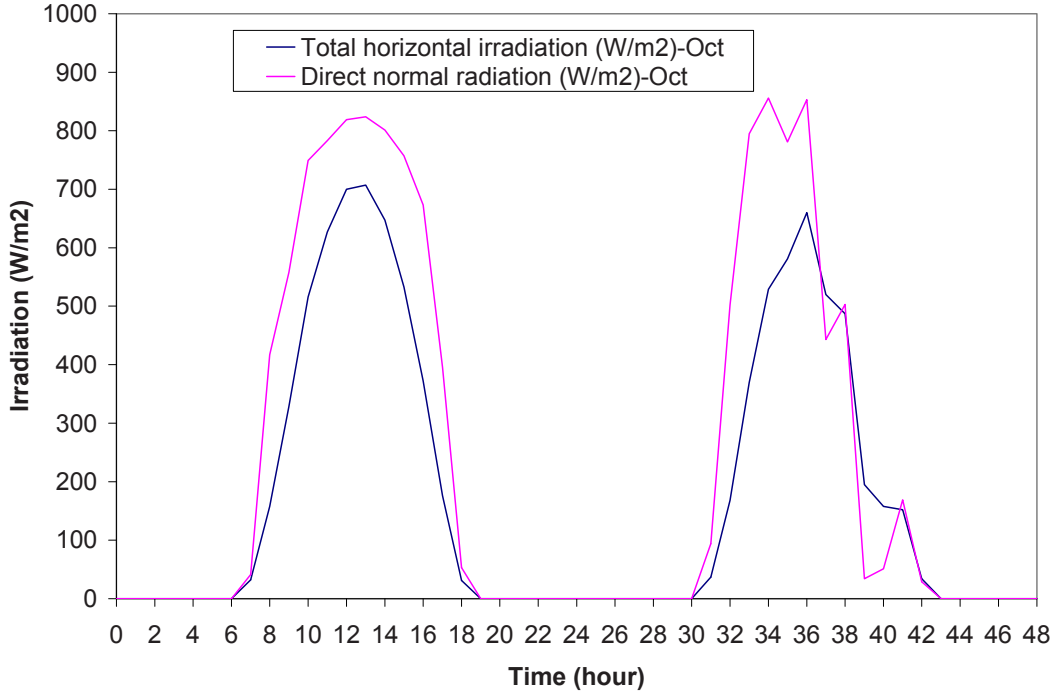

Figure 6.27 Solar Irradiation in October Cases

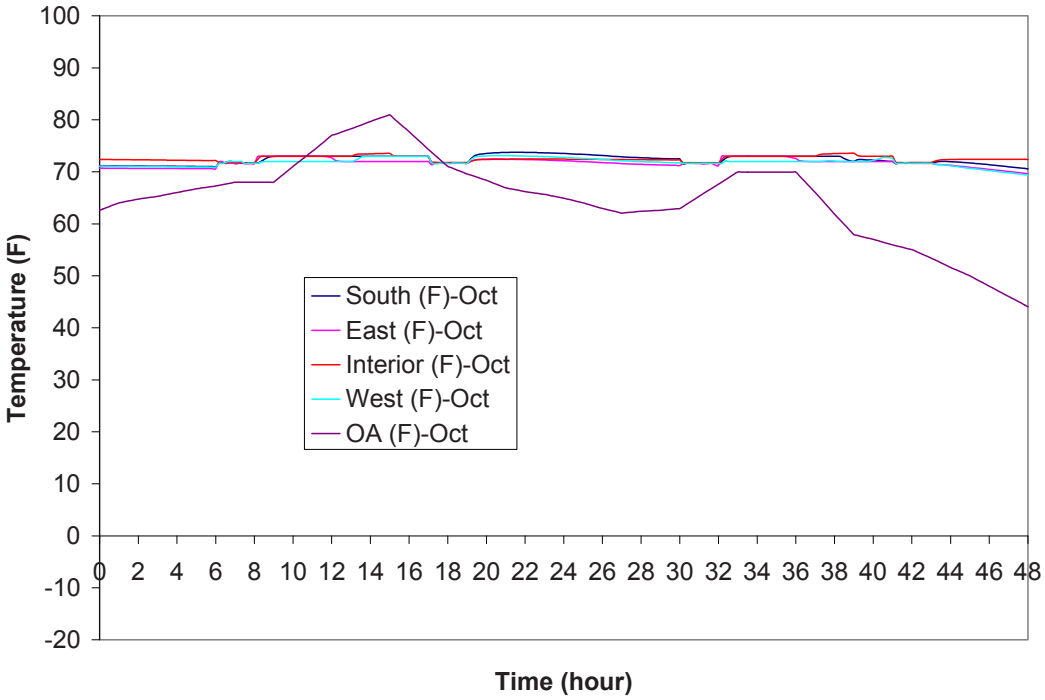

Figure 6.28 Temperature in October Cases

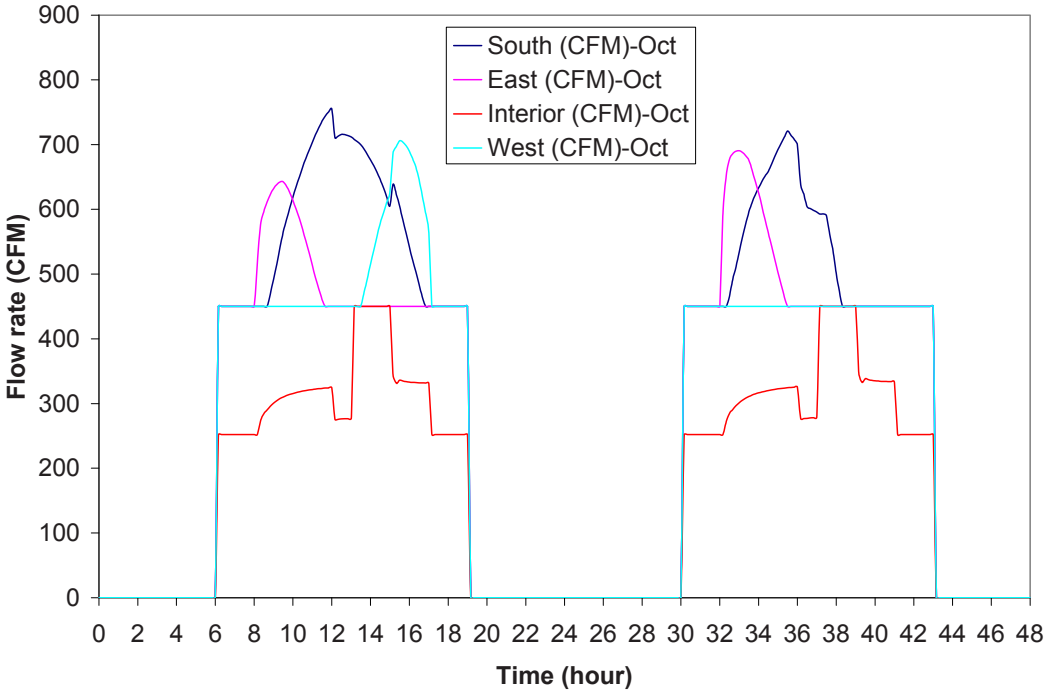

Figure 6.29 Airflow Rate to Each Room in October Cases

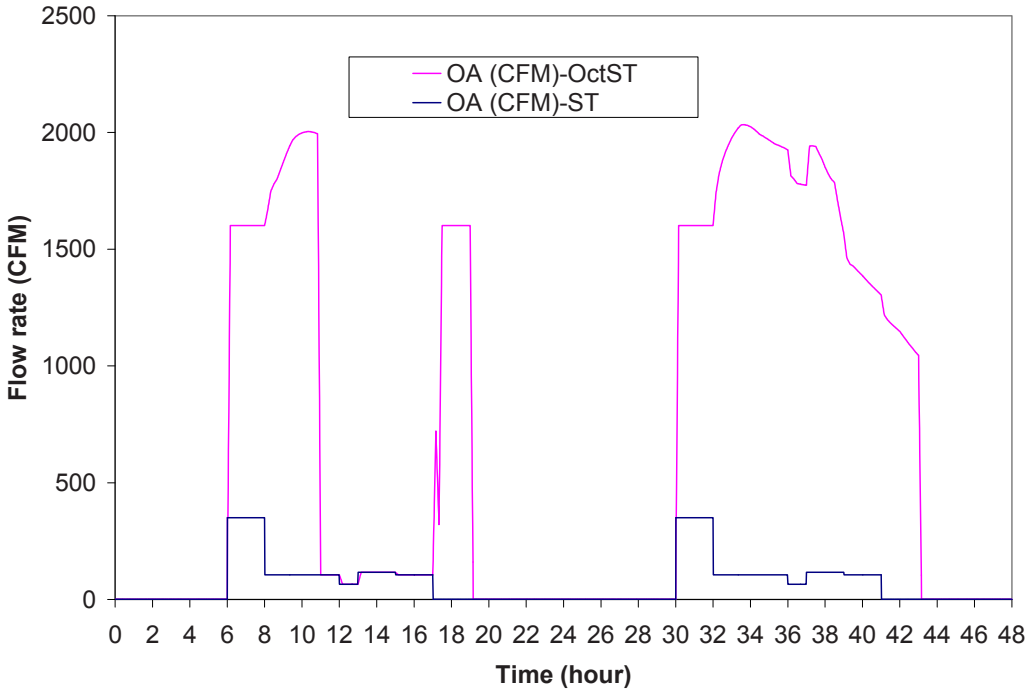

Figure 6.30 OA Flow rate comparison in October Standard Case

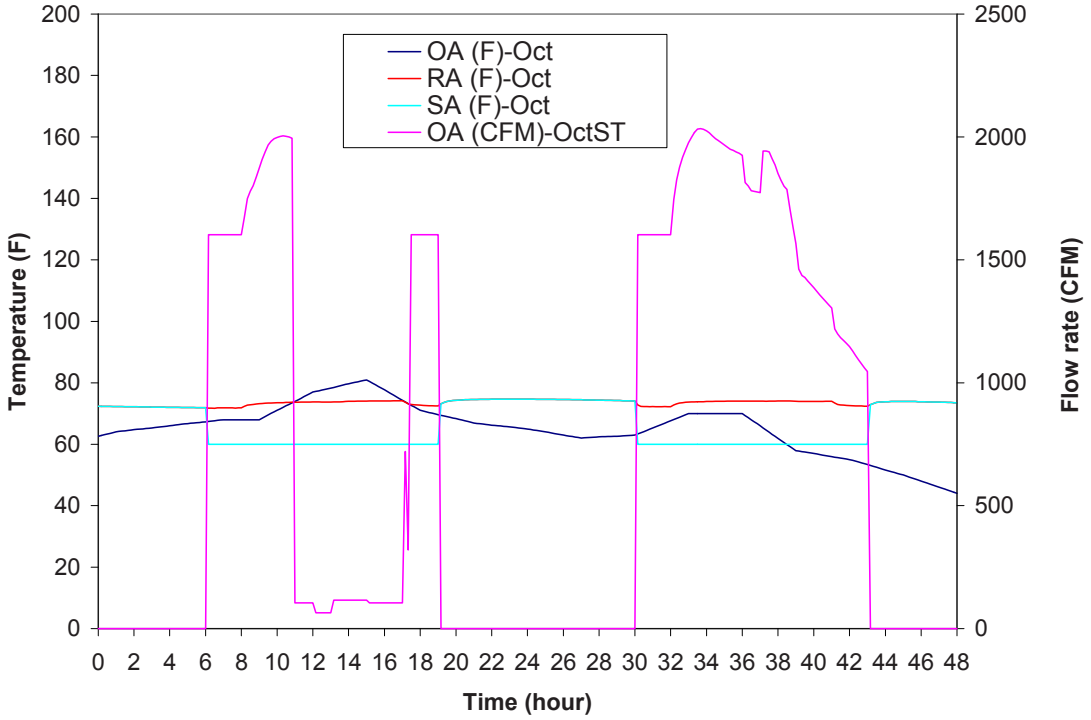

Figure 6.31 OA Flow Rate in October Standard Case

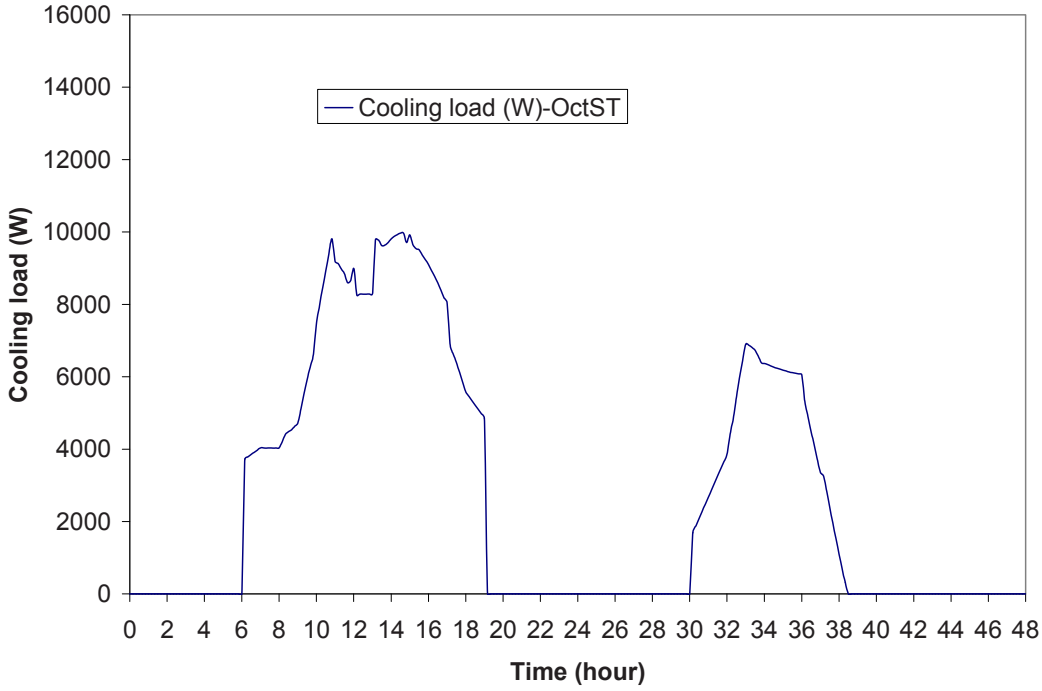

Figure 6.32 Cooling Load in October Standard Case

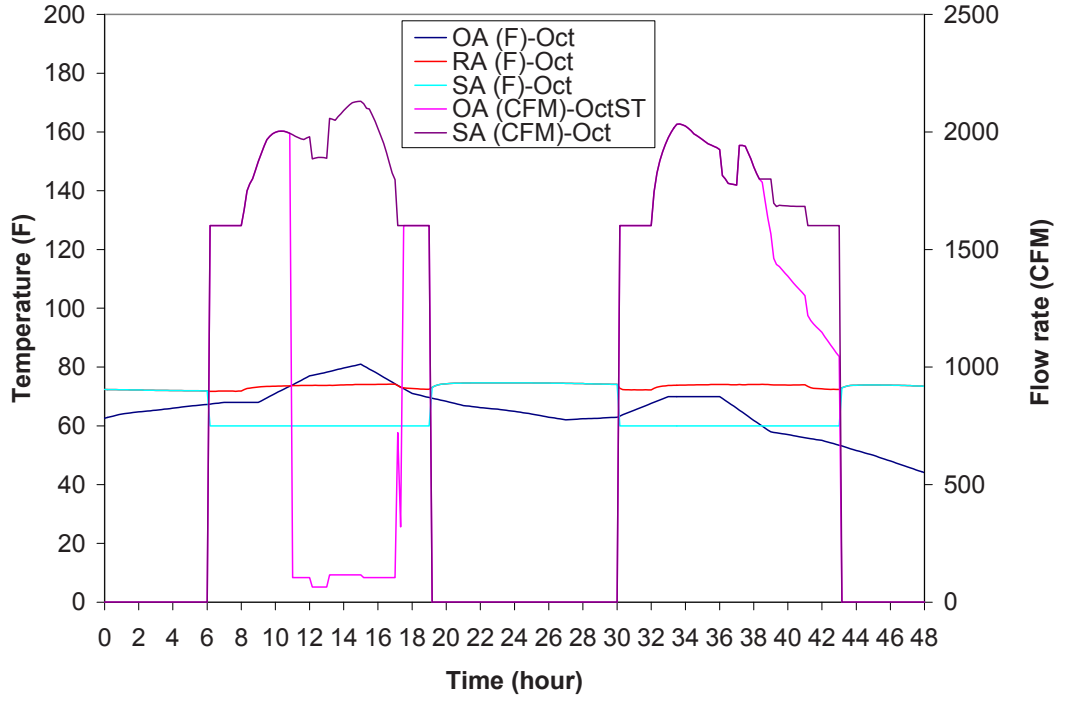

Figure 6.33 OA and SA Flow Rate in October Standard Case

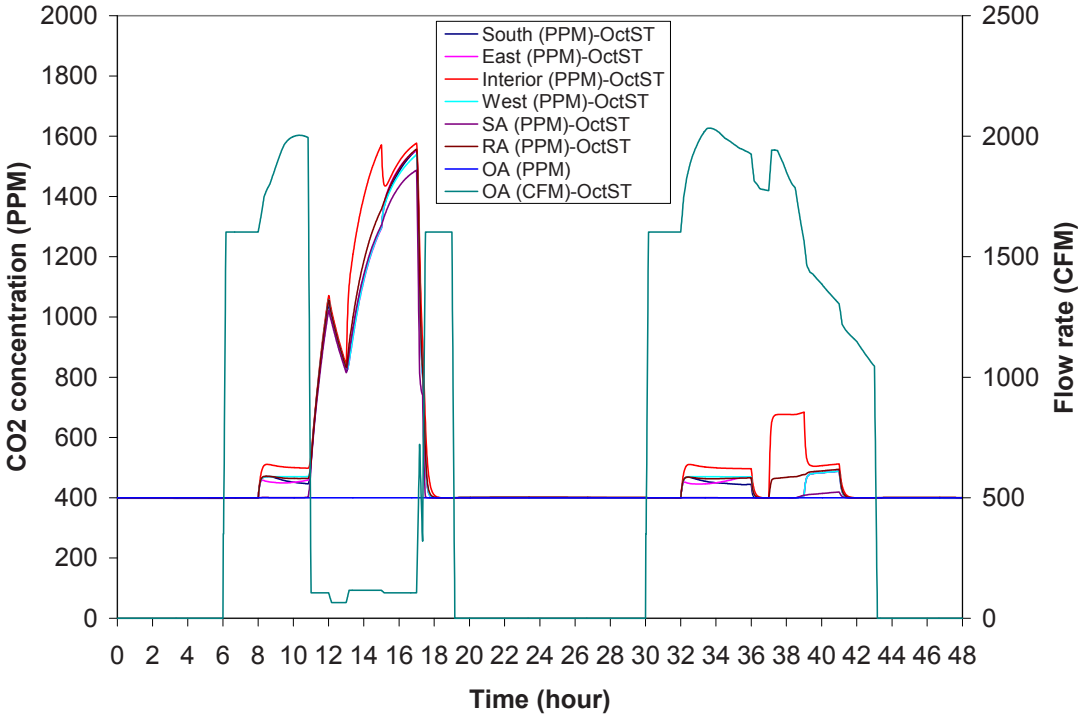

Figure 6.34 CO_2 Concentration in October Standard Cases

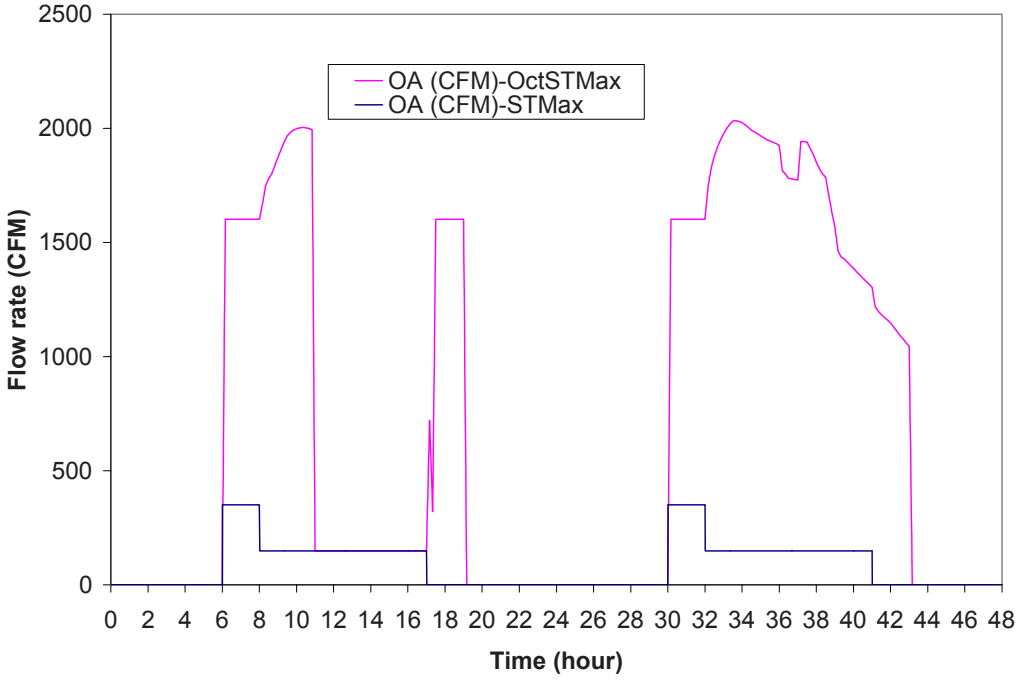

Figure 6.35 OA Flow rate comparison in October Standard Maximum Case

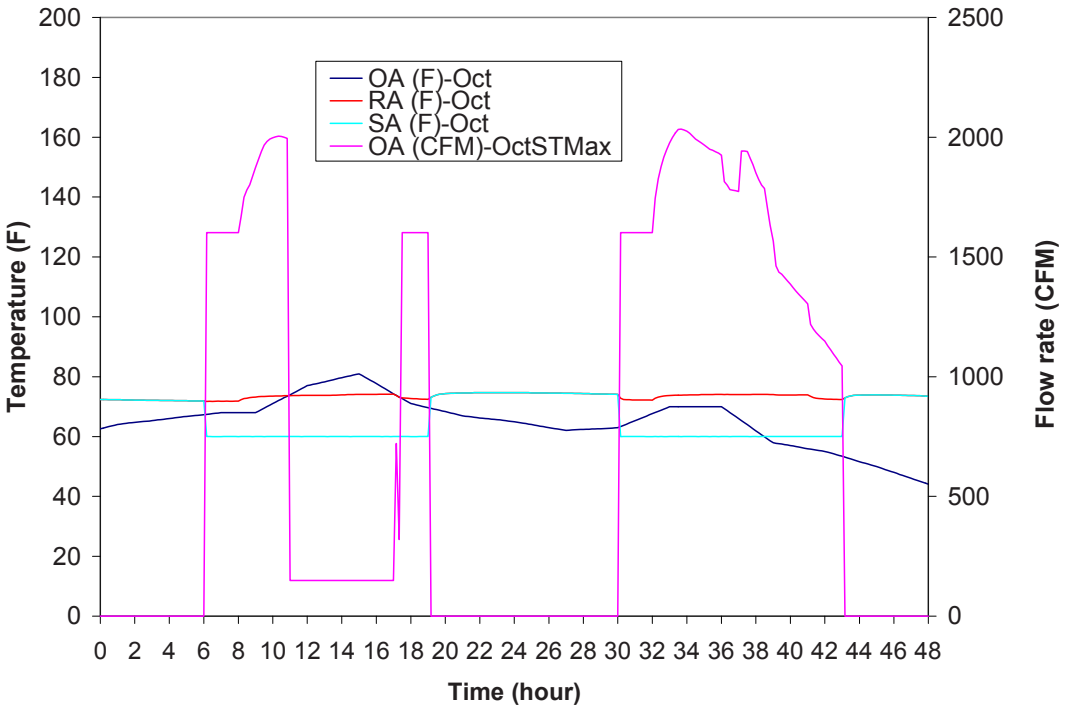

Figure 6.36 OA Flow Rate in October Standard Maximum Case

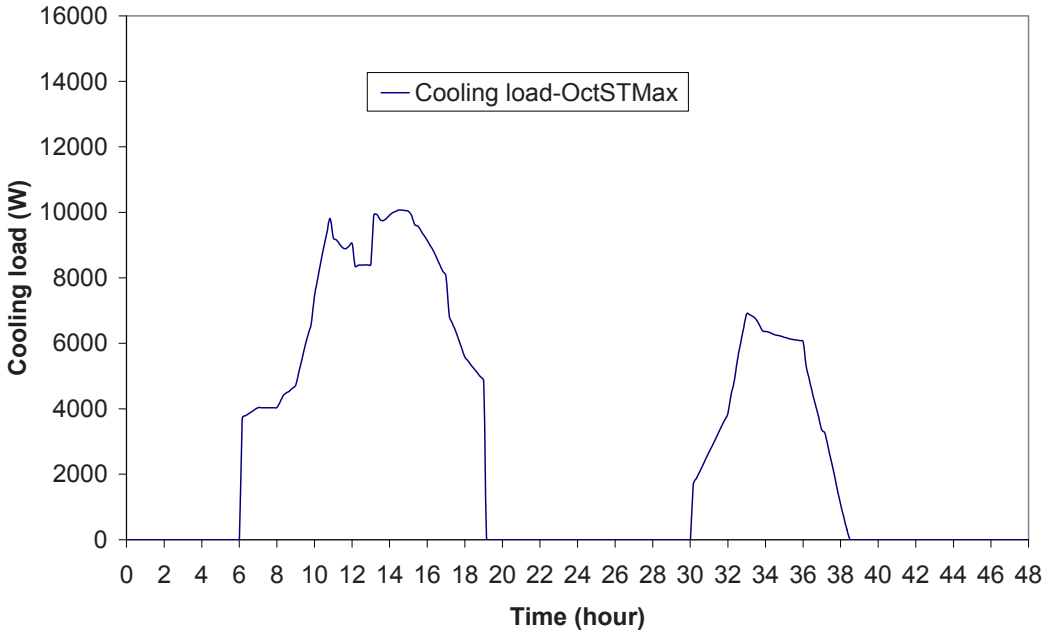

Figure 6.37 Cooling load in October Standard Maximum Case

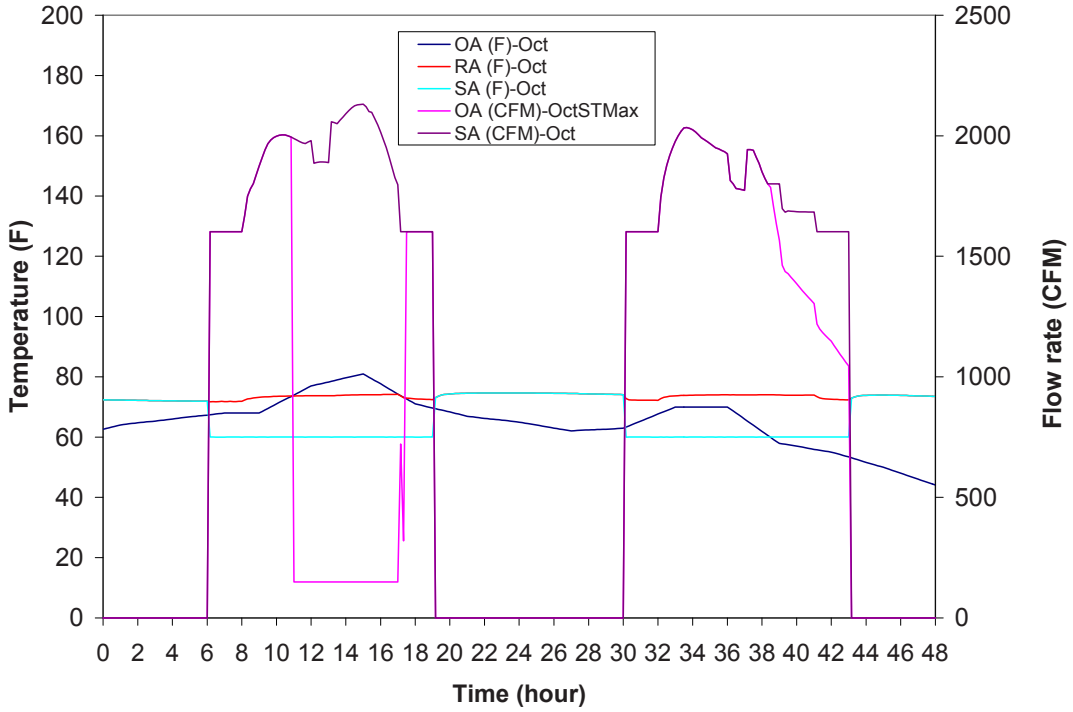

Figure 6.38 OA and SA Flow Rate in October Standard Maximum Case

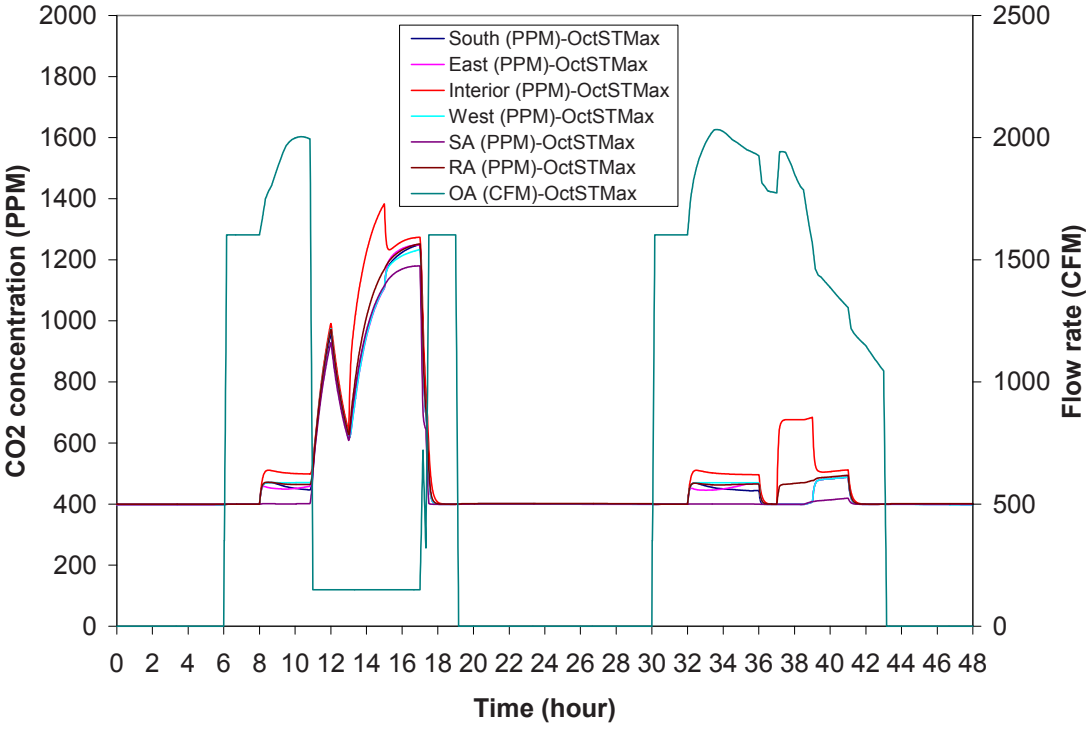

Figure 6.39 CO_2 Concentration in October Standard Maximum Case

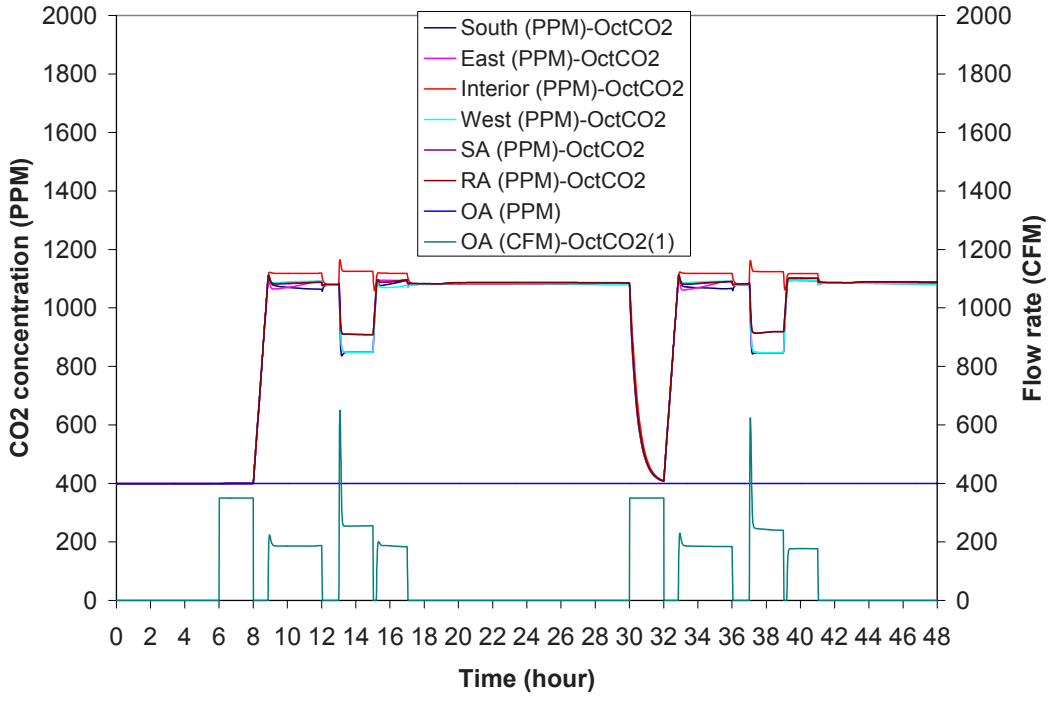

Figure 6.40 OA Flow rate in October based on CO_2 Control

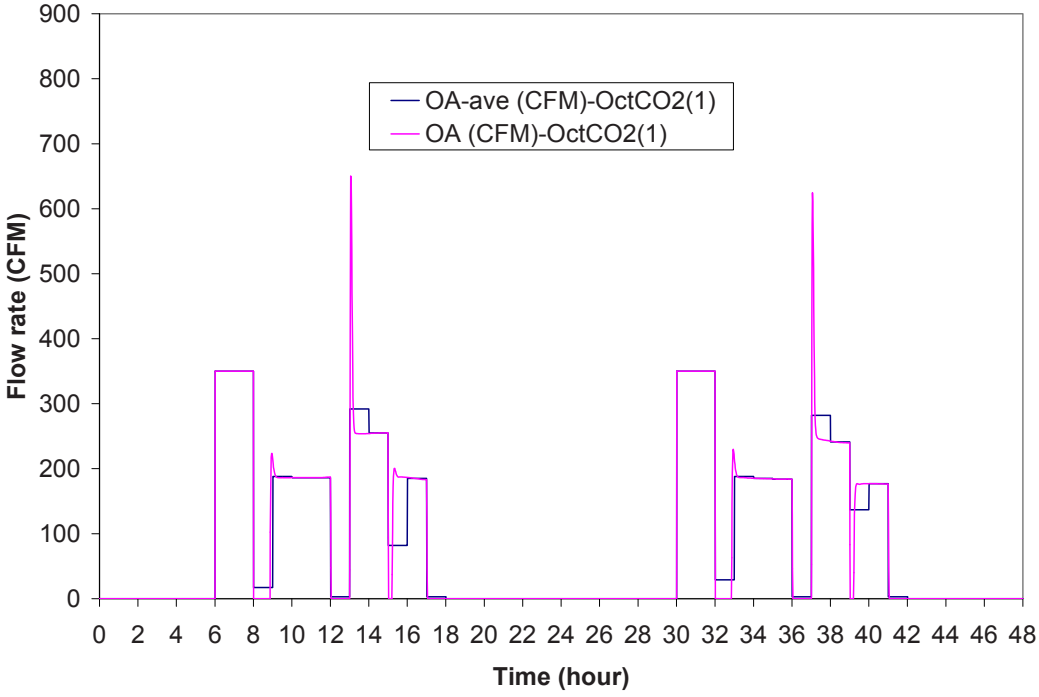

Figure 6.41 Hourly-Average OA Flow Rate in October Based on CO_2 Control

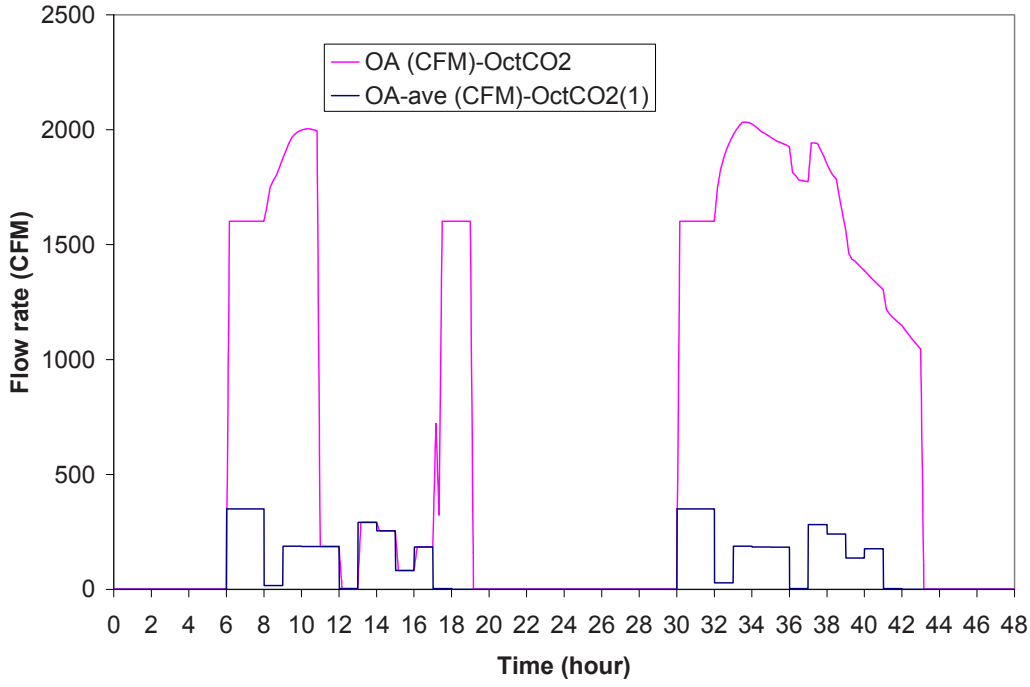

Figure 6.42 OA Flow rate comparison in October CO_2 Case

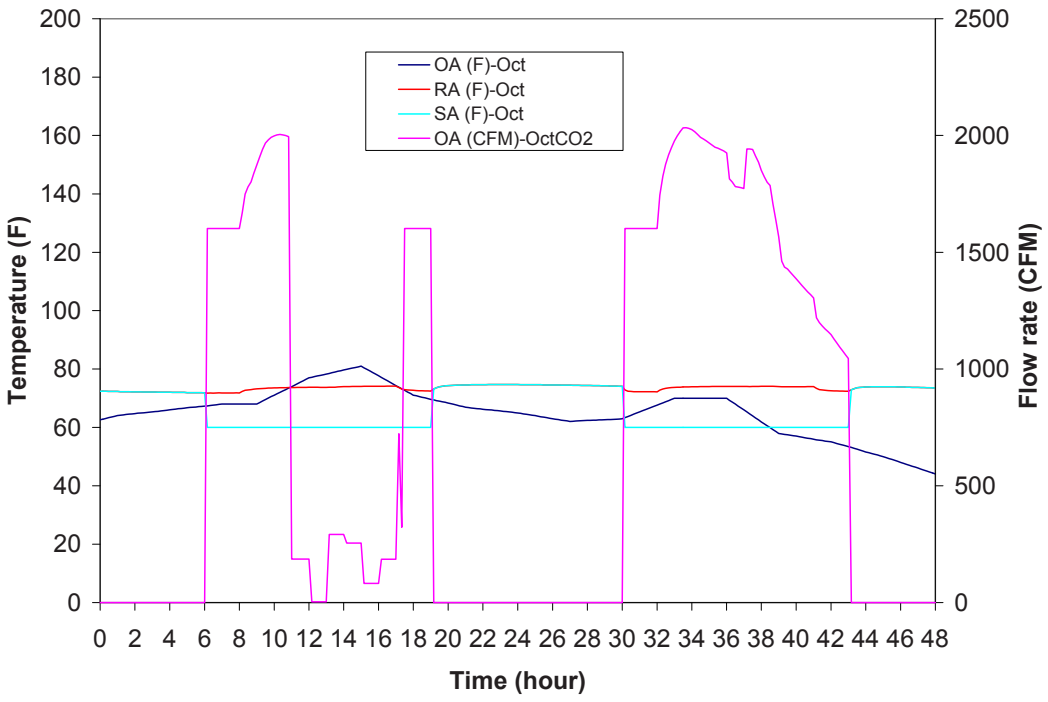

Figure 6.43 OA Flow Rate in October CO_2 Control Case

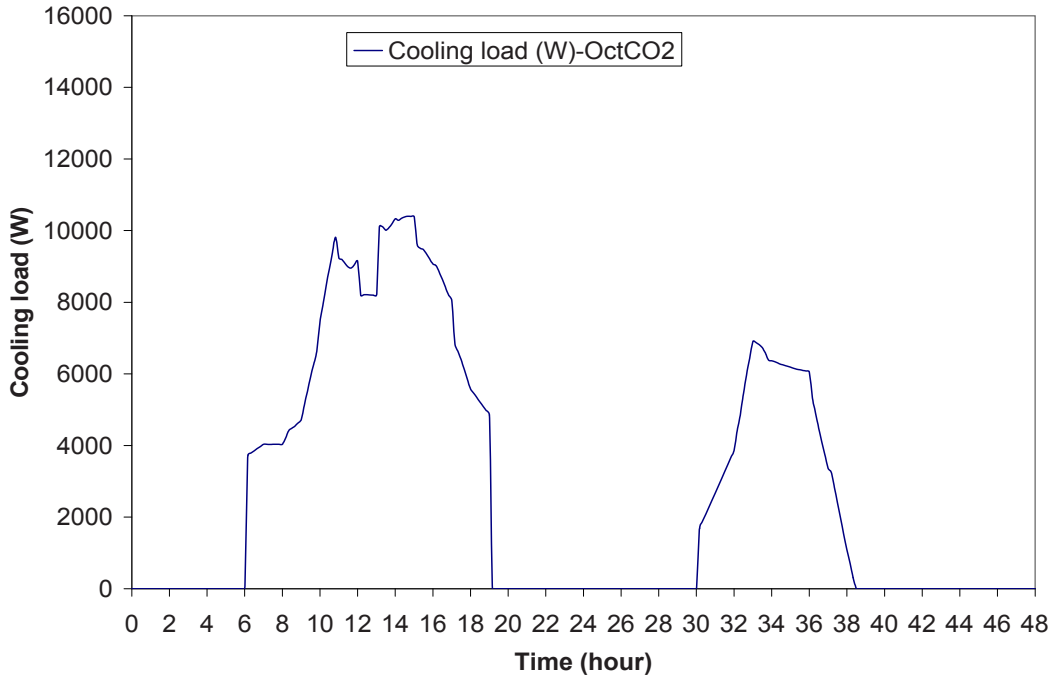

Figure 6.44 Cooling Load in October CO_2 Control Case

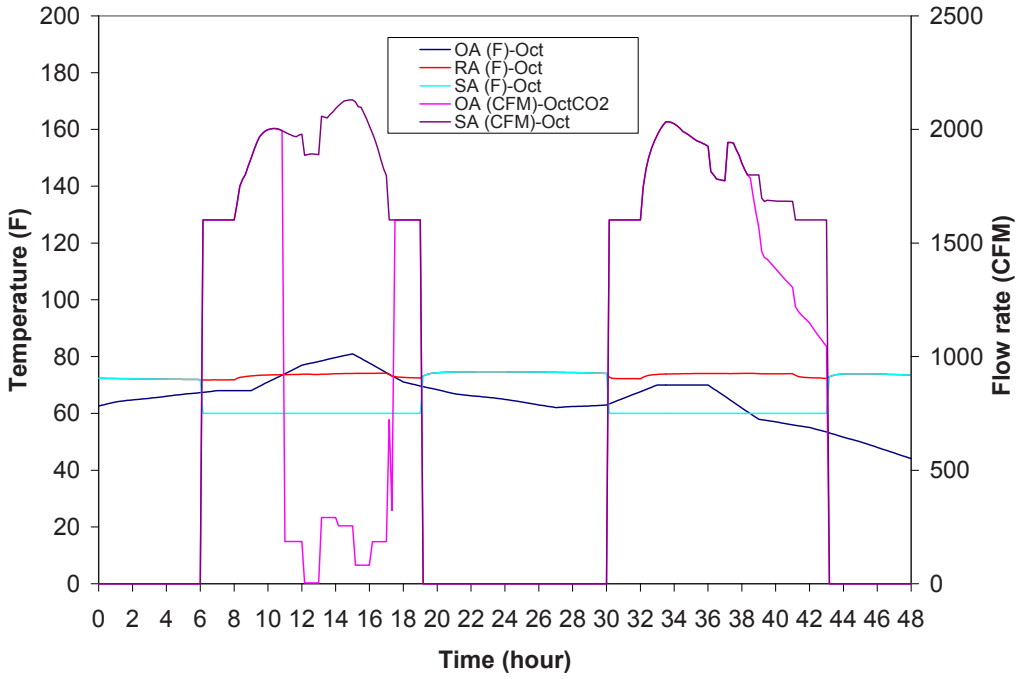

Figure 6.45 OA and SA Flow Rate in October CO_2 Control Case

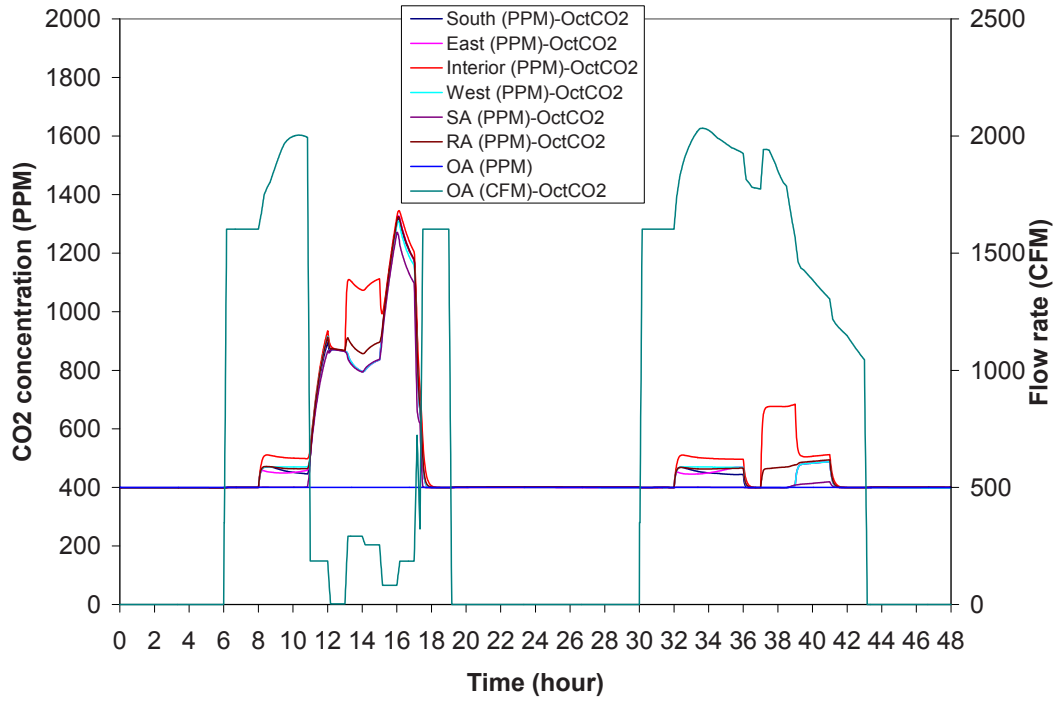

Figure 6.46 CO_2 Concentration in October CO_2 Cases

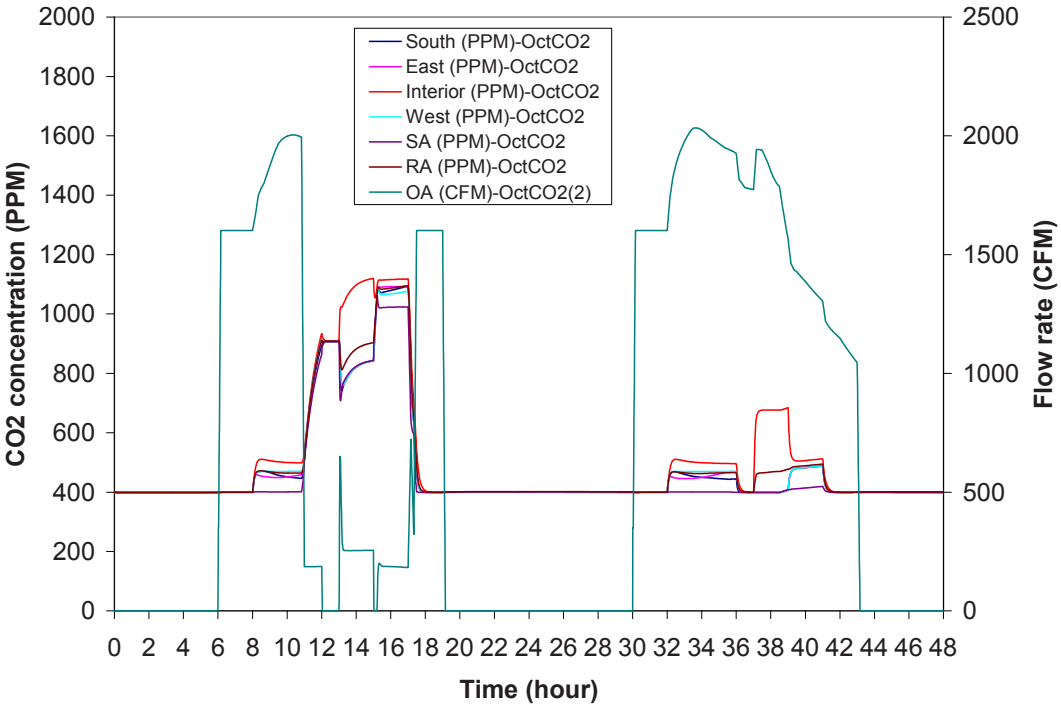

Figure 6.47 CO_2 Concentration in October CO_2 Cases (2)

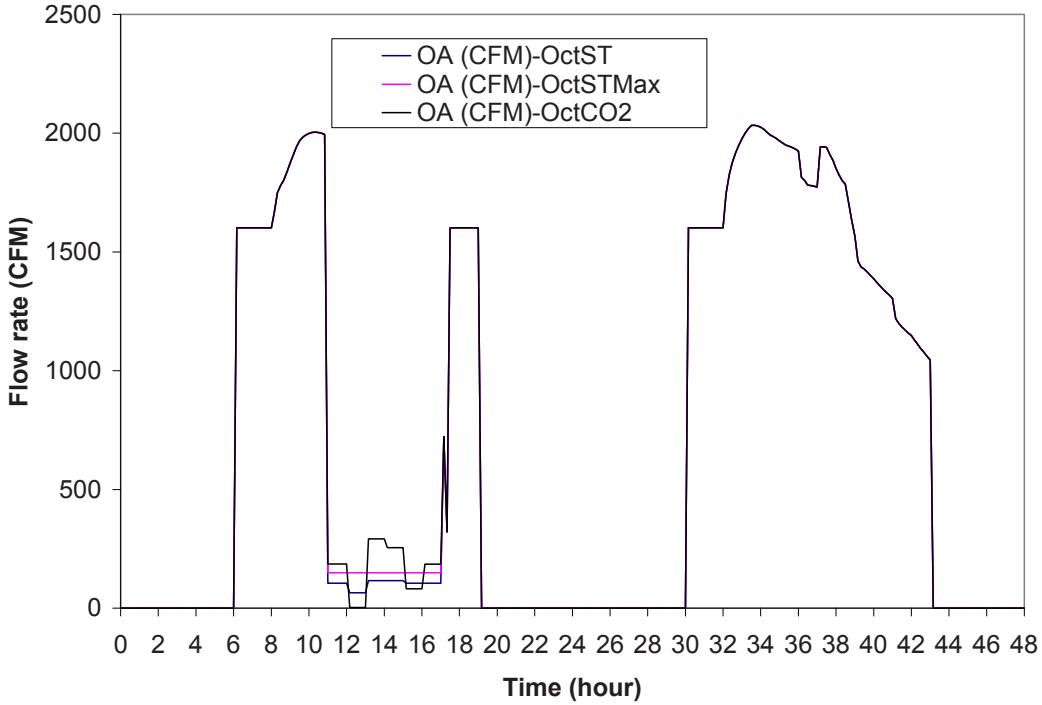

Figure 6.48 OA Flow Rate Comparison in October Cases

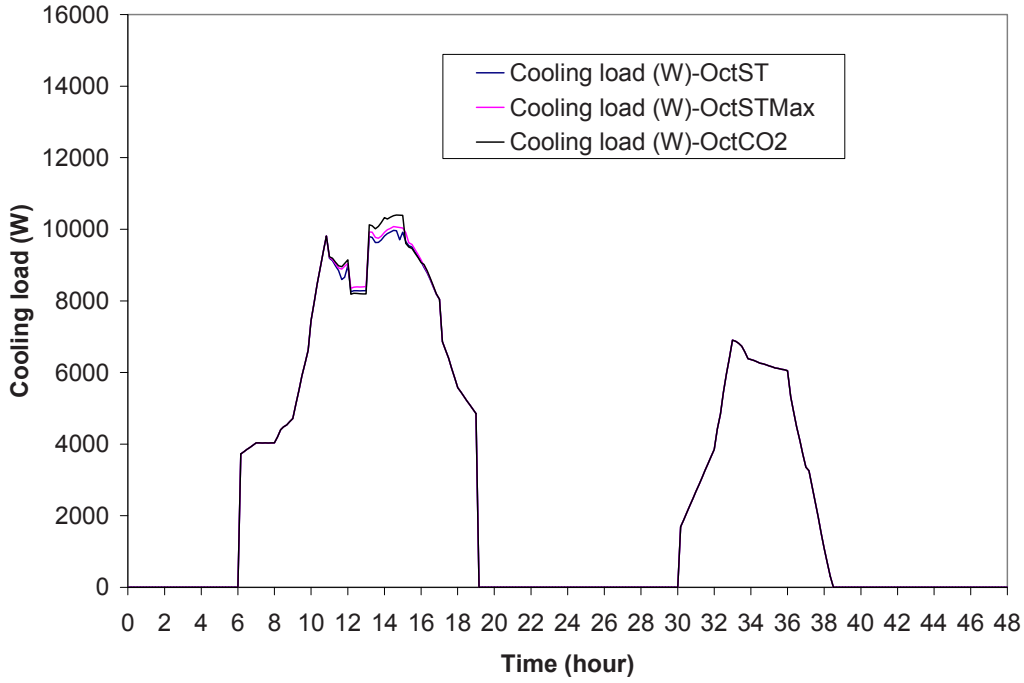

Figure 6.49 Cooling Load Comparison in October Cases

6.5 Summary

Table 6.2 summarized the cooling load results under different cases. In July which was in cooling season, the OA temperature was higher than the return air temperature, so the economizer was off, and the OA flow rate was completely determined by different ventilation control strategies. Different OA flow rate resulted in different cooling-coil load. The more the OA flow rate, the more the cooling load. The cooling load in CO_2-based DCV was 7.02% higher than that in Occupancy-based DCV, and 3.07% higher than that in constant control strategy. Different OA flow rate also resulted in different indoor CO_2 concentrations. The more the OA flow rate, the lower the indoor CO_2 concentrations. When using CO_2-based DCV, the indoor CO_2 concentrations were about 1100 ppm. When using constant OA flow rate control strategy, the highest CO_2 concentration was about 1400 ppm. When using Occupancy-based DCV, the highest CO_2 concentration was about 1600 ppm.

In January which was in the heating season, the OA temperature was lower than the return air temperature, so the economizer was on. The OA flow rate was totally determined by the use of economizer, thus three different control strategies had the same OA flow rate. Since the cold OA could make the supply air to reach the setpoint, the cooling load was 0. The indoor CO_2 concentrations in all ventilation control strategies were the same. The highest CO_2 concentration was about 900 ppm. It was much lower than that in summer cases because of much larger OA flow rate.

In October which was in the transition season, for most of the time, the OA temperature was lower than the return air temperature, and the economizer was on. For a short time, the OA temperature was higher than the return air temperature, so the economizer was off, and the OA flow rate was decided by different ventilation control strategies. The cooling load in CO_2-based DCV was 0.78% higher than that in Occupancy-based DCV, and 0.34% higher than that in constant control strategy. During the time the economizer was on, the indoor CO_2 concentrations in all ventilation control strategies were the same. The highest

CO_2 concentration was about 700 ppm. During the time the economizer was off, when using CO_2-based DCV, the indoor CO_2 concentrations were about 1100 ppm; when using constant OA flow rate control strategy, the highest CO_2 concentration was about 1400 ppm; when using Occupancy-based DCV, the highest CO_2 concentration was about 1600 ppm.

Table 6.2 Comparison of cooling load

	Total cooling load in CO_2-based DCV (MJ)	Total cooling load in Occupancy-based DCV (MJ)	Total cooling load in Constant OA flow rate (MJ)	Relative diff. (CO_2-based DCV and Occupancy based DCV	Relative diff. (CO_2-based DCV and Constant OA flow rate)
July 1-2	1024	952	993	7.02%	3.07%
Jan 13-14	0	0	0	-	-
Oct. 1-2	473	470	472	0.782%	0.338%

CHAPTER 7 CONCLUSIONS AND RECOMMENDATIONS

7.1 Conclusions

The experimental setup for DCV was built in Energy Resource Center (ERS) located on the Des Moines Area Community College in Ankeny, Iowa.

An IAQ model was built. It was based on a CO_2 balance and assumed a uniform concentration throughout the room.

The IAQ model was validated by the experimental data. Different factors including OA CO_2 concentration, CO_2 generation, and flow rate that affect the simulation results were studied. The results of IAQ model and experimental data agree with each other well.

An EnergyPlus model for the building and HVAC system was developed.

The integrated IAQ and EnergyPlus models were used to compare the cooling load and indoor air CO_2 concentrations for various ventilation control strategies in summer, winter and transition season applications.

In July which was in the cooling season, the cooling load in CO_2-based DCV was 7.02% higher than that in Occupancy-based DCV, and 3.07% higher than that in constant control strategy. When using CO_2-based DCV, the indoor CO_2 concentrations were about 1100 pm. When using constant OA flow rate control strategy, the highest CO_2 concentration was about 1400 ppm. When using Occupancy-based DCV, the highest CO_2 concentration was about 1600 ppm.

In January which was in the heating season, since the cold OA could make the supply air to reach the setpoint, the cooling load was 0. The indoor CO_2 concentrations in all ventilation control strategies were the same. The highest CO_2 concentration was about 900 ppm. It was much lower than that in summer cases because of much larger OA flow rate.

In October which was in transition season, the cooling load in CO_2-based DCV was 0.782% higher than that in Occupancy-based DCV, and 0.338% higher than that in constant

control strategy. During the time the economizer was on, the indoor CO_2 concentrations in all ventilation control strategies were the same. The highest CO_2 concentration was about 700 ppm. During the time the economizer was off, when using CO_2-based DCV, the indoor CO_2 concentrations were about 1100 ppm; when using constant OA flow rate control strategy, the highest CO_2 concentration was about 1400 ppm; when using Occupancy-based DCV, the highest CO_2 concentration was about 1600 ppm.

7.2 Recommendations

Future research could include the following consideration:

1. to develop IAQ model code in EnergyPlus code, so running EnergyPlus can produce all required results. Currently the IAQ model and EnergyPlus model are separate. Data processing is required to convert the output of one model to the input of another. If the two models could be combined, that will be very convenient for the user.
2. to run the simulations in different locations. The focus of current study was the area of Des Moines, IA. Different locations which represent hot, cold, dry and humid areas could be added.
3. to examine the technology required to implement Occupancy-based DCV such as radio frequency transmitters, optical sensors, or thermal sensors.

APPENDIX A. TECHNICAL DATA FOR

VAISALA GMW20 AND GMD20

	VAISALA GMW20	VAISALA GMD20
Measuring ranges	0-2000 PPM 0-5000 PPM 0-10000 PPM 0-20000 PPM	0-2000 PPM 0-5000 PPM 0-10000 PPM 0-20000 PPM
Accuracy at 25°C against certified factory references (includes repeatability and calibration uncertainty)	<+/- [30 PPM + 2% of reading]	<+/- [30 PPM + 2% of reading]
Non-linearity	<+/- 1.0 % FS	<+/- 1.0 % FS
Temperature dependence of output (typically)	0.15% FS/°C (reference 25°C)	0.15% FS/°C (reference 25°C)
Recommended calibration interval	5 years	5 years
Response time	1 minute	1 minute
Operating temperature range	-5- (+45) °C	-5- (+45) °C
Operating humidity range	0-85% RH, non condensing	0-85% RH, non condensing
Output signal for CO_2	0-20 mA or 4-20 mA or 0-10 V	0-20 mA or 4-20 mA or 0-10 V

APPENDIX B. CALIBRATION OF CO_2 SENSORS

Each CO_2 sensor was calibrated by using the standard gas whose CO_2 concentration was known. Figure B.1 shows the calibration results of one sensor. The x-axis shows the reading of the sensor. The y-axis was the actual CO_2 concentration of the standard gas. The equation of the trendline was used to correct the raw data read from the CO_2 sensor. The uncertainty of the sensor was calculated by the software JMP, which was about +/- 50ppm when the confidence interval was 95%.

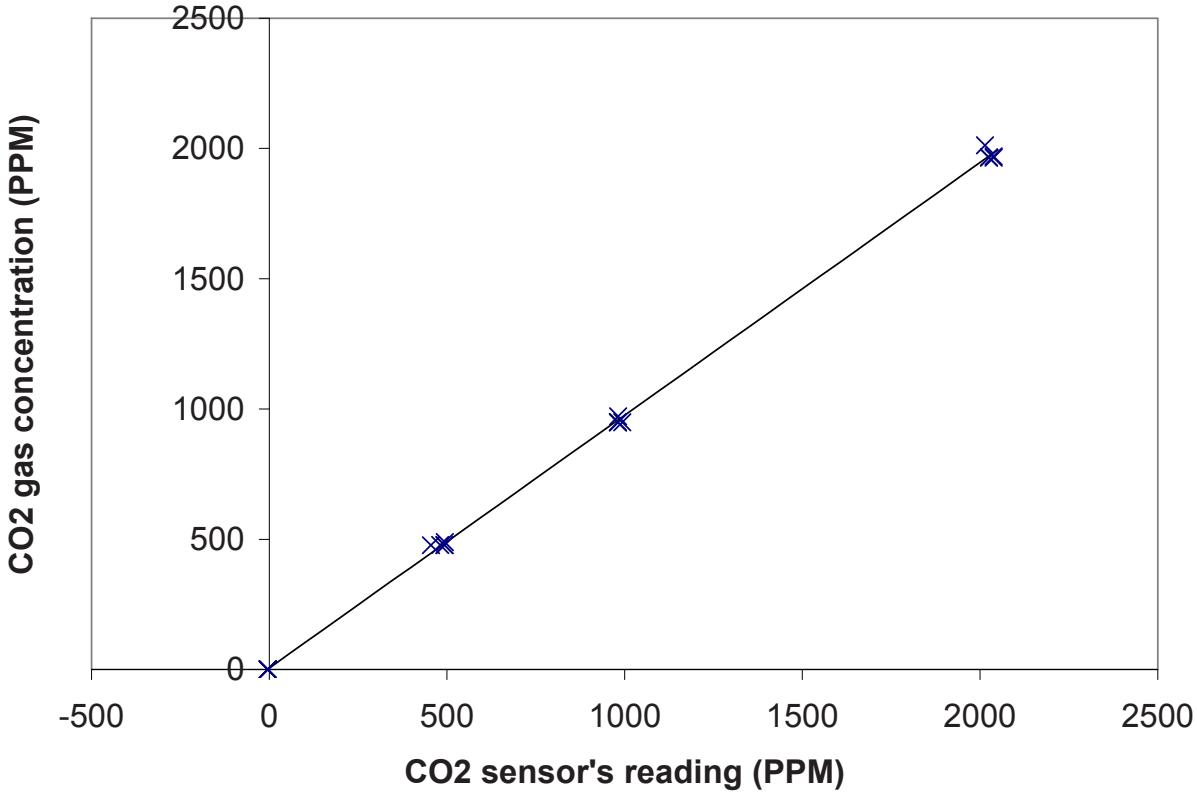

Figure B.1 Calibration results of one CO_2 sensor.

APPENDIX C. CALIBRATION OF FLOW METERS

Each flow meter was calibrated by using the wet meter. Figure C.1 shows the calibration results of one flow meter. The x-axis shows the reading of the flow meter. The y-axis was the flow rate measured by the wet meter. The equation of the trend line was used to correct the raw data got from the flow meter. The uncertainty of the flow meter was calculated by the software JMP, which was about +/- 0.00116 CFM (0.0328 L/min) when the confidence interval was 95%.

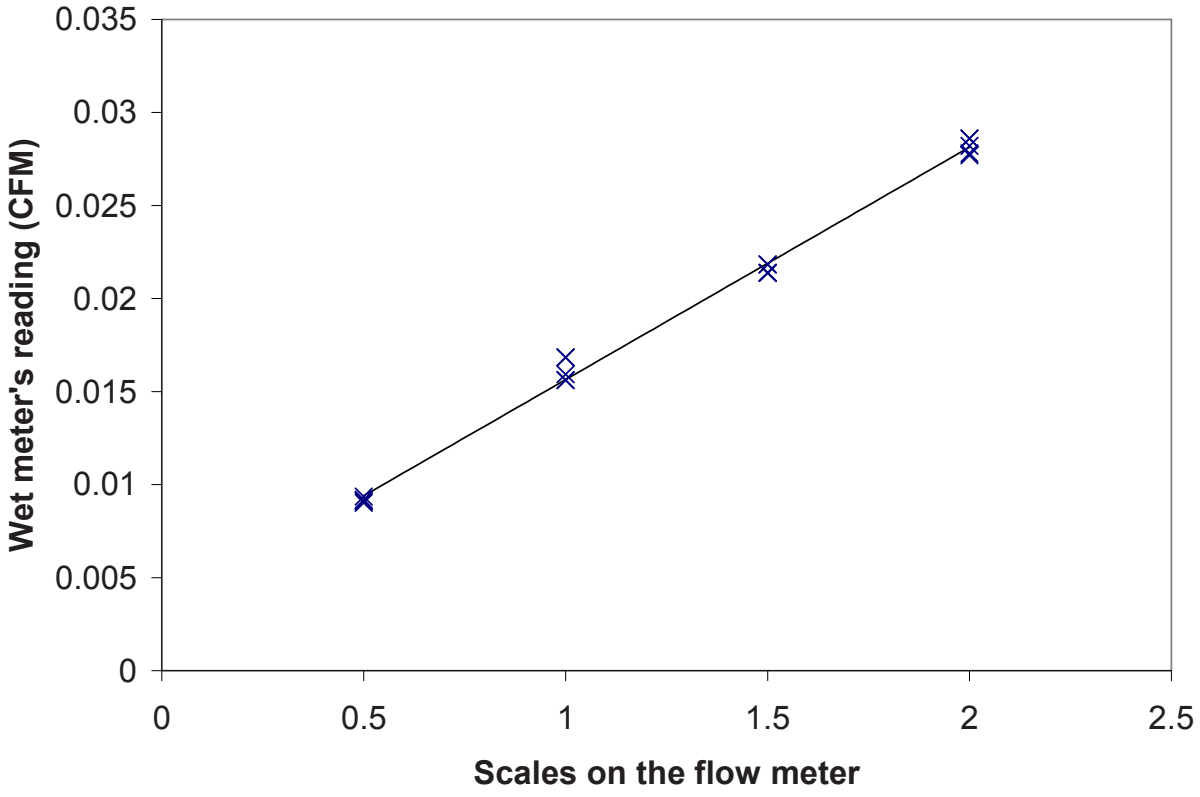

Figure C.1 Calibration results of one flow meter.

APPENDIX D. UNIT CONVERSION

Unit conversion for CO_2 concentration

Parts-Per-Million (PPM) was the unit of CO_2 concentration used in the experiment. The unit of density of CO_2 in the equations is mg/ft^3. The unit conversion for gases was given by

$$mg/ft^3 = \frac{PPM \ MWT}{2.897\,T} \tag{D.1}$$

where MWT was molecular weight of the gas with units of g/mol and T was the gas temperature with unit of K. CO_2 has M=44 g/mol, then

$$mg/ft^3 = \frac{15.19}{T} PPM \tag{D.2}$$

Unit conversion for CO_2 generation

In equation (3), the unit of CO_2 generation in the room G_j was mg/min. In the experiment, what was known was G_{qj}, the CO_2 generation in the room with the unit of ft^3/min.

G_j can be calculated from G_{qj} by using the following equation:

$$G_j = \rho \, G_{qj} \tag{D.1}$$

where

ρ Density of CO_2 gas (mg/ft^3)

The room temperature was controlled near 72°F, and the density of CO_2 gas at that temperature was $5.145 * 10^4$ mg/ft^3. So

$$G_j = 5.145 * 10^4 \, G_{qj} \tag{D.2}$$

REFERENCES

ASHRAE. (2004). ANSI/ASHRAE Standard 62.1-2004: Ventilation for Acceptable Indoor Air Quality

Alalawi, M. A., and M. Krarti. (2002). Experimental evaluation of CO_2-Based Demand-Controlled Ventilation Strategies. *ASHRAE Transactions*, 108 (2), 307-317.

Emmerich, S. J., and A. K. Persily. (1997). Literature review on CO_2-Based Demand-Controlled Ventilation. *ASHRAE Transactions*, 103 (2), 229-243.

EnergyPlus, version 1.3.0, Department of Energy, USA.

JMP, version 5.1.2. SAS Institute Inc. Cary, NC, USA.

Ke Y. P., and S. A. Mumma. (1999). Variable air ventilation control strategies analyzed in six climate zones. *International Journal of Energy Research*, 23, 371-387

Ke Y. P., and S. A. Mumma. 1997. Using Carbon Dioxide Measurements to determine occupancy for ventilation controls. *ASHRAE Transactions,* 103 (2), 364-374.

Krarti, M., and M. Alalawi. 2004. Analysis of the impact of CO_2-Based Demand-Controlled ventilation strategies on energy consumption. *ASHRAE Transactions*,110 (1), 274-286.

Lawrence, T. M., and J. E. Braun. 2007. Calibrated simulation for retrofit evaluation of Demand-Controlled ventilation in small commercial buildings. *ASHRAE Transactions,* 113 (2), 227-240.

Lee, S. S. 1999. Empirical validation of building energy simulation software: DOE2.E, HAP and TRACE. Iowa State University, Ames, IA

Mercer, K. B., and J. E. Braun. 2005. Evaluation of Demand-Controlled ventilation and enthalpy exchangers in small commercial buildings. *ASHRAE Transactions*, 111 (1), 873-889.

Price, B.A., and T. F. Smith. 1999. Description of the Iowa energy centre energy resources station: facility update II. The University of Iowa, Iowa City, IA

Stanke, D. 2005. Complying with Standard 62.1-2004: multiple-zone ventilation. *ASHRAE winter meeting seminar*, Orlando, FL

Simlink version 5.0. 2002. The MathWorks, Inc., Natic, MA, USA.

ACKNOWLEDGEMENTS

I would like to take this opportunity to express my thanks to those who helped me with various aspects of conducting research and the writing of this thesis. First and foremost, I would like to thank Dr. Gregory M. Maxwell for his guidance, patience and support throughout this research and the writing of this thesis. His insights and words of encouragement have often inspired me and renewed my hopes for completing my Ph.D. study. I would also like to thank my committee members for their efforts and contributions to this work: Dr. Ron M. Nelson, Dr. Michael B. Pate, Dr. Mark Bryden, and Dr. Steven J. Hoff. I would additionally like to thank the staff of the Energy Resource Station for their help of finishing the experiments, and the Iowa Energy Center which provided funding for this project under the Grant No. 96-08.